https://dspace.org/

Morphological and functional analysis of the postcranial anatomy of two dicynodont morphotypes from the cynognathus assemblage zone of South Africa and their taxonomic implications

Romala, Govender

2007-02-26T13:05:18Z
http://hdl.handle.net/10539/2134

Downloaded from a DSpace repository. https://dspace.org/

MORPHOLOGICAL AND FUNCTIONAL ANALYSIS OF THE POSTCRANIAL ANATOMY OF TWO DICYNODONT MORPHOTYPES FROM THE *CYNOGNATHUS* ASSEMBLAGE ZONE OF SOUTH AFRICA AND THEIR TAXONOMIC IMPLICATIONS

R. GOVENDER

WitsETD

A thesis submitted to the Faculty of Science, University of the Witwatersrand, Johannesburg, in fulfilment of the requirements for the degree of Doctor of Philosophy.

Johannesburg 2005

DECLARATION

I declare that this thesis is my own, unaided work. It is being submitted for the Degree of Doctor of Philosophy in the University of the Witwatersrand, Johannesburg. It has not been submitted before for any degree or examination in any other University.

_____

R. Govender

_____ day of _____ 2006

Wits ETD

ABSTRACT

Kannemeyeria simocephalus is probably the best known Middle Triassic dicynodont from South Africa and has been the standard against which other Triassic dicynodonts are compared. In the past studies have concentrated on the cranial morphology of *K. simocephalus* and how this affected Triassic dicynodont taxonomy and phylogeny. There has been little work on the postcranial anatomy of *K. simocephalus*, which remains poorly understood. This current study undertook a detailed descriptive analysis of the postcranial anatomy of *K. simocephalus* that lead to the identification of diagnostic characters of the postcranial skeleton. During the course of the analysis of the postcranial anatomy of *K. simocephalus* it was noted that material previously assigned to this taxon was significantly different from that recognised as *K. simocephalus*. Unfortunately, this material consists only of postcranial material and it is therefore referred to as Morphotype B rather than a new species of *Kannemeyeria* or as a new taxon from the *Cynognathus* Assemblage Zone (subzone B). A phylogenetic analysis was performed which included *K. simocephalus* and Morphotype B, and used cranial and postcranial characters. The preliminary phylogenetic results show that there are possibly two taxa of medium to large dicynodonts in the *Cynognathus* Assemblage Zone (subzone B); one a kannemeyeriid and the second a stahleckeriid. It has also evident that more attention needs to be paid to the study of the postcranial anatomy of Triassic dicynodonts, especially those from Africa and Asia.

Wits ETD

DEDICATION

For my Granny:

Phyllis Winifred Thomas

1907/10/19 – 2004/07/07

For inspiring us: For showing us convention does not define us and age should not deter us.

Wits ETD

ACKNOWLEDGEMENTS

My sincerest gratitude goes to Dr A. J. Renaut for providing me with this project and for his help during the early phases. To Dr P. J. Hancox, I truly appreciate him taking over the supervision this far into the project. I would like to express my appreciation to Dr A. Yates for his advice during the course of the project as well as for his assistance with phylogenetic analysis. I would like to thank Cecilio Vasconcelos for listening to ideas I had about my work. I would like to thank Dr R. Blob for his advice and assistance with the initial planning of the biomechanics (which was unfortunately omitted). I would like to extend my thanks to the preparators of the Bernard Price Institute (Palaeontology), Joseph Sithole, Samuel Tshabalala and Charlton Dube, for their advice and help during the preparation of study material. I am grateful to Dr M. A. Raath of the BPI, Mr Kevin Cole at the East London Museum and Mrs Sheena Kaal at the South African Museum for their assistance in making specimens available to me for study. Last but not least to my family and Johann I would like to express my sincerest thanks for all their help and support during this project, especially during those trying times.

Wits ETD

LIST OF FIGURES

Figure 1……..105

Lateral view of the scapula of *Kannemeyeria simocephalus* (Morphotype A) showing: a) scapula blade of the left scapula of BP/1/5624; b) Distal end of the right scapula of BP/1/6104 showing the glenoid and the coracoid articulation

Figure 2……..107

Medial view of the left scapula of *K. simocephalus* (Morphotype A) (BP/1/5624) showing the prominent tubercle on the porixmo-posterior corner of the acromion

Figure 3.....110

The left humerus of the small specimen (BP/1/6160) of *K. simocephalus* (Morphotype A) shown in dorsal view (a) and the ventral view (b), both showing the large proximal expansion and well developed delto-pectoral crest

Figure 4 ……112

Left ulna of *K. simocephalus* (Morphotype A) showing the narrow, triangular and low olecranon in a) lateral view of BP/1/5624 and b) medial view BP/1/6160

Figure 5……..114

Right radius of *K. simocephalus* (Morphotype A) showing a well developed tubercle above the distal end in a) anterior view (BP/1/5624 and the well developed ulna articulation in b) posterior view (BP/1/6160)

Figure 6.....117

Left femur of *K. simocephalus* (Morphotype A) (BP/1/5624) showing the medially inflected head in a) ventral view and the narrow greater trochanter and straight shaft in b) dorsal view

Figure 7…...……...119

Right tibia of *K. simocephalus* (Morphotype A) showing a prominent tibial tuberosity and cranial margin in anterior view (a) and a shallow groove that extends down the length of the shaft in posterior view (b)

Figure 8……..125

Lateral view of the left scapula of Morphotype B in a) lateral view and b) medial view showing a fossa at the proximo-posterior corner of the acromion.

Figure 9……..128

Proximal expansion of the humerus of Morphotype B showing an arc shaped delto-pectoral crest in a) dorsal view and the medial direction of the delto-pectoral crest in b) ventral view

Figure 10……130

Proximal end of the left ulna of Morphotype B (SAM –PK-1073) in a) lateral view and b) medial view

Wits ETD

Figure 11……....**132**
Right femur of Morphotype B (BP/1/3518) showing a wide proximal expansion and narrow greater trochanter in a) dorsal view and the third trochanter in b) ventral view
Figure 12……**153**
Muscle attachment sites on the lateral [a) i-ii] and medial [b) i-ii] surfaces of the scapulae of Morphotype A [a & b) i] and Morphotype B [b) ii] showing that in most instances there is a difference in the size of the muscles between the two animals
Figure 13……**154**
Muscle attachment sites on the dorsal [a) i-ii] and ventral [b) i-ii] surfaces of the humerus of Morphotype A [a & b) i] and Morphotype B [a & b) ii]
Figure 14……**155**
Muscle attachment sites on the lateral surface of the pelvic girdle of Morphotype A
Figure 15……**156**
Muscle attachment sites on the dorsal [a) i-ii] and ventral [b) i-ii] surfaces of the femora of Morphotype A [a & b) i] and Morphotype B [a & b) ii]
Figure 16……**161**
Phylogenetic tree showing the relationships of *K. simocephalus* (Morphotype A) and Morphotype B with certain Triassic dicynodonts using cranial and postcranial characters
Figure 17……**162**
Majority rule consensus tree of the relationships of *K. simocephalus* (Morphotype A) and Morphotype B among certain Triassic dicynodonts using cranial and postcranial characters
Figure 18……**163**
Consensus tree of the relationships of *K. simocephalus* (Morphotype A) and Morphotype B with some genera of Triassic dicynodonts using only postcranial characters
Figure 19……**164**
Relationships of *K. simocephalus* (Morphotype A) and Morphotype B among certain Triassic dicynodonts using cranial and postcranial characters and excludes *Dinodontosaurus*
Figure 20……**165**
Majority rule consensus tree of the relationships of *K. simocephalus* (Morphotype A) and Morphotype B among certain Triassic dicynodonts genera using cranial and postcranial characters, which excludes *Dinodontosaurus*
Figure 21 ……...**166**
Relationships of *K. simocephalus* (Morphotype A) and Morphotype B with certain Triassic dicynodonts using only postcranial characters and excludes *Dinodontosaurus*

WitsETD

Figure 22……167
Majority rule consensus tree for the postcranial analysis of the relationships of *K. simocephalus* (Morphotype A) and Morphotype B among certain Triassic dicynodonts and excludes *Dinodontosaurus*

Wits ETD

LIST OF PLATES

Plate 1……106

Lateral view of the scapula of *Kannemeyeria simocephalus* (Morphotype A) showing the left scapula in various states of preservation in a) i-ii and the distal end of the left scapula of BP/1/6104 in b).

Plate 2……108

Medial view of the left scapula of *K. simocephalus* (Morphotype A) showing the tubercle on the proximo-posterior corner of the acromion of BP/1/5624 and BP/1/6160.

Plate 3……109

a) Lateral view of the right glenoid of *K. simocephalus* (Morphotype A) (ELM 1) showing its postero-ventrally directed articulating surface;

b) Dorsal view of the interclavicle of *K. simocephalus* (Morphotype A) (ELM 1) showing damage along the distal end and along the lateral side;

c) Lateral view of the left clavicle of *K. simocephalus* (Morphotype A).

Plate 4……111

Humerus of *K. simocephalus* (Morphotype A) showing variation in the form of the left bone in three individuals studied a) i-iii shows the dorsal view of BP/1/5624, BP/1/6160, ELM1 respectively, and b) i-ii shows the ventral view of BP/1/5624 and BP/1/6160.

Plate 5……113

Ulna of *K. simocephalus* (Morphotype A) showing the low olecranon and the variation in form between the left one of the larger individual [a)i BP/1/5624] and the smaller individual [a) ii BP/1/6160] and b) shows the medial view

Plate 6……115

Radius of *K. simocephalus* (Morphotype A) showing the well developed tubercle above the distal end in anterior view a)i BP/1/5624 and the well developed ulna articulation in anterior view a) ii BP/1/6160 and posterior view b) BP/1/6160.

Plate 7……116

Lateral view of the right and left pelvic girdles of *K. simocephalus* (Morphotype A) incomplete in a) BP/1/5624 and fairly complete in b) R 3761 showing an elongated oval obturator foramen.

Plate 8……118

Femora of *K. simocephalus* (Morphotype A) showing different types of distortion in right (a (i) & b (i)) and left (a (i) & b (ii)) viewed in a) ventral view and b) dorsal view.

Plate 9……120

a) Tibia of *K. simocephalus* (Morphotype A) (BP/1/5624) showing a prominent tibial tuberosity.

b & c) Shows the thin right and left fibula of *K. simocephalus* (Morphotype A) (ELM 1).

WITS ETD

Plate 10……..121

The atlas-axis complex of *K. simocephalus* (Morphotype A) showing the lateral view of the atlas (a (i) left; a(ii) right) and the lateral view of the axis in (b(i)) and anterior view in b(ii).

Plate 11……..122

a) Lateral view of a possible dorsal vertebrae of *K. simocephalus* (Morphotype A) (SAM-pk-3017) showing a posteriorly inclined neural spine and a prominent rib articulation on the centrum; while b) shows lateral view of four Caudal vertebrae showing a decrease in size in the posterior direction.

Plate 12…….123

a) Lateral view of a possible dorsal vertebrae of *K. simocephalus* (SAM-pk-3017) showing a posteriorly inclined neural spine and a prominent rib articulation on the centrum; while b) shows lateral view of four Caudal vertebrae showing a decrease in size in the posterior direction.

Plate 13……..126

Left (BP/1/994D) and right (BP/1/1669) scapula of Morphotype B showing that BP/1/1669 is much larger in a) lateral view and b) medial view.

Plate 14……..127

Medial view of the left [a) BP/1/994D] and right [b) BP/1/1669] scapula of Morphotype B showing the fossa at the proximo-posterior corner of the acromion.

Plate 15……..129

Proximal end of the left humerus of Morphotype B showing the arc shaped delto-pectoral crest in a) i-ii dorsal view [i. BP/1/994a; ii SAM-PK-1073] and that it is slightly medially directed in b) ventral view (BP/1/994A).

Plate 16……..131

Proximal end of the left ulna of Morphotype B (SAM-PK-1073) in a) lateral view and b) medial view showing the low, wide olecranon.

Plate 17……..133

Right femur of Morphotype B (BP/1/3518) the narrow greater trochanter in a) dorsal view and the short third trochanter and antero-dorsally directed head in b) ventral view.

Plate 18……..134

Scapulae (left and right) of British Museum specimen previously identified as *K. simocephalus* (by Pearson 1924b) (Morphotype A) show features that show them to more closely resemble Morphotype B.

Wits ETD

Plate 19……..135

Ulna (left) of British Museum specimens that was previously identified as *K. simocephalus* (by Pearson 1924b) (Morphotype A) but closer examination of photographs of the material shows that it more closely resembles Morphotype B.

Plate 20……..136

Left and right femora of a British Museum specimen (R 3740) previously identified as *K. simocephalus* (by Pearson 1924b) (Morphotype A), which resembles Morphotype B more closely.

Plate 21……..138

Comparison of the scapula of Morphotype B [b)i & ii] with that of *K. simocephalus* (Morphotype A) showing the tubercle [b)i] and the fossa [b) ii] at the proximo-posterior corner of the acromion.

Plate 22……..139

Comparison of the proximal end of the humerus of Morphotype B (BP/1/994A) with the humerus of *K. simocephalus* (Morphotype A) (BP/1/6160) showing the difference in the shape of the delto-pectoral crest (a) i-ii and the biccipital fossa in b) i-ii.

Plate 23……..140

Comparison of the proximal end of the ulna of Morphotype B (SAM-PK-1073) with that of *K. simocephalus* (Morphotype A) (BP/1/6160), which shows the difference in the olecranon of the two morphotypes.

Plate 24……..141

Comparison of the right femur of Morphotype B (BP/1/3518) and the left femur of *K. simocephalus* (Morphotype A) (BP/1/5624) clearly showing the medially inflected head in *K. simocephalus* (Morphotype A) [b)i] and the antero-dorsally directed head in Morphotype B [b)ii].

Plate 25……..143

Comparison of the scapula of Morphotype B with that of *Zambiasaurus* showing the narrow scapula blades (a) and the antero-ventrally directed coracoid articulation (b).

Plate 26……..144

Comparison of the humerus of Morphotype B with that of *Zambiasaurus* showing the more posteriorly positioned head and arc shaped delto-pectoral crest [a) i-ii] and medially directed delto-pectoral crest and slightly deep biccipital fossa [b) i-ii].

Plate 27……..145

Comparison of the lateral view of the ulna of Morphotype B with *Zambiasaurus* showing that Morphotype B has a wider olecranon in a) i-ii lateral view and a deeper groove in b) i-ii medial view.

Wits ETD

Plate 28……..146

Comparison of the femur of Morphotype B with that of *Zambiasaurus* showing that the proximal end of the femur Morphotype B is wider than that of *Zambiasaurus* [a)i-ii] and that the head of the femur of *Zambiasaurus* is less well developed in this specimen [b) i-ii].

Plate 29……..147

Comparison of the scapula of Morphotype B with *Angonisaurus* showing that *Angonisaurus* has a larger more robust scapula and the acromion is directed more laterally in *Angonisaurus* [a)i-ii] and there is no fossa present on the medial surface of the scapula *Angonisaurus* [b) i-ii].

Plate 30……..148

Comparison of the humerus of Morphotype B with *Angonisaurus,* showing the triangular delto-pectoral crest in *Angonisaurus* [a)i-ii] and in b)i-ii showing an almost trapezoidal biccipital fossa in *Angonisaurus*

Plate 31……..149

Comparison of the ulna of Morphotype B with *Angonisaurus* that shows the wedge-shaped olecranon in *Angonisaurus* [a)ii] compared with the wider one in Morphotype B [a)i] and shows a more elongated proximal end in *Angonisaurus* [b)ii] than in Morphotype B [b)i] as seen in medial view (b).

Plate 32……..151

Shows some elements from the skeleton of ELM 1 that does not conform with the features of what is currently recognised as *K. simocephalus* (Morphotype A): a) radius and ulna; b) ilium and c) pubo-ischiadic plate.

Plate 33……..174

Proximal articulating surface of the humerus of *K. simocephalus* (a & b) and Morphotype B (c).

Plate 34……..175

Distal articulating surface of the humerus of *K. simocephalus*.

Plate 35……..176

a) Proximal articulating surface of the ulna and radius of *K. simocephalus*; b) Distal articulating surface of the radius of *K. simocephalus*; c) Distal articulating surface of the ulna of *K. simocephalus*.

Plate 36……..177

Proximal articulating surface of the femur of a)i. *K. Simocephalus* (dorsal view); a) ii Morphotype B (ventral view). Distal articulating surface of the femur of b) i. *K. simocephalus* (dorsal view); b) ii Morphotype B (dorsal view).

Wits ETD

Plate 37……..178

a) Proximal articulating surface of the tibia of *K. simocephalus*; b) Distal articulating surface of the tibia of *K. simocephalus*.

LIST OF TABLES

Table 1……..162

List of characters that diagnose each clade

Table 2……...169

Data Matrix of taxa and characters used in the phylogenetic analysis

Wits ETD

ABBREVIATIONS

3rd Tr.	Third Trochanter
Acet. n.	Acetabular notch
Acet. r.	Acetabular ridge
Acet.	Acetabulum
Acr.	Acromion
Ant. Cond.	Anterior condyle
Ant. Proc.	Anterior Process
Atl.	Atlas
Ax.	Axis
Biccip. F.	Biccipital Fossa
Cent.	Centrum
Cor. Artic.	Coracoid articulation
Cran.margin	Cranial margin
Dist.	Distal articulation
D-P Cr.	Delto-pectoral crest
Ectepic.	Ectepicondyle
entepic. For.	Entepicondylar Foramen
entepic.	entepicondyle
Fem. H.	Femoral head
Fib. artic.	Fibula articulation
Glen.	Glenoid
Gr.	Groove
H. Art.	Haemel arch Articulation
Hum. H.	Humeral head
I. *M. bic.*	Insertion *M. biceps*
I. *M. corac.*	Insertion *M. coracobracahialis*
I. *M. Ilio-fem.*	Insertion *M. Ilio-femoralis*
I. *M. Ischio-troch.*	Insertion *M. Ischio-trochanterica*
I. *M. latis. dors.*	Insertion *M. latissimus dorsi*
I. *M. pect.*	Insertion *M. pectoralis*

WisETD

I. *M. trap.*	Insertion *M. Trapezius*
Ic	Intercentrum
Intercond. F.	Intercondylar Fossa
Isch.	Ischium
N. S.	Neural Spine
N. A.	Neural Arch
O. *M. pub-isch. Fem.*	Origin *M. Pubo-ischio femoralis*
O. *M. delt.*	Origin *M. deltoideus*
O. *M. Fem.-tib.*	Origin *M. femoro-tibialis*
O. *M. Gastroc.*	Origin *M. gastrocnemius*
O. *M. Ilio-fem.*	Origin *M. ilio-femoralis*
O. *M. scap.-hum. Ant.*	Origin *M. scapulo-humeralis anterior*
O. *M. scap.-hum. lat.*	Origin *M. triceps caput lateralis*
O. *M. scap.-hum. post.*	Origin *M. scapulo-humeralis posterior*
O. *M. serr. Ant.*	Origin *M. serratus anterior*
O. *M. subscap.*	Origin *M. subscapularis*
O. *M. Triceps cap. Med.*	Origin *M. Triceps caput medialis*
O. *M. Triceps scap.*	Origin *M. Triceps caput scapularis*
Obt. For.	Obturator foramen
Odont.	Odontoid Process
Olec. F.	Olecranon Fossa
Olec.	Olecranon
Post. Cond.	Posterior condyle
Post. Proc.	Posterior Process
Postzyg.	Postzygapophysis
Presp. A.	Prespinous Area
Prezyg.	Prezygapophysis
Proj.	Projection
Prox.	Proximal articulation
Pub. Tub.	Pubic tubercle
Rad. Artic.	Radial articulation
Rad. Cond. (capit.)	Radius condyle (capitulum)
Rad. F.	Radial facet
Sc. bl.	Scapula blade

WisETD

Sig. fac.	Sigmoidal Facet
Sk. Artic.	Skull Articulation
Sp.	Scapula spine
Tr. M.	Trochanter major
Tr. Min.	Minor Trochanter
Tub.	Tubercle
Tuberos. tib.	*Tuberositas tibiae*
Tv. Proc.	Transverse Process
Ul. Cond. (troch.)	Ulna condyle (trochlea)

WitsETD

INSTITUTION ABBREVIATIONS

(BMH) R – British Museum of Natural History

BP – Bernard Price Institute (Palaeontology), Johannesburg

ELM – East London Museum

GSR – Geological Survey, Pretoria

GSPR – Geological Survey, Namibia

HMV – Hofmuseum, Vienna, Austria

SAM – South African Museum, Cape Town

UCMP – University of California Museum Palaeontology

CONTENTS

DECLARATION ii

ABSTRACT iii

DEDICATION iv

ACKNOWLEDGEMENTS v

LIST OF FIGURES vi

LIST OF PLATES ix

LIST OF TABLES xiii

ABBREVIATION xiv

INSTITUTION ABBREVIATIONS xvi

CHAPTER ONE - INTRODUCTION

1.1 General Introduction...……...1

1.2 Historical Review of *Kannemeyeria simocephalus*.……3

CHAPTER TWO – MATERIALS AND METHODS

2.1 *Kannemeyeria simocephalus*……..……..…….9

2.2 Morphotype B…….....12

2.3 Methodology…….....14

2.4 Phylogenetics…….....15

2.5 Aims…….....16

CHAPTER THREE - POSTCRANIAL ANATOMY OF *KANNEMEYERIA SIMOCEPHALUS*

3.1 General Introduction…….....18

3.2 Pectoral Girdle

3.2.1 Scapula…….....19

3.2.2 Precoracoid……..22

3.2.4 Coracoid……...22

Wits ETD

3.2.5 Clavicle……22
3.2.6 Sternum……23
3.3 Forelimb
3.4.1 Humerus……...23
3.4.2 Ulna……..27
3.4.3 Radius……...28
3.4 Pelvic Girdle
3.4.1 Ilium…….....29
3.4.2 Pubis…….....30
3.4.3 Ischium…….31
3.5 Hindlimb
3.5.1 Femur…….....32
3.5.2 Tibia…….....33
3.5.3 Fibula…….....34
3.6 Axial Skeleton
3.6.1.1 Atlas..…….....35
3.6.1.2 Axis……....35
3.6.1.3 Postaxial Cervical vertebrae……..36
3.6.2 Dorsal vertebrae……....36
3.6.3 Caudal vertebrae……...37
3.7 Functional Morphology of *K. simocephalus*
3.7.1 Pectoral Girdle and Forelimb……....37
3.7.2 Pelvic Girdle and Hindlimb…….....40
3.7.3 Glenoid and Elbow……41
3.7.4 Acetabulum and Knee……...42

CHAPTER FOUR – POSTCRANIAL ANATOMY OF MORPHOTYPE B

4.1 Introduction…….....43
4.2 Pectoral Girdle
4.2.1 Scapula……44
4.2.2 Precoracoid……...46

Wits ETD

4.2.3 Coracoid……...46
4.3 Forelimb
3.3.1 Humerus……...47
3.3.2 Ulna…….....47
4.4 Hindlimb
4.4.1 Femur……...48
4.5 Functional Morphology of Morphotype B
4.5.1 Pectoral Girdle and Forelimb…….……..50
4.5.2 Glenoid and Elbow joint…….…51
4.5.3 Pelvic Girdle and Hindlimb……..…52

CHAPTER FIVE – PRELIMINARY PHYLOGENETIC ANALYSIS OF THE POSTCRANIAL SKELETON OF *K. SIMOCEPHALUS* AND MORPHOTYPE B

5.1 Introduction…….....53
5.2 Results…….....55

CHAPTER SIX– DISCUSSION

6.1 *Kannemeyeria simocephalus*
6.1.1 Comparative Analysis……..58
6.1.2 Diagnosis of *Kannemeyeria simocephalus*…..……..65
6.2 Morphotype B
6.2.1 Comparison with *K. simocephalus.*…….....66
6.2.2 Comparison with African Triassic dicynodonts...……..71
6.2.3 Comparison with New World Stahleckeriids…….73
6.3 Comparative Functional Morphology
6.3.1 Comparative Functional Morphology……..75
6.3.2 Comparative Muscle Architecture……...76

6.4 Phylogenetics

6.4.1 Relationships of *K. simocephalus* and Morphotype B……85

Wits ETD

6.4.2 Palaeobiogeography Implications……...89

6.5 Possible Identification of Morphotype B……...90

CHAPTER SEVEN – CONCLUSION…….....92

CHAPTER EIGHT– REFERENCES…….....97

APPENDIX A
Plates and Figures of *K. simocephalus*……105

APPENDIX B
Plates and Figures of Morphotype B…….....125

APPENDIX C
Comparison of Morphotype B with *K. simocephalus*……138

APPENDIX D
Comparison of Morphotype B with other Triassic dicynodonts……143

APPENDIX E
Material of Uncertain affinity.....…… ....…….…..…….151

APPENDIX F
Comparative Muscle Architecture of *K. simocephalus* and Morphotype B..….....153

APPENDIX G
Phylogenetics……...158

APPENDIX H
Articulating surfaces of the long bones *K. simocephalus* and Morphotype B……174

Wits ETD

CHAPTER ONE

INTRODUCTION

1.1 General Introduction

Dicynodonts are a diverse group of non-mammalian synapsids that range in age from the Middle Permian to the Late Triassic and show a specialisation for herbivory (Angielczyk 2001; King 1990a). Dicynodonts rose to be the dominant herbivorous fauna during the Late Permian (King 1990a). During the Late Permian and Triassic they had a world wide distribution (Angielczyk 2001; Cox 1998; Lucas & Wild 1995; King 1990b), particularly during the Middle Triassic (Lucas & Wild 1995).

During the Late Permian dicynodonts are known from Africa, China, Russia and western Europe (King 1990a) as well as more recently India (Ray 2001), Laos (Battail *et al* 1995), Madagascar (King 1992; Mazin & King 1991) and South America (Barbarena *et al.* 1985). The mass extinction at the end of the Permian resulted in a great reduction in the number of dicynodont genera (Cox 1965; King 1990a). Even though dicynodonts staged a recovery in the Middle Triassic their diversity was considered to be low (King 1990c). More recent discoveries, however, (e.g. tuskless *Kannemeyeria* Renaut *et al* in press) might show that dicynodont diversity was greater than previously thought (Renaut pers comm.).

The study of dicynodonts has shown that they are of use in ecological reconstructions, biostratigraphic correlations and in the development of global biochrons. In South Africa their remains are estimated to be ten times that of the contemporaneous carnivores, which has been used as a component of the ecological evidence that they were the primary consumers (Rubidge & Sidor 2001; King 1990b). South Africa has the most complete and best exposed Early Triassic terrestrial sequence (Hancox 2000), which along with the Pangaean-wide distribution of dicynodonts during the Triassic (Lucas & Wild 1995) allowed Lucas (1998) to establish eight temporally successive land vertebrate faunachrons which formed the framework for the correlation of nonmarine Triassic deposits.

Over the past century the majority of dicynodont studies have been based on cranial material. Although there have been a significant number of postcranial studies, including aspects of anatomy and functional morphology, however, the postcranial skeletons of this group of animals remain poorly known (Angielczyk 2001). More recent studies of Triassic

WITS ETD

dicynodonts have focused on taxa from Africa, China, India, China and South America and the detailed nature of some of these studies have allowed for the postcranial skeleton to be used in determining the relationships of Triassic dicynodonts (e.g. Cox 1965; Camp 1956) as well as in determining the evolutionary trends in the postcranial skeletons of Triassic dicynodonts (e.g. Surkov 1998a).

Even though the postcranial anatomy has been studied in a number of instances, there remains a lack of understanding of the morphology and evolution of the postcranial skeleton of dicynodonts (Surkov 1998a). Lucas and Wild (1995) also found that the taxonomy of dicynodonts is largely based on cranial morphology and this has made the precise identification of isolated elements very difficult. The cranial basis for dicynodont taxonomy is largely as a result of the lack of associated cranial and postcranial remains, along with early collecting concentrating on the skulls of these animals. Another consideration is the time it takes to excavate an entire specimen.

Recently there has been a need for a holistic approach to the understanding of the anatomy of dicynodonts, their lifestyle and relationships. This study focuses on the postcranial anatomy of *Kannemeyeria simocephalus*, currently the only medium to large dicynodont known from the middle part of the *Cynognathus* Assemblage Zone. *Kannemeyeria simocephalus* has been found to be restricted to the *Cynognathus* Assemblage Zone (subzone B) of South Africa. The re-evaluation of the cranial anatomy of *Kannemeyeria* (Renaut 2000) and the recognition of two African species of *Kannemeyeria* has rekindled an interest in the postcranial anatomy of *K. simocephalus* the South African species of *Kannemeyeria*. The need to re-examine the postcranial anatomy of *K. simocephalus* is also exacerbated by the conclusion of Renaut (2000) that stated that the cranial morphology of *Kannemeyeria* although specialised allowed it to be a generalist as far as the use of food source was concerned. This therefore removed the cranial morphology as a limiting factor both geographically and temporally.

Only one study, Pearson (1924b), attempted a detailed examination of the postcranial skeleton of *Kannemeyeria*. The material used in this study was incomplete and crushed so that some regions were reconstructed using small dicynodont material (Pearson 1924b). Cruickshank (1975) provided a brief description of the *Kannemeyeria* specimen at the East London Museum. During the years of collecting most of the material of medium to large

Wits ETD

dicynodonts collected in the *Cynognathus* Assemblage Zone has been assigned to *Kannemeyeria simocephalus*. In order to better understand the postcranial anatomy of *Kannemeyeria simocephalus* the material assigned to this taxon was re-examined.

1.2 Historical Review of *Kannemeyeria*

Weithofer (1888) described *Dicynodon simocephalus* based on an imperfect skull (HMV 8173) from the farm, Elliot (originally thought to come from the farm Dwasvlei), in the Aliwal North District. Broom (1899) described another species of *Dicynodon, D. latifrons*, which he considered to resemble *D. simocephalus*. Seeley (1908) further described the skull of a dicynodont from the Karoo that had two tusks or canines like *Dicynodon*. He felt that the shape of the skull suggested the possible presence of a trunk; he therefore proposed the name *Kannemeyeria proboscoides*. Based on a large dicynodont skull form the Burgersdorp (Albert) district Jäckel (1911) described a new genus and species, *Sagecephalus pachyrhynchus*. Watson (1912) concluded that the skull of *Dicynodon simocephalus* was similar to that of *Kannemeyeria proboscoides* and thus referred *D. simocephalus* to *Kannemeyeria* and created the new combination *Kannemeyeria simocephalus*. Haughton (1915) described a smaller, but well preserved and complete skull and lower jaw and erected the species *K. erithrea* for it. Two years later, Haughton (1917) referred *D. latifrons* Broom 1899 to *Kannemeyeria* as *K. latifrons*.

Pearson (1924a) reviewed the early work that had been done on *Kannemeyeria*. She re-examined the specimens described by Seeley (1908), finding that only the features of the palate were clearly visible. She further found that the skull of *K. erithrea* (Haughton 1915) was very similar to *K. simocephalus* (Pearson 1924a). Pearson (1924a) also re-examined the skull of *Sagecephalus pachyrhynchus* Jäckel 1911 and concluded that it was the distorted anterior part of the skull of *Kannemeyeria*. Pearson (1924a) added to the list of characters originally proposed by Haughton (1915). Her second paper that year (Pearson 1924b) was a detailed description of the reconstruction of the *Kannemeyeria* skeleton at the British Museum of Natural History. Some of the bones were reconstructed using the bones of small Permian dicynodonts while the foot bones were few and poorly preserved

WITS ETD

(Pearson 1924b). Pearson (1924b) concluded that from the shape of the feet they were more than likely used for digging.

In 1935 Broom helped identify a skeleton, which consisted of the skull, lower jaw, six vertebrae, partial femur and tibia, fragments of the left pectoral girdle, ribs and humerus, was excavated and brought back to the East London Museum (Courtney-Latimer 1948). It was identified as a new species of *Kannemeyeria*, *K. wilsoni* by Broom (1937). According to Broom (1937) this new species was distinguished by its pointed and flatter beak, in having flatter nasals than *K. simocephalus* and in that the tusks were directed further forward. This specimen was unique at the time because it was the first near complete specimen of *Kannemeyeria*. Broom (1937) also reviewed the genus *Kannemeyeria* and pointed out that in 1932 he considered that *K. proboscoides, Sagecephalus pachyrhynchus* and *K. erithrea* belonged to *Kannemeyeria simocephalus*, but defended his species *K. latifrons*. After reviewing the existing species of *Kannemeyeria* Camp (1956) erected a new species based on a well preserved skull and lower jaw from the farm Bethel, *K. vanhoepeni*.

Cruickshank (1965) described another specimen (UMZC T757) of *K. latifrons* from Tanzania. The weakly developed tusks, the thinness of the bones, little fusion of the postorbital-jugal junction, the displacement of the occipital bone and the small size of the skull led him to the conclusion that this was a juvenile specimen (Cruickshank 1965).

In 1966 Bonaparte described a new kannemeyeriid from Argentina, *K. argentinensis,* which he considered showed a number of affinities with *K. erithrea*. Roy-Chowdhury (1970) described a large dicynodont from India, *Rechnisaurus cristarhynchus*, which superficially resembled *Kannemeyeria*. The presence of distinctive cranial features (Roy-Chowdhury 1970) suggested that it belonged to the family Stahleckeridae, and was therefore not a close relative of *Kannemeyeria*. In the same year Crozier (1970) described two new dicynodonts specimens from the N'tawere Formation of the Luangwa Valley, Zambia, as *R. cristarhynchus* and a new species, *K. latirostris*. *K. latirostris*, being a small kannemeyeriid that showed a number of differences that distinguished it from other species (Crozier 1970).

Wits ETD

Cruickshank (1970) reviewed the taxonomy of the genus *Kannemeyeria*, and re-examined the type species assigned to *Kannemeyeria*. This investigation led him to synonymise *"D." simocephalus, "D." latifrons, K. proboscoides, Sagecephalus pachyrhynchus* and *K. erithrea* with *K. simocephalus* (Cruickshank 1970). He considered *K. wilsoni* as the most complete skeleton of *Kannemeyeria* known, and because of differences in cranial morphology retained it as a separate species, but noted the possibility that it was a female of the species *K. simocephalus* (Cruickshank 1970). *K. argentinensis* and *K. latirostris* were also retained as separated species (Cruickshank 1970). Since only the specimens assigned to *K. erithrea* had reliable locality information, and was complete and undistorted, Cruickshank (1970) used this skull to redefine the genus *Kannemeyeria*. Cruickshank (1970) recognised that "*K.*" *vanhoepeni* resembled *Placerias* and therefore erected the new genus *Proplacerias* (Cruickshank 1970). After re-examining a cast of *Placerias* Cruickshank (1972) found that *Proplacerias* actually more closely resembled *Kannemeyeria* and he considered that it most likely another specimen of *K. wilsoni* (Cruickshank 1972) which made it the only specimen (other than the type) referred to *K. wilsoni*.

Keyser (1973) described a specimen of *K. simocephalus* (GSPR 313) from the Omingonde Formation of Namibia. From the same beds he also recognised the skull of a new dicynodont, *Dolichuranus primaevus,* which was found to be very similar to *K. latirostris* (Keyser 1973). This investigation prompted Keyser (1973) to refer *K. latirostris* to *Dolichuranus*. A further investigation of the evolutionary trends in Triassic dicynodonts led Keyser (1974) to conclude that the specimen of *Rechnisaurus* from the Yerrapalli Formation of India (Chowdhury 1970) and the one from the N'tawere Formation of Zambia (Crozier 1970) were similar to *Kannemeyeria*. He therefore suggested that *Rechnisaurus* should be placed in the Kannemeyeriidae and doubted that the generic distinction could be upheld.

Cruickshank (1975) briefly described the postcranial skeleton of *K. wilsoni*, which he concluded was not very different from that of the specimen described by Pearson (1924b). Kitching (1977) reviewed the known specimens of *Kannemeyeria* and he concluded that the variation in the skull morphology was due to age, sexual dimorphism and distortion, and that this had resulted in the identification of the five species of *Kannemeyeria*

Wits ETD

(Kitching 1977). Kitching (1977) therefore thought it reasonable to accept that there is only one species of *Kannemeyeria*, *K. simocephalus*.

Keyser and Cruickshank (1979) also compared *K. simocephalus* from Namibia with the Zambian specimen of "*Rechnisaurus*", and both of these with *Kannemeyeria* specimens from the Beaufort Group (Keyser & Cruickshank 1979). Keyser and Cruickshank (1979) found that the specimens from Namibia (R313), and Zambia (BP/1/3638, *R. cristarhynchus*), were similar to each other, but differed from the *Kannemeyeria* specimens from South Africa. They therefore felt that these two specimens represented a different species of *Kannemeyeria*, *K. cristarhynchus* Roy-Chowdhury 1970. Keyser and Cruickshank (1979) concluded that *Rechnisaurus* was indistinguishable from *Kannemeyeria* and that it was an "offshoot" of *Kannemeyeria*, and they also upheld Keyser's (1973) inclusion of *K. latirostris* in the genus *Dolichuranus*. A list of characters that unified Triassic dicynodonts was provided, and *Kannemeyeria* retained their characters 1 to 6 and 9 to 13 (p97), which are considered pleisomorphic, while other Triassic dicynodonts had more derived characters, thus making *Kannemeyeria* the "oldest" (*sic* Keyser & Cruickshank, 1979) known Triassic dicynodont, according to them. However, it should be noted that although *Kannemeyeria* has a number of pleisomorphic characters this has a bearing on its phylogenetic status and not on its temporal position. Keyser & Cruickshank 1979 suggested that *Kannemeyeria* is the genus against which all other Triassic dicynodonts should be compared, however, with more information being made available about previously not well know Triassic dicynodonts this statement will need to be re-evaluated.

Cheng (1980) described a kannemeyeriid from China, *Shaanbeikannemeyeria*, which was found to share a number of features with *K. erithrea* as well as *Uralokannemeyeria* Danilov 1971, indicating a possibly close relationship between the three taxa (Cheng 1980). Cruickshank (1986) suggested a possible close relationship between yet another dicynodont genus, *Sangusaurus* Cox 1969 and *K. erithrea* and also stated that *K. argentinensis* was probably a juvenile *K. cristarhynchus*-like form (Cruickshank 1986). King (1988) reviewed the current work on the dicynodonts and placed *Kannemeyeria* in the tribe Kannemeyeriini. She considered *Rechnisaurus* as *incertae sedis* (King 1988). Bandyopadhyay (1989) re-evaluated the genus *Rechnisaurus* and concluded that the synonymy of *Rechnisaurus* with *Kannemeyeria* by Keyser and Cruickshank (1979) could

Wits ETD

not be accepted because their analysis was based solely on the Zambian specimen. A re-examination of the holotype by Bandyopadhyay (1989) showed that *Rechnisaurus* was distinct from other dicynodonts, but he agreed that it should be considered *incertae sedis* until more complete material is found. *Rechnisaurus* was again synonymised with *Kannemeyeria* by Lucas and Harris (1996) because they considered that the differences could be explained by species variation.

In the past *Kannemeyeria* was thought to range over the entire *Cynognathus* Assemblage Zone in South Africa (Keyser & Smith 1979). Hancox *et al*. (1995), however, noted that *Kannemeyeria* was limited to the middle part of the zone. Hancox (1998) found that *Kannemeyeria* was restricted to subzone B (Hancox *et al* 1995; Shishkin *et al* 1995) and that the lower limit of the subzone was marked by the First Appearance Datum (FAD) of *Kannemeyeria*.

Lucas and Wild (1995) considered *Kannemeyeria* to straddle the Early –Middle Triassic boundary and defined a worldwide *Kannemeyeria* biochron. Their biochron (Lucas & Wild 1995), however, depends on the synonymy of *Rechnisaurus*, *Uralokannemeyeria* and *Shaanbeikannemeyeria* with *Kannemeyeria* and the presence of *Kannemeyeria* in South America. They believe that the difference between *Kannemeyeria* and *Rechnisaurus* can be explained by species variation (Lucas & Wild 1995). Renaut (2000) also questioned the validity of the species *K. argentinensis* and based on a re-examination of the holotype of *K. argentinensis* found that the resemblance to *Kannemeyeria* was as a result of distortion, and that the taxon should rather be included with the genus *Vinceria* Bonaparte 1967 (Renaut & Hancox 2001). This means that *Kannemeyeria* does not occur in Argentina; thereby weakening the case for Lucas and Wild's (1995) global *Kannemeyeria*-biochron (Renaut & Hancox 2001).

Renaut (2000) carried out an extensive study of cranial morphology of *Kannemeyeria*, in which he identified a number of diagnostic characters. This study also showed that the cranial morphology of *Kannemeyeria* was derived, and this study called into question the conclusion of Pearson (1924a) that *Kannemeyeria* showed only extreme advances over the "Lower Beaufort" dicynodonts. He also identified two skull types within the genus, and therefore only recognised two African species, *K. simocephalus* and *K. cristarhynchus*, which was supported by an allometric analysis (Renaut 2000). A final taxonomic clarification resulted in a new species *K. lophorhinus* being erected to accommodate the

Wits ETD

specimens referred to *K. cristarhynchus*, because the species name *cristarhynchus* was based on the Indian, *Rechnisaurus* material (Renaut et al. 2003).

During the course of the cranial study Renaut (2000) recognised a '*Kannemeyeria*-morphotype' that had palaeoecological implications, which meant it probably, occupied a wide range of habitats or niches. *Kannemeyeria* and the *Kannemeyeria*-ecotype were "ecological generalists" (Renaut 2000), and this pattern was present in diverse habitats geographically and temporally, which suggests that a specialised cranial morphology resulted in a generalist organism that was able to utilise all available resources in an effective manner. This eliminated the cranial morphology as a limiting factor, which would have limited *Kannemeyeria* middle part of the *Cynognathus* Assemblage Zone in South Africa.

An allometric analysis also led Renaut (2000) to include *K. erithrea* Haughton 1915, *K. latifrons* Broom 1899 and *K. wilsoni* Broom 1937 in *K. simocephalus*. The same analysis also showed that *K. erithrea* and *K. latifrons* were probably based on juvenile specimens of *K. simocephalus*.

More recently Renaut (2000) suggested that some of the Russian, Chinese and Indian Triassic dicynodonts may be accommodated within *Kannemeyeria*, which would give this taxon a wider geographic range and have implications for survival and migration of these animals. *Kannemeyeria* is of importance to the stratigraphy of the Karoo as it has considered an index taxon for the *Cynognathus* Assemblage Zone, and the stratigraphic range of *Kannemeyeria* has helped define subzone B (Hancox *et al* 1995). Although *Kannemeyeria* has been considered crucial to these various aspects, the postcranial anatomy is poorly known.

Wits ETD

CHAPTER TWO

MATERIALS AND METHODS

The following material formed the core specimens for the examination of the postcranial anatomy of *Kannemeyeria simocephalus*. Among the material previously identified as *Kannemeyeria* some were found to have a different morphology and were therefore treated separately and not included in the material of *K. simocephalus*. This material is referred to as Morphotype B. It must also be noted that by referring to material as a separate morph does not preclude it from being included in a single species as that species may consist of more than one structural form.

2.1 *Kannemeyeria simocephalus*

BP/1/5624

Since the holotype specimen of *Kannemeyeria simocephalus* (HMV 8173) has no associated postcrania, the descriptions of the postcranial morphology provided here are based on specimen BP/1/5624, a referred specimen (Renaut 2000). This skeleton was discovered by P. J. Hancox in 1994 and excavated during two field trips to the farm Bethel/Slootkraal. Where the bones are damaged and cannot provide any information, the specimen EL1 and BP/1/6160 were used to supplement the descriptions. BP/I/5624 is the possibly the second specimen to have a well documented provenance with an associated skull and lower jaw.

Locality: Bethel/Slootkraal, Rouxville District, South Africa. *Cynognathus* Assemblage Zone, Subzone B.

Preservation: The skeletal elements are well preserved, but all the bones have experienced some damage. The skeletal material consists of eight vertebrae, a number of rib fragments, all the elements of the forelimb, the scapula, the pelvic girdle and two elements of the hindlimb (femur and tibia). A closer examination of the material previously assigned to BP/1/5624 has shown it to represent three different individuals. The first is an adult (BP/1/5624), the second is another adult (renumbered BP/1/6104) and the third a very small individual (renumbered BP/1/6103). The material of the very small individual is

Wits ETD

fragmentary while the second adult is larger and the material consists of a complete but distorted right scapula, the right pubo-ischiadic plate and other fragments.

Distortion: Renaut (2000) notes that the left and right sides of the skeleton of BP/1/5624 showed different types of distortion. The distortion is more visible on bones of the girdles and limb bones. This is clearly evident in the femora. The left femur has been dorso-ventrally flatted so that the natural shape is exaggerated, while the right femur has been rolled and possibly compressed along the anterior and posterior margins. This compression has resulted in the shaft of the femur having a circular shape in transverse section. The scapulae from BP/1/5624 and BP/1/6104 also show different types of distortion; with the scapula of BP/1/5624 twisted so that the anterior dorsal end of the bone approached the distal end. The scapula of BP/1/6104 has been broken into a number of pieces which have been distorted individually so that they no longer fit together well. The ulna and radius have been medio-laterally flattened and the posterior surface of the radius is damaged.

BP/1/6160

In 2002 a new specimen of *Kannemeyeria* (BP/1/6160) was discovered on the farm Bethel/Slootkraal. Due to time constraints only the foot bones were collected during this fieldtrip. In August 2003 the remainder of the specimen was collected. It was discovered during the excavation that most of the skeleton caudal to the pectoral girdle was lost previously when a road was cut through the area. The head of this individual plunged into the hill, therefore only the pectoral girdle, some vertebrae, the forelimbs, and the skull and lower jaw could be collected.

Locality: Bethel/Slootkraal, Rouxville District, South Africa. *Cynognathus* Assemblage Zone (subzone B). This specimen (BP/1/6160) was found in a channel in green, sandstone with abundant rip up clasts. This specimen was orientated north-northeast to west-southwest.

Preservation: The body of this specimen (BP/1/6160) was preserved such that it listed to the right, so that the bones of the left side lay slightly higher than those of the right. The forelimbs are sprawled and lay so that the posterior surface was visible. On the left, the olecranon of the ulna is directed up the hill while the radius lies diagonally beneath it. The

Wits ETD

humerus forms an angle of 45° to the ulna with its head directed towards the midline of the body. Due to the listing of the fossil to the right, the left scapula, which was associated with a clavicle, lay above the humerus.

On the left, the scapula was preserved in a horizontal position, while the right scapula was preserved in a vertical position, which may even be the life position. In the middle of the specimen a large block of matrix was collected that lay below the left scapula. Preparation of this large central block has thus far delivered part of the precoracoid, parts of the left and right clavicles, as well as possibly part of the interclavicle. A dorso-ventrally flattened skull and the anterior cervical vertebrae were also found in association with the pectoral girdle and forelimbs, however, the cervical vertebrae remain attached to the skull which is still being prepared.

SAM-PK-3017

This specimen consists mainly of a skull and a series of vertebrae. There are fragments of other bones.

Locality: Winnaarsbaken, Burgersdorp District, South Africa. *Cynognathus* Assemblage Zone (subzone B).

Preservation: The material is well preserved and shows details of the bone morphology. However it must be noted that although the vertebrae might form a sequence there is no point of reference as to its position in the vertebral column.

ELM 1

This specimen consists of a skull and a number of postcranial elements which includes vertebrae, ribs, scapulae, coracoid plates, clavicles, sternum, humeri, radii, ulnae, pelvic girdles, femora, tibia and fibulae. The material that has been mounted belongs to a single specimen according to Courtney-Latimer (1948). This mounted specimen was used to augment the description of BP/1/5624.

Locality: Losberg Mountain on the farm ‘Ravenskloof’, Tarkastad. *Cynognathus* Assemblage Zone (subzone B).

Wits ETD

Preservation: The material is well preserved and shows details of the bone morphology. The shape and position of the articulating surface of the acetabulum of ELM 1 suggests that it does not conform to what is expected for *Kannemeyeria simocephalus*. In ELM 1 the lower forelimb, i.e. radius and ulna, are significantly different from that of BP/1/5624 and BP/1/6160. It is therefore considered best that at this juncture that these elements be considered as material of uncertain affinity until further collecting is undertaken.

2.2 Morphotype B

BP/1/994

This specimen consists of a complete scapula, a femur, and the proximal and distal ends of the lower forelimb bones. The specimen belongs to a medium sized animal.

Locality: Winnaarsbaken, Burgersdorp District, South Africa. *Cynognathus* Assemblage Zone (subzone B).

Preservation: The skeletal elements are well preserved. The scapula is complete and has suffered no distortion or damage. Unfortunately, the lower forelimbs are only represented by the ends of the bones. The femur is well preserved but the shaft has been sectioned for use in a histological study (Chinsamy & Rubidge 1993).

BP/1/3518

A complete, well preserved left femur.

Locality: Winnaarsbaken, Burgersdorp District, South Africa. *Cynognathus* Assemblage Zone (subzone B).

Preservation: A closer examination of the femur shows that the distal end of the bone has been slightly affected by distortion. The dorsal surface of the distal articulating condyles has been flattened slightly. The dorsal surface of the anterior condyle is also flattened and

Wits ETD

its concavity is exaggerated, while the ventral surface of the distal condyles has been damaged.

BP/1/1669

After examining this specimen two large individuals were identified, however, they have not been separated into two separate specimens. One is represented by both cranial and postcranial material and has been identified as *K. simocephalus*. Mixed in with this large specimen of *K. simocephalus* are postcranial remains that do not conform to the known characteristics of *K. simocephalus*. These postcranial elements are that of a large dicynodont.

Locality: Grootdam, Burgersdorp District, South Africa. *Cynognathus* Assemblage Zone (subzone B).

Preservation: The large specimen is represented by a scapula and coracoid plate, which are damaged and slightly flattened. These bones, however, are still articulated. The glenoid is complete and its articulating surface is clearly visible. There are also a number of foot bones, however, it has still to be determined to which specimen they belong.

SAM-PK-11262

The specimen was originally assigned as undetermined dicynodont material. This specimen consists of a proximal and distal end of a femur.

Locality: Winnaarsbaken, Burgersdorp District, South Africa. *Cynognathus* Assemblage Zone (subzone B).

Preservation: Only the proximal and distal ends of the femur have been preserved. Although the shaft has been lost, the remaining parts of the femur have suffered no discernible effects of distortion. The features present on the proximal and distal ends are clearly visible.

WitsETD

SAM-PK-1073

This specimen consists of at five boxes of material. This specimen is currently identified as *Kannemeyeria simocephalus*. An examination of the material has led to the conclusion that this specimen also belongs to the second morphotype.

Locality: Aliwal North, Burgersdorp District, South Africa. *Cynognathus* Assemblage Zone (subzone B).

Preservation: This material consists mainly of fragments; however, the proximal end of the ulna is used in the description of this animal. The material consists of the proximal and distal ends of long bones. There are also fragments of cranial material which may have the potential to eventually can confirm the taxonomic identify the second morphotype.

2.3 Methodology

The medial surface of the scapula of Morphotype B (BP/1/994D) was covered by plaster and the lateral surface was covered by a thin a layer of matrix. These were removed mechanically using an air scribe. Matrix was removed from BP/1/3518 to make the distal end of the dorsal surface more clearly visible. The plaster was also removed from the humerus of Morphotype B (BP/1/994A) along with matrix.

The comparison of Morphotype B with *Zambiasaurus* and *Angonisaurus* are based on the photographs of the original material taken by Dr P. J. Hancox. *Angonisaurus* material (BP/1/5531) collected and housed at the BPI (Palaeontology) was also used in the analysis.

Photographs of the material were taken using a digital camera. The photographs were corrected for the purpose of drawing Adobe Photoshop™. Adobe Illustrator™ was used to trace the photographs, and guidelines were drawn marking the fossae, sulci and ridges.

WITS ETD

2.4 Phylogenetics

Based on the analysis of gross morphology, two morphotypes have been identified in the *Cynognathus* Assemblage Zone (subzone B) of South Africa, viz. *K. simocephalus* and Morphotype B. The lack of cranial material means that Morphotype B remains unidentified at this time therefore a preliminary phylogenetic analysis was undertaken to determine the relationship between these two forms.

As the current study does not include a cranial analysis, rather than replicate the process it was decided to use the data matrix of Vega – Dias *et al* (2004) because the analysis included both cranial and postcranial characters. No changes have been made to their coding for the cranial and postcranial characters of a number of taxa. The following taxa have been included in the current analysis: *Shansiodon, Tetragonias, Wadiasaurus, Parakannemeyeria, Sinokannemeyeria, Angonisaurus, Stahleckeria, Ischigualastia, Jachaleria, Dinodontosaurus, Placerias, K. simocephalus* and Morphotype B.

The current study focused on the postcranial anatomy of *K. simocephalus* therefore the postcranial characters of Vega – Dias *et al* (2004) for *Kannemeyeria* were re-coded. Twelve new postcranial characters were included in this analysis. This was done to aid in determining the relationship between *K. simocephalus* and Morphotype B, because Morphotype B consists of only postcranial material. Character 27 (Vega – Dias *et al* 2004) was modified (Appendix G).

Coding of the additional characters was based on the literature and is therefore highly suspect: Yeh (1959) for *Shansiodon*, Cruickshank (1967) for *Tetragonias*, Bandyopadhyay (1988) for *Wadiasaurus*, Sun (1963) for *Parakannemeyeria* and *Sinokannemeyeria*, Cox and Li (1983) and BP/1/5531 for *Angonisaurus*, Cox (1965) for *Ischigualastia* and *Dinodontosaurus*, Camp and Welles (1956) for *Placerias* and Vega – Dias and Schultz (2004) for *Jachaleria*.

This phylogenetic analysis was based on 56 characters (Table 1; Appendix F). The analysis was performed using Paup 3.1.1 for Macintosh. A heuristic search using random stepwise addition (20 replicates) was performed and characters were optimised using DELTRAN. The bootstrap analysis was carried out using a heuristic search with 500 replications with

WitsETD

random replicates set at 20. In addition an analysis was performed using only the postcranial characters. This involved a general heuristic search that found the minimum number of trees. The trees were rooted using *Dicynodon trigonocephalus* as the default outgroup. The multistate characters were unordered except for the modified character 27 which was ordered. The taxon *Dinodontosaurus* has been considered problematic because it is considered to consist of more than one taxon therefore analysis was performed which excluded this taxon.

2.5 Aims

Renaut (2000) concluded that although *Kannemeyeria* has an advanced cranial morphology, it was an ecological generalist which allowed *Kannemeyeria* to exploit any food source. It therefore implies that *Kannemeyeria* was capable of entering and surviving any habitat, however, according to Hancox (2000; 1998) *Kannemeyeria* was restricted to the *Cynognathus* Assemblage Zone (subzone B) in South Africa. This again brought to the fore lack of knowledge of the postcranial anatomy of *Kannemeyeria*. The main aim of this project was to describe the postcranial anatomy of *Kannemeyeria simocephalus,* South African species, and to determine if the postcranial skeleton of *K. simocephalus* had any diagnostic features that would set it apart from other Triassic dicynodonts.

In South Africa *K. simocephalus* is the only medium to large known from *Cynognathus* Assemblage Zone (subzone B) and therefore all isolated postcranial material has been assigned to this taxon. In order to make this a significant investigation of the postcranial anatomy of *K. simocephalus* the isolated elements were included in the study. The isolated elements were included in the study because even though there 350 or more *Kannemeyeria* skulls in collection world wide there are few postcranial skeletons. A detailed analysis of the isolated elements would also give an indication if they had a morphology that was different from that of *K. simocephalus*.

A phylogenetic analysis was to be undertaken to determine if *K. simocephalus* would nest within the Triassic dicynodont clade. This analysis would also give some indication as to

WITS ETD

whether *K. simocephalus* and Morphotype B would nest in the same clade or in different clades among the Triassic dicynodonts.

Wits ETD

CHAPTER THREE

DESCRIPTION OF THE POSTCRANIAL ANATOMY OF *KANNEMEYERIA SIMOCEPHALUS*

3.1 General Introduction

As has already been noted in the introduction there have only been two studies that have focused on the postcranial skeleton of *Kannemeyeria* (viz. Pearson 1924b; Cruickshank 1975). The most serious problem faced by Pearson (1924b) was that there was serious damaged to the bones caused by crushing while Cruickshank (1975) provided only a brief description of what was considered a fairly complete specimen. Since this time *Kannemeyeria* was not studied in any detail until Renaut (2000) undertook a detailed analysis of the cranial morphology and the taxonomy of *Kannemeyeria*.

In the past one of the problems with the postcranial material has been poor preservation, however, recent collecting efforts has provided more complete and well preserved material. A large proportion of the material is made up of isolated material that has been collected over the years. All of which have been assumed to be *Kannemeyeria* based on previous knowledge of the biozone and *Kannemeyeria* itself. The inclusion of isolated elements in this study presented a new set of problems. Preliminary visual examination of all material currently assigned to *Kannemeyeria simocephalus* raised a number of questions about the identification of the isolated material. This once again brought fore the current understanding of postcranial anatomy of dicynodonts.

This resulted in greater discrimination in the choice of material used in the study and reduced the number specimens to those that included only postcranial material associated with known *K. simocephalus* cranial material. It must be noted at this point that although there may be postcranial material assigned to *K. lophorhinus* it remains undescribed and due to the questions raised about what is currently understood by *K. simocephalus* this material was not included in the current study.

The uncertainty about what the postcranial skeleton of *K. simocephalus* looks like has lead to a renewed interest in the postcranial anatomy. Material described by Pearson (1924b) and Cruickshank (1975) were also re-examined. The Pearson material was only examined

Wits ETD

by way of photographs while ELM1 described by Cruickshank (1975) was examined in person as these two works have formed the basis of all work done on *Kannemeyeria*. Re-examination of the pictures of the scapula, ulna and femur described by Pearson (1924b) has raised questions about this material being included in *K. simocephalus*. Only the pelvic girdle and lower forelimb of ELM1 appear to be of uncertain affinity.

3.2 Pectoral Girdle

3.2.1 Scapula

The scapula of *Kannemeyeria simocephalus* (figure 1a; plate 1a) is a long and gracile bone that is laterally convex. Anteriorly and posteriorly the margins of the scapula blade are straight and the scapula blade is broad antero-posteriorly. Dorsally, the blade forms a broad border. Approximately a third of the way below the dorsal border there is a scapula spine that projects beyond the anterior border, and is continuous with the proximal margin of the triangular acromion. Below this the scapula widens distally to form the glenoid facet posteriorly, and the coracoid plate articulation anteriorly. Between these articulations, at the anterior edge of the glenoid, the distal end of the scapula projects slightly ventrally.

Dorsally, the scapula blade is antero-posteriorly expanded to form a thin, wide margin (figure 1a; plate 1a). The dorsal margin projects beyond the anterior and posterior borders of the scapula blade on the right scapula of ELM1, whereas on the left it does not project beyond the anterior and posterior border. In the small individual (BP/1/6160) as well as the large individual (BP/1/5624) the proximo-posterior part of the scapula blade projects posteriorly. Below this the blade of the scapula is antero-posteriorly narrow, however, the width of BP/1/5624 is wider than that of ELM1 (plate 1a (iii)) and BP/1/6160 (plate 1a (ii)).

About a third of the way below the dorsal border the scapula spine begins (figure 1a; plate 1a). The scapula spine of the two small individuals is not very prominent and is very low (plate 1a (ii & iii). It does not extend far anteriorly in these small individuals, and its distal extent is marked by a raised area in BP/1/6160. The base of the scapula spine is marked by a prominent ridge on the lateral surface of the scapula blade in ELM1 and BP/1/5624. In

WitsETD

BP/1/5624 the spine is raised and directed antero-lateral so that it extends over the anterior margin thereby forming a groove (prespinous fossa *sic* Cruickshank 1975) between itself and the anterior margin (figure 1a; plate 1a). The surface of this groove is concave; however, the length and shape of the groove would suggest that it is more likely that a muscle passed along the groove. Distally, the scapula spine is continuous with the proximal margin of the acromion in BP/1/5624and ELM1 while in BP/1/6160 its distal end is marked by the raised oval tuberosity. The tuberosity is directed proximo-anteriorly and the surface is covered by striations and is visible on the medial surface. Below this the anterior part of the scapula is damaged in the smaller individuals (BP/1/6160 & ELM1).

In both BP/1/5624 and BP/1/6160 the acromion is broken anteriorly, while on the right scapula of ELM1 the acromion is triangular and directed slightly antero-laterally. It is proximo-distally narrow with a flattened anterior surface that is broad and convex distally, and concave proximally. The slightly concave lateral surface of the posterior end of the acromion of the large individual is limited posteriorly by a ridge, and is covered by striations. Distally, the acromion of ELM1 merges with anterior edge of the glenoid on the lateral surface of the scapula. Below the acromion of ELM1 the lateral surface of the glenoid is concave, and this concavity extends proximally to the distal end of the groove between the scapula spine and the posterior border.

The posterior border of the scapula of *K. simocephalus* is straight and projects posteriorly just below the dorsal border (figure 1a; plate 1a). In *K. simocephalus* the proximal half of the posterior margin is thin, but it becomes thick and flat distally. Distally, on the posterior border of the large individual (BP/1/5624) towards the lateral surface is a small, oval tubercle. On the small individual (ELM1), however, the origin of the scapula head of the triceps is a small round tubercle. In BP/1/6160 there is a broad rugose area fir the origin for the scapula head of the triceps rather than a tubercle as in other two individuals. The surface is rugose and it extends almost to the medial border. Although in ELM1 and BP/1/5624 the origin of the scapula head of the triceps ends as a tubercle the base of this tubercle is broad and extend over the same area as in BP/1/6160. BP/1/5624 has been affected by distortion but on ELM1 the base of the tubercle extends onto the lateral surface of the distal end.

Wits ETD

Distally, the scapula blade widens below the acromion to flare in ELM1 and BP/1/6104. Here it consists of the coracoid and glenoid articulation (figure 1b; plate1b). In the small individual (BP/1/6160) distortion has resulted in the distal end of the scapula being twisted so that the coracoid articulation is directed medially. In ELM1 and BP/1/6104 the distal end is antero-posteriorly wide, with the coracoid articulation directed anteriorly. In front of the glenoid facet the bone extends slightly ventrally beyond its anterior edge. In ventral view this extension ends as a round, thick and convex surface, and it is limited to the lateral side of the glenoid (figure 1b; plate 1b). The glenoid is set at an angle to the coracoid articulation and the presence of the ventral extension gives the ventral end of the bone a V-shape. It is directed postero-ventrally and has a wide, circular concave surface, which is limited by a rim that becomes flat anteriorly.

Medially (figure 2; plate 2), the surface of the scapula blade is only slightly concave. In the small individual (BP/1/6160) the anterior margin passes close to the tubercle that marks the distal extent of the scapula spine. In both the large (BP/1/5624) and small individual (BP/1/6160) the anterior margin extends down the medial surface and forms the posterior border of the acromion process. The tubercle that forms the distal extent of the scapula spine on BP/1/6160, when viewed from the medial surface, is located above the acromion on the left scapula, while it is below the acromion on the right scapula.

In *K. simocephalus* (ELM1) the acromion's triangular medial surface is concave longitudinally. Its concave surface is deepest at its posterior border and becomes flat in an anterior direction. The anterior end is convex along the edges. On the proximo-posterior border of the acromion's medial surface is a broad triangular shaped tubercle (figure 2; plate 2) in BP/1/5624 and a smaller horse-shoe shaped tubercle in BP/1/6160 and BP/1/6104. The tubercle on ELM1 is low and the surface is very rugose with a concave ventral border. The surface of the tubercle is rugose and the dorsal border is 'concave' and forms a low ridge. On the medial surface the anterior border/margin extends below the acromion to end at the distal end of the scapula. On the medial surface of the coracoid articulation of the scapula there is a broad, shallow groove extends down the bone onto the medial surface of the precoracoid to the coracoid foramen (figure 2; plate 2).

Wits ETD

3.2.2 Precoracoid

Based on its presence in ELM1 *K. simocephalus* has a semi-circular precoracoid (Plate 3a). In ELM1 the bone is broken anteriorly and ventrally, which may be as a result of the thinness of the bone. Along the posterior border the precoracoid is fused with the coracoid. Although the contact is not very distinct the surface is slightly raised and thick. Dorsally, it forms a distinct suture contact with the scapula. The coracoid foramen is located in the proximo-posterior 'corner' close to the coracoid and glenoid. It is elliptical in the proximo-posterior to antero-ventral direction. The lateral surface of the precoracoid is concave in an anterior and ventral direction, resulting in the formation of two possible attachment sites. On the medial surface there is a groove at the proximal end of the coracoid foramen.

3.2.3 Coracoid

The coracoid (ELM 1) (Plate 3a) is almost sickle shaped and is thicker than the precoracoid. Most of the dorsal part of the coracoid is made up of the glenoid facet. The facet is triangular and faces laterally and very slightly posteriorly. Its surface is undulating and concave proximally, and is thickened at the distal end of the glenoid facet. The distal end of the glenoid facet is marked by a thin ridge and the surface below it is concave. Posteriorly, the coracoid tapers to a narrow rounded end that is thicker than the anterior end of the bone. It projects beyond the glenoid facet of the scapula. Laterally, the surface is concave and the ventral edge of the bone is thick posteriorly and thins in an anterior direction.

3.2.4 Clavicle

Study of ELM1 shows the clavicle (Plate 3c) is a thin bone that is expanded proximally and distally. Laterally, the head of the bone is thickened in the dorsal direction and the surface is rugose. The antero-lateral corner is round with a broad, shallow groove on the proximal end. Laterally, the surface of the shaft is slightly rugose and thick. Along the distal end of the clavicle is a broad, shallow groove. Proximally, along the medial surface of the clavicle the posterior border is thickened. In front of this the surface is concave forming a groove. The medial surface of the clavicle shaft is broad and concave. On the proximo-anterior corner there is an oval tubercle that projects above the surface of the

WitsETD

bone. The dorsal surface is convex. The posterior border is concave and has a bow-shape. Distally, the bone is broken but what remains show is that the bone is flat, broad and thin.

3.2.5 Sternum

The sternum (ELM 1; Plate 3b) of *K. simocephalus* is a thin, proximo-distally oblong and the anterior end has a thick, rugose surface. On the dorsal surface there are two tubercles and two grooves. The grooves are broad, shallow and are medial to the tubercles. Distally, the sternum is rounded. At the proximal end of the ventral surface there is an oval tubercle on either side. Lateral to the tubercle the surface is broad and concave, and this is only visible from the left.

3.3 Forelimb

3.3. 1 Humerus

In dorsal view the proximal expansion of the humerus of *K. simocephalus* is larger than the distal expansion (figure 3a; plate 4a). The head of the humerus of *K. simocephalus* (BP/1/6160 & BP/1/5624) is positioned anteriorly on the dorsal border and forms an inverted triangle. The head overhangs the dorsal surface and its articulating surface becomes flat distally (figure 3a; plate 4a). Below the head there is a broad, low ridge, which is more prominent in the large individual (BP/1/5624). There are concave surfaces anterior and posterior to the ridge, with the posterior narrower than the anterior. In the small individual (BP/1/6160) the surface posterior to and below the head is a shallow, concave fossa.

Dorsally, the proximal expansion of BP/1/5624 is almost triangular (plate 4a (i), whereas in BP/1/6160 the proximal expansion is rectangular (plate 4a (ii), and in ELM1 it is semi-circular (plate 4a (iii)). This may be an indication of individual variation but it could also relate to the age of the individuals. The proximal expansion is directed antero-ventrally terminating as the delto-pectoral crest, which is lower than the posterior border in BP/1/5624. In BP/1/6160 and ELM1 the proximal expansion is directed anteriorly and terminates as the delto-pectoral crest which is at the same level as the posterior border. The

WITS ETD

delto-pectoral crest of BP/1/5624 is short, broad and flared. The delto-pectoral crest of BP/1/6160 is long, broad and rectangular while in ELM1, although it is rounded anteriorly, it is still rectangular, and like that of BP/1/6160 is directed 90° to the shaft. On the dorsal surface of the delto-pectoral crest of the humerus of *K. simocephalus* is a very shallow fossa (figure 3a; plate 4a).

Proximally, the striations in the fossa are clearly visible on the large individual (BP/1/5624) and are parallel to each other following the long axis of the bone. At the posterior boundary of the fossa the striations form a diagonal pattern. The striations at the distal end are orientated at 90º to the horizontal and are close together. At the distal end the surface becomes rugose and slightly above this is an oval tubercle that has a rugose surface.

The proximo-posterior 'corner' of the humerus of BP/1/5624 and ELM1 (plate 4a (i) & (iii) projects beyond the posterior border and below this the posterior border is straight in all specimens of *K. simocephalus*. Posterior to the head is a broad, shallow groove that extends as far as the proximal end of the ridge below the head. At the proximo-posterior corner of the bone there is a narrow, oval tubercle that thins distally to form the posterior border. A third of the way below the dorsal border in BP/1/5624 there is a small triangular tubercle while in ELM1 it forms an elongated oval (figure 3a; plate 4a).

The broad proximal expansion narrows as it grades into the shaft of the humerus. In the smaller individual (BP/1/6160) the shaft is short and narrow while in BP/1/5624 and ELM1 the shaft is short and broad. On the posterior surface of the shaft a groove extends down the entire length of the shaft.

In BP/1/5624 the twist on the shaft has resulted in the ectepicondyle being directed dorsally therefore in dorsal view it is actually the anterior margin of the ectepicondyle that is visible. This margin is narrow and rectangular. Due to the ectepicondyle facing antero-dorsally and anteriorly in the two smaller individuals BP/1/6160 and ELM1 respectively the dorsal surface of the ectepicondyle is visible. On the dorsal surface the ectepicondyle projects above the surface as a round tubercle in ELM1 and BP/1/6160 while in BP/1/5624 it is flat.

WITS ETD

The distal articulating surface is visible when the humerus is viewed from dorsally. This articulating surface of the ectepicondyle is directed ventrally, but it extends onto the edge of the dorsal surface of the ectepicondyle where it is separated from the dorsal surface by a thin ridge. In BP/1/6160 the ectepicondyle is directed slightly antero-dorsally and is slightly elongated. The articulating surface is directed ventrally and is dorso-ventrally narrow. The ectepicondyle has a round tubercle that projects above the dorsal surface at it distal end.

Anteriorly, the margin of the delto-pectoral crest is antero-ventrally broad with the widest part distally in BP/1/6160 while in ELM1 the anterior margin is thin along the entire length, but it is slightly thicker distally. The distal end of the delto-pectoral crest of the small individual (BP/1/6160) is inclined towards the ventral surface. On the distal border of the delto-pectoral crest of BP/1/6160 and ELM1 is a small, oval tubercle that projects ventrally. In anterior view, the oval entepicondylar foramen enters the shaft at a shallow angle to the bone surface in the large individual (BP/1/5624) while the entepicondylar foramen is not visible in anterior view in the small specimen (BP/1/6160). The ridge above the entepicondyle foramen opening is directed toward the dorsal surface in BP/1/5624. The bone texture is rugose and the bone surface becomes slightly concave towards the dorsal surface. It is covered by striations that are directed towards the entepicondyle. At the distal end of the shaft, the bone surface dorsal to the articulation is slightly concave. In anterior view, in front of the capitulum, is an elongated, concave groove that extends as far as the ectepicondyle in the large individual (BP/1/5624). This groove is the only feature visible in the anterior view of the small individual (BP/1/6160) and it extends onto the anterior surface of the ectepicondyle, which projects ventrally and is round. In the large individual the ectepicondyle is smooth and almost glossy with striations that are close together, but at the distal end it becomes rugose where it reaches the lower part of the anterior extent of the articulation.

The ventral articular surface extends onto the anterior surface and its proximal border is a thin, undulating ridge. Due to the damage on the distal end of the humerus of the large individual part of the trochlea (ulna articulation) is lost, while the oval capitulum (radius articulation) has flattened articulation and is separated from the trochlea by a narrow, shallow groove (plate 34). The remains of the trochlea suggest that this feature was not very large, but like the capitulum it was raised above the surface of the bone, with a flat

articulation. In BP/1/6160 the capitulum is oval with a concavo-convex surface and the triangular, concave trochlea is slightly below the capitulum and closer to the entepicondyle. The groove separating the capitulum and trochlea in the larger specimen (BP/1/5624) is very distinct which would suggest that the articulating surfaces are separated whereas in the smaller specimen (BP/1/6160) the articulating surfaces grade toward the groove. It is therefore possible that the depth of the groove is an ontogenetic development.

In ventral view the proximal expansion is almost completely made up by the delto-pectoral crest and the biccipital fossa (figure 3b; plate 4b). The biccipital fossa of the large individual (BP/1/5624) and the right humerus of the small individual (BP/1/6160) is shallow, broad dorsally and narrows distally. In the small individual (BP/1/6160), however, the biccipital fossa is broad and square in the left humerus. Its posterior boundary is formed by a ridge in front of the posterior border, and distally it grades into the broad, thick shaft. Behind the posterior boundary of the biccipital fossa the bone slopes towards the posterior border. This surface is concave proximally and the parallel striations are directed towards the posterior border. The ventral surface of the delto-pectoral crest is covered by diagonally directed striations that are parallel to each other. On the distal end of the crest the surface is rugose and the striations appear to form whorls. The very short shaft is slightly narrower than the proximal expansion. Ventrally, the oval opening of the entepicondylar foramen is directed towards the posterior border of the humerus. It is surrounded by a thin ridge that becomes flat as it reaches the posterior border. The opening of the foramen makes a steep angle to the bone surface and maintains this steep angle as it passes through the bone. Above the opening of the entepicondylar foramen is a narrow, shallow groove.

The straight posterior border of the humerus passes onto the entepicondyle. On the proximal third of the humerus, below the dorsal border, there is a shallow groove, which becomes deeper as it reaches the proximal end of the entepicondyle. The groove is limited to the shaft of the humerus and is shallow in the small individual. A deep and triangular olecranon fossa occurs in front of this groove in the large individual while in BP/1/6160 a shallow concave, triangular olecranon fossa is located below this groove. It is, however, possible that the depth of the olecranon fossa in the large individual may be as a result of damage, because above the damaged area the surface is only slightly concave. The distal

Wits ETD

articular surface extends onto the posterior surface forming a very shallow and narrow fossa, just posterior to the ectepicondyle.

The ectepicondyle is larger than the entepicondyle and is dorso-ventrally thicker. Anteriorly, the ectepicondyle narrows to form a thin edge and its round articulating surface projects ventrally. It is also situated lower than the entepicondyle, and the direction of the striations suggests that growth of the ectepicondyle occurs in an antero-ventral direction. The entepicondyle is thinner than the ectepicondyle and does not project as far ventrally. Based on the examination of the material there is no ectepicondyle present.

3.3.2 Ulna

In lateral view the ulna of BP/1/5624 is antero-posteriorly flattened (figure 4a; plate 5a (i)) while that of BP/1/6160 is not as flat (plate 5a (ii)), even though it is antero-posteriorly expanded. It is broad proximally and narrows to form the shaft, which has the same width as the distal end. The proximal part of the ulna is triangular, and narrows to form the olecranon proximally in BP/1/5624 and BP/1/6160. The low olecranon is narrow and triangular with a round dorsal border in BP/1/5624 and BP/1/6160 (figure 4a; plate 5a; plate 35a). There is no evidence of a suture contact between the olecranon and the rest of the ulna.

The sigmoidal facet faces laterally and has slightly concave surface in BP/1/5624 and BP/1/6160 (figure 4a; plate 5a). In the middle of the sigmoidal facet the surface faces antero-laterally. Part of the articulating surface is directed ventrally and forward toward the anterior border. The sigmoidal facet projects laterally thus forming a thin ridge in BP/1/5624 and BP/1/6160. The surface of the sigmoidal facet in BP/1/6160 and BP/1/5624 is triangular and laterally broad. This lateral projection of the sigmoidal facet merges with the shaft below the distal end of the radial facet.

The radial facet (figure 4a; plate 5a) is located below the anterior border of the sigmoidal facet of the ulna, and forms an inverted triangle. The base is formed by the anterior border of the sigmoidal facet and it narrows distally and ends at the same level as the ridge on the lateral surface. The surface of the radial facet is concave along its entire length and rugose

WitsETD

proximally. Distally the surface is not deeply concave and is smooth. The anterior and posterior borders of the radial facet are sharply demarcated.

Distally, along the anterior border of the ulna of *K. simocephalus* is a shallow fossa that starts about halfway down the bone. It is elongated with its narrowest part proximally and widest distally. The entire surface is concave, but it is deeply concave distally. Its distal border is a round thin ridge. In BP/1/6160 the distal fossa does extend onto the medial surface while in BP/1/5624 it is limited to the anterior margin. On the lateral border of this fossa there is an elongated tubercle with a rugose surface. The position of this tubercle suggests that it may have been the attachment site for a ligament or ligaments. Posterior to the sigmoidal facet is a narrow, deep groove. In the middle of the shaft is a shallow fossa that extends to the postero-distal end and was separated from the anterior fossa by a narrow ridge.

The medial surface of the olecranon (figure 4b; plate 5b) is flattened postero-proximally with a raised rugose surface that extends from the olecranon, and is bound posteriorly by a ridge. A fossa occurs in front of the ridge, which is broad proximally, narrowing distally. A groove begins near the distal end of the fossa and extends to the distal end of the bone, where it ends as a deep depression. This groove most probably accommodated the tendons of muscles of the forelimb.

The distal articulation is directed ventrally and forms an elongated oval (plate 35c). Its surface is concave and broad posteriorly, while it is narrow anteriorly. The articulating surface extends onto the distal medial surface.

3.3.3 Radius

The radius of *K. simocephalus* is a slender bone that is essentially featureless except for the expanded ends and constricted shaft (figure 5a; plate 6a). Proximally, the expansion is slightly smaller than the distal expansion. The distal expansion is more flared than the proximal one.

In both BP/1/5624 and BP/1/6160 the proximal and distal articulating surfaces are narrow and concave (plate 35a & b). This narrow proximal articulation forms a continuous

Wits ETD

articulating surface with the sigmoidal facet of the ulna for the distal end of the humerus. Anteriorly, the proximal end has a straight margin which becomes concave along the shaft. Along the proximo-posterior border of the radius there is an oblong tubercle with a convex surface. The striations along the lateral surface of the tubercle suggest that its growth occurred in a proximal direction. This narrow, oblong tubercle forms the ulna articulation. Below this articulation the posterior border of the radius is concave. In the large and small specimens the posterior border is more concave than the anterior.

The distal end of the radius is marked by an undulating rim that projects more ventrally closer to the posterior border (plate 35b). Along the distal third of the anterior border there is a rectangular, medio-laterally and antero-posteriorly narrow tubercle. In BP/1/6160 this tubercle is very narrow when compared with the larger BP/1/5624. There is also a very low, round tubercle along the rim of the distal end of the radius. It is located more towards the middle of the rim in the large individual and closer to the posterior border in the smaller individual.

In medial view there is a groove close to the anterior border (figure 5b; plate 6b). This groove extends from below the proximal rim to a third of the bone length above the distal end. The groove is shallow and wide proximally, and narrows towards the distal end. Medially, the distal end is thickened towards the anterior border to form a wide, flattened surface. Although this surface narrows towards the posterior border it is still broad, however, in BP/1/6160 this part of the distal end is very narrow. This part of the rim in the small individual is also directed more proximally, which has made the distal articulating surface visible in medial view.

Wits ETD

3.4 The Pelvic Girdle

3.4.1 Ilium

In BP/1/5624 the dorsal border of the ilium is not preserved therefore the description is based on R3761. The dorsal border of the ilium (R 3761) is convex and is slightly lower towards the posterior border (plate 7b). Laterally, the surface of the blade is concave and the anterior process is directed laterally (BP/1/5624). The anterior process is short and

wide and is situated higher than the posterior one. It projects far in front of the pubis. The posterior process is located close to the acetabulum and its ventral surface is concave giving it a hook-like appearance. It is dorso-ventrally wide and short antero-posteriorly. Below the anterior process the anterior border of the ilium narrows gradually to form an almost straight border, while the posterior border narrows drastically resulting in a concave border. Anteriorly, the pillar like neck narrows more than posteriorly.

The medial wall of the acetabulum is lower than the lateral wall, and its ventral surface is rugose (plate 7b). The anterior two-thirds of the acetabular facet is separated from the posterior part by the supra-acetabular notch, however, the articulating surface remains continuous. The posterior part of the rim is narrow and sharply demarcated. The acetabulum is circular, broad, deep and faces laterally.

Dorsally, the acetabulum facet is bound by the supra-acetabular buttress. This buttress is narrow anteriorly and posteriorly, and broad in the middle. Two-thirds of the way up the posterior border of the supra-acetabular buttress is the supra-acetabular notch (plate 7a), which is narrow and deep in BP/1/5624. The anterior border of the ilium, above the acetabular facet and the dorsal part of the anterior border of the pubis is flattened with a roughened surface.

Anteriorly, on the dorsal border of the acetabulum, in front of the acetabular facet, is a facet for the pubis. This elongated and concave facet is located on the medial border. Behind the acetabular facet is a concave, almost square facet for the ischium, which is situated higher than the pubic facet. Medially the surface of the iliac blade is convex dorsally and becomes concave above the acetabulum. Although the bone has been damaged, five sacral rib facets are visible.

3.4.2 Pubis

The pubis and ischium are fused in *K. simocephalus* (plate 7b). This has resulted in the formation of the pubo-ischiadic plate. The left pubis of BP/1/5624 is broad proximally and narrows distally. Dorsally, the anterior part of the bone is higher and is directed more medially than posteriorly. The ventral part of the pubis is narrow, and the anterior part of the bone is directed more antero-ventrally. Anteriorly the pubis narrows to form a round

Wits ETD

tubercle that is directed anteriorly and ventrally. The lateral surface of the tubercle in BP/1/5624 is very rugose. Behind the tubercle the bone extends posteriorly towards the ischium. This part of the bone is thin and the surface is concave.

A small, oval acetabular facet is present on the dorsal surface (plate 7b). The surface of this facet is smooth and only slightly concave, and is continuous with the ischial facet. Laterally, the border of the facet is distinctly lower and the facet faces laterally. The medial wall of the pubic facet extends dorsally to meet the medial wall of the iliac acetabular facet. In front of the acetabular facet is the rectangular, convex facet for articulation with the ilium, which has a rugose surface that projects dorsally creating forming small pillars. This surface matches the surface of the facet anterior to the ilial acetabular facet. It would suggest that these bones interdigitate in order to form a secure join. Laterally, the surface below the articulation is rough and is covered by thin ridges. It narrows in the anterior direction to end in a round, concave facet that also has a rugose surface. Along the posterior border of the pubis there is a C-shaped groove that extends across the surface of the bone. It forms the sub circular anterior border of the obturator foramen.

3.4.3 Ischium

The ischium is triangular and is expanded ventrally (plate 7a & b). Dorsally, the ischial acetabular facet is elongated and has a slightly concave surface. It is separated from the rest of the bone by a ridge. The lateral wall of the facet is lower than the medial one, which rises to form a rugose dorsal border. Posterior to the acetabular facet is the facet that articulates with the ilium. It is a narrow, elongated triangle that has a convex surface. Anteriorly, the ischium meets the pubis below the acetabular facet to form the concave dorsal border of the obturator foramen (plate 7b). The short, concave, almost circular posterior border of the obturator foramen is formed by the ischium. In *K. simocephalus* the obturator foramen forms a narrow, elongated oval that is slightly wider towards the ischium (plate 7b).

Wits ETD

3.5 Hindlimb

3.5.1 Femur

The femur of *K. simocephalus* is a long, dorso-ventrally flattened (figure 6; plate 8) bone with a straight shaft that has concave anterior and posterior borders. The proximal and distal expansions are of equal width. It has been noted that the right femur of BP/1/5624 has been compressed antero-posteriorly which has resulted in the shape of the bone being completely different. As a result of this drastic change the right femur does not form part of this description (plate 8a (i) & (ii)).

The greater trochanter is elongated and extends along the proximal third of the posterior border of the femur and is almost straight (parallel to the long axis of the bone) (figure 6b; plate 8b (ii)). It is antero-posteriorly narrow with a rugose surface and is clearly demarcated from the rest of the bone. Dorsally, the greater trochanter is rounded and thick.

Distally, the articular condyles are separated by a circular intercondylar fossa (figure 6b; plate 8b (ii)). It is deep and is situated slightly above and between the proximal borders of the condyles. The posterior condyle's projection above the dorsal surface of the bone is round and is higher than the anterior condyle. It is directed more ventrally and is slightly lower than the anterior condyle. Postero-dorsally to the posterior condyle is a broad, shallow groove that terminates at the proximal end of the ventral border. The anterior condyle is smaller than the posterior condyle with its dorsal surface skewed in the proximal direction and it is rugose with pits. Distally, the condyles are separated by a broad, fairly deep groove which is steeper towards the posterior condyle.

The femoral head is round and medially inflected (figure 6a; plate 8a (ii); plate 36a(i)). In ventral view the head of the left femur of BP/1/5624 is surrounded by a shallow groove that is steep towards the head. This groove makes the head more prominent in ventral view. In front of the head is a shallow fossa that is broad proximally and narrows distally where it merges with the shaft. The posterior boundary is marked by the presence of the greater trochanter. Below the head of the bone is a low, flat ridge that extends to the posterior border. No internal trochanter is present.

WITS ETD

The ventral articulating surface is reflected on the distal end of the condyles (figure 6a; plate 8a (ii)). The articulating condyles are separated on the ventral surface by a broad, antero-posteriorly oblong fossa. This fossa has a shallow, concave surface that is bordered anteriorly and posteriorly by prominent ridges. It extends above the condyles to merge with the shaft above. Distally, the articulating surface of the condyles is directed ventrally and is convex. The articulating surface of the posterior condyle projects more ventrally than that of the anterior condyle.

3.5.2 Tibia

Only the right tibia of BP/1/5624 has been preserved (figure 7a; plate 9a). It has been 'rolled' and is antero-posteriorly compressed. Both the proximal and the distal ends are expanded with the proximal being larger than the distal.

Proximally, the *Tuberositas tibiae* faces antero-laterally (figure 7a; plate 9a). A round tubercle projects laterally from this surface and is bounded ventrally by a narrow ridge. The surface of the tuberculum is rugose and extends slightly medially. This surface is raised above the rest of the bone and grades down into the *Margo cranialis*. Anteriorly, the surface of the margin is broad and roughened.

Lateral to the *Tuberositas tibiae* is a shallow groove that extends halfway down the bone. It is narrow proximally where the *Tuberositas tibiae* projects over this groove and is bound by a lateral ridge. The lateral border of the tibia flares out and a shallow fossa is present below the proximal ridge, which represents the articulation for the fibula. Below this the bone has been damaged. Approximately halfway down the shaft there is a shallow fossa. Distally the bone curves laterally forming a ridge that gives the bone a squared off appearance. Anteriorly the shaft has lost all definitive features due to cracking and damage. Medially the bone was damaged resulting in the middle of the shaft being compressed.

The proximal end of the bone is round and higher anteriorly than posteriorly. It has a single slightly concave articulating surface. Posteriorly, the head is bound by a thick, flat ridge. This structure extends onto the posterior surface and has a roughened appearance. It merges with the surface, which grades into the shaft. Below this the bone is damaged.

WitsETD

Posteriorly, in the middle of the shaft, is a shallow fossa that has a surface texture that is rough. Distally, the concave surface of the shaft ends as a broad ridge above the articulating surface. The medial articulation is located more ventrally, has a round, convex surface that is directed ventrally, while the lateral articulation is squarish and directed ventrally with a flat to slightly concave surface.

3.5.3 Fibula

The fibula of *K. simocephalus* is along, thin bone and is represented here by ELM1 (plate 9b & c). Laterally, the border is only slightly concave while the medial border is straight. Proximally, the bone is expanded and a small, hemispherical tubercle rises above the surface. Along the lateral border of the distal expansion is a groove that extends to the distal end. Both the proximal and distal ends have convex surfaces.

3.6 Axial Skeleton

The axial skeleton of *K. simocephalus* is described from both isolated and associated vertebrae. Only the vertebrae are described here because the ribs are represented by fragments even though they are from a single specimen no complete rib could be pieces together. BP/1/5624 has eight vertebrae preserved but all have been damaged to some degree. The atlas is the best preserved while the remaining vertebrae are all damaged dorsally. The neural spine, transverse processes, prezygapophyses and postzygapophyses are no longer present.

SAM-PK-3017 has at least fifteen vertebrae preserved. The axis is complete and well preserved while the remaining vertebrae are mostly complete with a few that have suffered some damage. Structurally the remaining vertebrae are very similar which suggests that they may belong to the same section of the vertebral column, however, the lack of other associated vertebral columns does make it difficult to determine exactly where these vertebrae fit in. All the vertebrae are amphicoelous.

Wits ETD

3.6.1 Cervical Region

3.6.1.1 Atlas

In BP/1/5624 both sides of the atlas are preserved, but it has suffered some damage dorsally and posteriorly (plate 10a). The neural arches do not meet in the midline when viewed from dorsally. On the medial side of the neural arch are two concave facets (plate 11). These facets lie next to each other resulting in a 'butterfly' shape, but are separated by a flat, raised ridge. The postero-dorsal border of the posterior facet is higher than the antero-dorsal border, while the antero-ventral border is lower than the postero-ventral border (plate 11).

The anterior facet is deeply concave in the cranial direction and is C-shape (plate 11). It becomes raised in the medial direction towards in the middle of the bone. The ventral end of the ridge separating the two facets is very broad (plate 11). In the atlas the centrum is not fused to the rest of the atlas vertebral body.

3.6.1.2 Axis

The axis of *K. simocephalus* in SAM-PK-3017 is a well preserve, robust and relatively large bone (plate 10b (i)). The dorsally projecting neural spine is short, antero-posteriorly broad and is directed antero-ventrally. Anteriorly, the neural spine is thickened, is directed more anteriorly, and is lower than the posterior border (plate 10b (i)). When compared with the remaining vertebrae the axis is more gracile. In dorsal view the surface of the neural spine is rugose and is wide at its anterior and posterior ends.

In SAM-PK-3017 the prezygapophyses are small, flared and project slightly beyond the anterior end of the neural spine (plate 10b (ii)). It has a smooth, slightly convex articulating surface that is directed antero-dorsally. Posteriorly, the postzygapophyses are wide, and are in line with the posterior end of the neural spine (plate 10b (i & ii). The wide, smooth and convex articulating surface is directed ventro-laterally. On the axis the postzygapophyses are positioned closer together than the prezygapophyses. Close to the prezygapophyses, and below the level of the zygapophyses, lies the transverse process. It is short and becomes wider towards the free end (plate 10b (i & ii)). The transverse process is narrow, and is triangular with a rounded lateral tip.

Wits ETD

In lateral view the centrum is antero-posteriorly elongated with the posterior end larger and extending lower than the anterior end. Laterally, the surface of the centrum is concave and extends to the proximal end of the ventral keel (plate 10b).

The centrum of the atlas of *K. simocephalus* is not fused to the rest of the atlantal components. Instead it is fused to the axis forming the odontoid process (Romer 1956). In anterior view it is crescent shaped (plate 10b (ii)) with an incomplete dorsal border in *K. simocephalus* (SAM-PK-3017) with three possible articulating sites. Laterally on the odontoid process there are two oval flat to convex articulating facets, while the third articulating facet is situated ventrally and is laterally oval with a concave articulating surface. In anterior view the intercentrum of the axis is visible ventrally and is oval. When viewed laterally it is difficult to distinguish between the axis intercentrum and the odontoid process. Ventrally, the intercentrum is triangular when seen in lateral view (plate 10b (i)).

3.6.1.3 Post–axial Cervical Vertebra

BP/1/5624 has two vertebrae in articulation and from the form of the damaged neural spine the one is the axis. It is preserved in articulation with another vertebra, which due to its position can be assumed to be the first cervical vertebra. Due to the extent of the damage there are no details of the dorsal part of the vertebrae preserved. The centrum is antero-posteriorly elongated, narrow with no ventral keel.

3.6.2 Dorsal Vertebrae

The remaining vertebrae of SAM-PK-3017 have the similar morphology and are therefore considered to belong to the same section of the vertebral column. The neural spine is antero-posteriorly narrow, long and inclined posteriorly (plate 12a). It projects well beyond the posterior extent of the centrum. In dorsal view the surface of the neural spine is rugose and broad.

Anteriorly, the prezygapophyses are located well in front of the neural spine. The flat articulating surfaces face dorso-medially, and the distal ends of the prezygapophyses almost meet in the midline. This makes the articulating surface appear continuous and that

Wits ETD

it forms a cup or cradle for the postzygapophyses. The postzygapophyses are very short and do not extend beyond the neural spine in lateral view (plate 12a). The articulating surface is flat and directed ventrally, and almost meets in the midline.

The transverse processes are wing-like. They are short and are directed dorsally (plate 12a). The lateral ends of the transverse processes are thickened are have rugose surfaces. From dorsal view the surface of the transverse process is concave towards the body of the vertebra.

The centrum is antero-posteriorly short with deeply concave sides (plate 12a). Along the proximo-anterior margin of the centrum there is an elongated, concave facet that extends almost to the ventral end of the centrum. This facet most likely represents the articulation for the rib.

3.6.3 Caudal Vertebrae

There are four poorly preserved caudal vertebrae associated with BP/1/5624 (plate 12b). The neural spines are broken off dorsally. Although damaged the ventral surface of the centrum the presence of articulating facets on the ventral surface of the anterior and posterior ends of the vertebra suggests the possible presence of a haemal arch. The centrum is very short and round and there is no evidence that transverse processes were present (plate 12b). Laterally the centrum is concave. The neural spine of the smallest caudal vertebra is not completely fused to the rest of the vertebra.

Wits ETD

3.7 Functional Aspects of the Postcranial Skeleton of *Kannemeyeria simocephalus*

3.7.1 The Pectoral Girdle and Forelimb

The scapula blade of *K. simocephalus* is long, broad and straight with an antero-posteriorly expanded dorsal border. The blade is convex laterally while the acromion and scapula spine lie above the anterior border (figure 12; plate 1a). Posterior to the scapula spine there is a shallow fossa on the proximal lateral surface of the blade (figure 1a; plate 1a). The

acromion itself is directed away from the distal expansion of the scapula, in a lateral direction. This has resulted in a groove that passes from the acromion onto the lateral surface of the distal expansion, lying between the acromion and the anterior border (Plate 1a).

On the medial surface the scapula is slightly concave proximally forming a very shallow fossa. This fossa is elongated and its distal extremity is marked by a low ridge (figure 1b). The surface is covered by long, parallel striations and is smooth to the touch (figure 12). There is a horse-shoe shaped facet is present at the proximo-posterior end of the acromion. The surface of the facet is pitted and rugose, and is incomplete proximally resulting in a broad, shallow groove. Medially, the acromion surface is longitudinally concave (plate 2). Anteriorly, the shallow prespinous area is covered by thin, parallel ridges which would suggest that this was an area for attachment.

The posterior margin of the scapula has become flattened as far as the distal articulation. On this posterior margin close to the lateral surface is a small, round tubercle that has a rugose surface. It is located below the level of the distal end of the acromion. Distally, the scapula consists of the glenoid and the precoracoid articulation. In BP/1/6160 the glenoid facet is circular with a concave surface. The glenoid facet is directed postero-ventrally.

Laterally the surface of the precoracoid is concave in the anterior and posterior direction thus forming two possible attachment sites (plate 3a). The glenoid facet of the coracoid is triangular and faces slightly postero-laterally. Posteriorly, the coracoid tapers to a point that extends beyond the glenoid. The lateral surface of the coracoid is concave with the thickest part of the bone posteriorly.

Although the clavicle and interclavicle are described here, these descriptions remain tentative as these descriptions are based on a specimen that probably consists of elements belonging to both morphotypes. BP/1/5624, the specimen which forms the basis of the description of *K. simocephalus*, does not have these elements preserved and the material described by Pearson (1924b) has also been found to be a mix of both morphotypes.

WitsETD

The clavicle is a thin bone with expanded proximal and distal ends. Antero-laterally on the clavicle there is a broad, shallow groove. Laterally, the shaft is thick and rugose while medially the surface is concave. There is a tubercle on the proximo-anterior corner.

Anteriorly, the oblong interclavicle of *K. simocephalus* is thick and rugose (plate 3b). On the dorsal surface there are two tubercles and two grooves that lie medial to the tubercles. At the proximal end of the ventral surface there is an oval tubercle on either side of the surface and lateral to this the surface is broad and concave.

The humerus is a robust, stout bone in the large individual (BP/1/5624); however, in the small individual (BP/1/6160) the humerus is more slender and less robust. The degree of twist on the small individual is not as great as that seen in the adult specimen (plate 4a).

Anteriorly, the dorsal border merges with the delto-pectoral crest forming a rounded dorsal margin. The delto-pectoral crest is short, antero-posteriorly narrow and relatively thin. In BP/1/6160 the delto-pectoral crest is directed anteriorly, is antero-posteriorly shorter, being thicker dorso-ventrally (figure 3a; plate 4a. The dorsal surface of the delto-pectoral crest is concave, resulting in a shallow fossa with a smooth surface. Striations on the fossa surface form an irregular pattern. At the distal end of the delto-pectoral crest is an oval tubercle with a rugose surface. Below the proximal third of the humerus on the posterior surface is a small triangular tubercle that is surrounded by a groove. The shaft of the humerus of BP/1/5624 is twisted so that the ectepicondyle is directed dorsally, however, in BP/1/6160 and ELM 1 the twist on the shaft is such that the ectepicondyle faces anteriorly (plate 1a). As in BP/1/5624 there is a tubercle on the proximal part of the ectepicondyle in BP/16160. On BP/1/6160 there is a ridge that runs from the shaft onto the anterior border and ends at the ectepicondyle. The articulating surface of the distal articulation is directed ventrally and extends onto the ventral and slightly on the surface below olecranon fossa.

Ventrally, the proximal half of the humerus is made up mostly by the biccipital fossa. It is broad and not very deep but becomes deeper towards the posterior border. Proximally, the fossa is broad and shallow. In BP/1/5624 the delto-pectoral crest forms a shallow anterior border of the biccipital fossa while in BP/1/6160 it forms a steeper border. Its surface is covered by diagonal, parallel striations. On the posterior surface a shallow, elongated

Wits ETD

groove is present below the dorsal border and the concavity of the groove increases towards the entepicondyle. In front of this groove is the shallow triangular olecranon fossa.

The ulna does have a low ossified olecranon. It has a rugose surface. The sigmoidal face projects laterally but the proximal third of the bone is smaller in the new specimen. Another notable feature of the ulna is the ridge that projects laterally from the sigmoidal face. Proximally, along anterior border is the inverted triangular facet for the radius. Along the anterior border below the radial facet is an elongated concave facet that is deepest distally. On the lateral surface at the distal end of the facet is an elongated tubercle with a rugose surface.

On the proximo-posterior border of the radius is an oblong tubercle occurs with a convex surface that articulates with the ulna. Proximally, the articulating surface is concave while on the posterior surface the proximal articulation is thick, broad and flat. A shallow broad groove extends down the shaft on the lateral side of the radius possibly for the passage of tendons and blood vessels. Along the distal third of the anterior margin is a narrow, rectangular tubercle, which is distinctly different from that of the ulna articulation in that its margins are distinctly demarcated. The surface of the tubercle is rugose and convex.

3.7.2 Pelvic Girdle and Hindlimb

In *K. simocephalus* the iliac blade has a wide anterior process and narrow posterior one (plate 7a). The anterior process is positioned higher than the posterior one and the blade is fan-shaped, providing a large area for muscle attachment with the smooth and slightly concave lateral surface. Distally, the distance between the posterior process and the acetabular facet is smaller than that of the anterior process and the acetabular facet. Posteriorly, the dorsal border of acetabular facet is divided in two by a groove; however, the articulating surface is still continuous. The ilial acetabular facet is deep, large and faces laterally (plate 7a). Above the acetabular facet the anterior surface is concave. In front of the acetabular facet is the facet for the pubis, which is lower than that for the ischium. The anterior margin of the ilium in front of the pubic articulation forms a flattened facet with the distal end on the anterior border of the pubis.

Wits ETD

The pubo-ischiadic plate is shorter than the ilium (plate 7a). Antero-ventrally, the pubis narrows to form the pubic tubercle and its lateral surface is covered by ridges (plate 7a & c). At its antero-ventral end it is round and the surface is rugose. The acetabular facet of the pubis is continuous with that of the ischium, but it is smaller and faces slightly postero-laterally. The ischial facet is slightly deeper and faces more laterally. The articulating surface of the femoral condyles is directed ventrally.

Kannemeyeria simocephalus has a dorso-ventrally flat femur with a round medially inflected head (plate 8; figure 6). In front of the head on the ventral surface is a shallow fossa, and below the head is a low ridge (plate 8a). Distally, the fossa between the condyles is concave. The greater trochanter is narrow, flat antero-posteriorly and narrow distally (figure 6b; plate 8a). It is also clearly demarcated from the rest of the bone. On the dorsal surface it forms the posterior border of the shallow fossa in front of the head. The femoral head is pitted and very rugose and is not separated from the trochanter major.

A groove passes down the middle of the dorsal surface to reach the fossa between the condyles. The fossa is round to oval and relatively deep, and it is separated from the distal concave surface by a thin ridge. The concavity that separates the condyles is broad and shallow. In front of the ectocondyle is an elongated concavity for the articulation of the fibula (figure 6b; plate 8b).

The tibia is more gracile and narrower than the femur (figure 7; plate 9a). The *Tuberculum tibia* faces antero-laterally with a round tubercle at the proximal extend that is directed laterally. It is bound ventrally by a ridge that grades into the *Margo cranialis*. Posteriorly, the tibial tuberculum is bordered by a groove, and on the posterior border is an elongated, shallow fossa for the articulation of the fibula.

3.7.3 The Glenoid and Elbow Joint

The glenoid is made up of the scapula and coracoid facets (plate 3a). In BP/1/6160 the distal end of the scapula is twisted so that facet for the glenoid is round and directed postero-ventrally while the anterior part of the lateral surface is directed more medially (plate 1a). The humeral head has its articulating surface directed dorsally, and it projects slightly onto the dorsal surface. On the two specimens studied the olecranon fossa is

WitsETD

located on the posterior surface in BP/1/5624 and is on the dorsal surface in the small individual (BP/1/6160). In the smaller individual the olecranon fossa is directed "dorso-posteriorly" while in the adult it is directed posteriorly. When compared with the humerus the bones of the antebrachium are gracile. The radius and ulna form a single articulating surface for the humerus and are probably situated at 90° to the humerus resulting in a sturdy forearm.

3.7.4 The Acetabulum and Knee Joint

The acetabulum faces laterally and the ilium facet is directed slightly ventrally. Dorsally, the thick supra-acetabular ridge prevents the femur from moving upwards and out of the acetabulum. There is only a thin ridge on the lateral surface of the pubo-ischiadic acetabular facet and therefore there is little to stop the femur from slipping downwards. The head of the femur is inflected medially, and with the incipient neck, this means that the head of the femur is not in the same plane as the long axis of the femur. This position of the head means that the femur does not take up a horizontal position but rather it is drawn towards the body.

The distal articulating surface of the femur is directed ventrally, which would allow the tibia and fibula to be in a more upright position. They would be probably at approximately right angles to the femur. This probably allowed greater flexion and extension during locomotion.

Wits ETD

CHAPTER FOUR

A SECOND POSTCRANIAL MORPHOTYPE FROM THE *CYNOGNATHUS* ASSEMBLAGE ZONE

4.1 Introduction

The investigation into the dicynodonts of the *Cynognathus* Assemblage Zone (subzone B) of South Africa has so far identified two taxa, *Kombuisia* and *Kannemeyeria simocephalus*. The cranial morphology of *Kannemeyeria* was studied by Renaut (2000) after which he recognised two skull types. This led him to recognise two species of *Kannemeyeria, K. simocephalus)* and *K. lophorhinus* Renaut *et al* 2002 (= *K. cristarhynchus* Chowdhury 1970) (Renaut 2000; Renaut *et al* 2002). These species are separated both temporally and geographically. *K. simocephalus* is found in the subzone B of the *Cynognathus* Assemblage Zone of South Africa while *K. lophorhinus* is found in the *Cynognathus* Assemblage Zone (subzone C) Namibia and Zambia respectively.

It must once again be noted that all isolated postcranial elements belonging to medium to large dicynodonts that have been collected in the *Cynognathus* Assemblage Zone (subzone B) of South Africa has in the past been assigned to the genus *Kannemeyeria*, specifically *K. simocephalus*. The re-examination of the postcranial anatomy of *K. simocephalus* has shown some features that diagnose the postcranial anatomy of *K. simocephalus*. These include: A postero-ventrally facing glenoid; on the medial surface of the scapula at the proximo-posterior corner of the acromion process has a horseshoe shaped tubercle; the radius is a slender bone with expanded proximal and distal ends; on the posterior corner of the proximal end is a rectangular, convex ulna articulation; the femur is slightly dorso-ventrally flattened with narrow proximal and distal ends; along the proximal posterior border is the narrow greater trochanter which is parallel to the long axis of the bone; the posterior distal articulating condyle is located lower than the anterior condyle, and the articulating surface is also directed more ventrally on the posterior condyle.

During the examination of the postcranial skeleton of *K. simocephalus* the isolated elements were also examined and it was found that some of these differ from those that have been identified as *K. simocephalus*. This material is known from a limited number of localities, some of which has also produced *K. simocephalus* postcranial material that is

Wits ETD

associated with a skull. In some instances the postcranial elements are associated with each other but there is no associated cranial material. A possible complication with the material associated with known *K. simocephalus* skeletons, is that they were thought to be *Kannemeyeria* material therefore material was not separated when it was collected.

4.2 Postcranial Anatomy of Morphotype B

4.2.1 Pectoral Girdle

4.2.1.1 Scapula

This description is based on two scapulae BP/1/994D, the smaller, and BP/1/1669, a scapula belonging to a very large individual (figure 8; plate 13) The scapula of the larger individual (BP/1/1669) is incomplete along the dorsal and anterior borders. The acromion is broken anteriorly and the coracoid plate is broken ventrally. BP/1/994D is the smaller individual and is complete.

In lateral view (figure 8a; plate 13a), the surface of the scapula blade is markedly convex whilst the anterior margin of the scapula blade is concave. The posterior border is straight. The concavity of the anterior border has resulted in the proximal part of the blade being directed slightly anteriorly with respect to the distal end of the bone. Dorsally, the border of the scapula is rugose. The antero-proximal border is round and thinner than the posterior border, which projects slightly posteriorly. On the lateral surface of the blade posterior to the scapula spine is a slight concavity (which may be due to distortion). Below the rounded proximo-anterior border is a tubercle (possibly distortion related) that is surrounded by a groove. Approximately halfway down the blade the scapula spine begins. The spine is very thin and damaged proximally. It would appear that the spine does not project far anteriorly and the ‘cleithral groove’ or prespinous area is very narrow and concave. This area extends onto the proximal part of the medial surface of the acromion.

The acromion of the scapula of BP/1/994D is triangular and broad proximo-distally, and does not extend beyond the anterior end of the distal expansion as in *Kannemeyeria simocephalus* (figure 8a; plate 13a). Anteriorly, the acromion has a flat and slightly concave surface, which extends onto the medial surface. Its concave lateral surface is

Wits ETD

covered by long, parallel striations. On the distal border of the acromion posterior to the tip of the acromion is a groove, which forms a concavity that ends as a ridge on the distal anterior surface. Above the distal expansion the scapula blade is narrow and in BP/1/1669 there is a shallow groove posterior to the scapula spine that extends to the glenoid.

Distally, the scapula blade expands to form the distal articulation (figure 8a; plate 13a). It is narrow anteriorly and widens posteriorly to form the glenoid facet. The thick, round glenoid facet is directed postero-ventrally, and the articulating surface of the glenoid projects laterally. Laterally, the margin of the glenoid facet is thin and becomes thick medially, extends onto the medial surface of the distal end of the scapula. The articulating surface of the glenoid is concavo-convex, with the concave surface posteriorly. The convex anterior articulating surface extends onto the medial surface and forms a bulbous condyle. Anteriorly, the distal expansion narrows to forms the oblong concave precoracoid articulation. This articulation is directed medially and antero-ventrally. The coracoid articulation lies medial to the acromion. In the large individual the glenoid is twisted slightly so that it is visible in lateral view.

The posterior border of the scapula is thin proximally and widens distally. Halfway down the expanded distal end of the posterior border is an oval tubercle for the origin of the scapula head of the triceps muscle. It is very prominent and almost on the lateral margin of the posterior border. The surface of the bone in this area is rugose.

On the medial surface the anterior border is thin with a narrow groove lying between it and the scapula spine. The groove between the anterior border and the scapula spine extends to the proximal end of the acromion process. This anterior border passes distally, posterior to the acromion process, to terminate as a thick distal border.

The medial surface of the acromion forms an elongated triangle with its base distally (figure 8b; plate 14). Its surface is an elongated concavity with its deepest point at it posterior extent. The thick anterior tip of the acromion is directed more medially. At the proximo-posterior corner of the medial surface acromion is an elongated oval, wide concave fossa. This fossa extends in the proximal direction to end just above the distal end of the scapula spine (figure 8b; plate 14).

Wits ETD

Distally, the bone widens and is thick. Both the distal articulations extend onto the medial surface, resulting in the distal end having an "A"-shape (figure 8b; plate 13b). A deep groove on the medial surface of the distal articulation separates the coracoid articulation and the glenoid, however, the groove extends more onto the coracoid articulation. The distal end of the groove is marked by a sharp ridge, and its posterior border marks the anterior extent of the glenoid on the medial surface of the distal end, while the middle of the groove is located on the posterior part of the coracoid plate articulation. Proximally, the groove extends almost to the postero-distal end of the acromion. In front of this groove, the medial surface of the coracoid articulation is rounded and elongated. In BP/1/1669 the groove extends to below the coracoid foramen. The groove is at its widest between the coracoid foramen and the distal end of the scapula and narrows towards the acromion and below the coracoid foramen.

4.2.1.2 Precoracoid

The precoracoid, preserved only in BP/1/1669, has been broken anteriorly and ventrally, which has resulted in the bone having lost its shape (plate 13a (ii)). Away from the anterior margin and close to the dorsal border is an incomplete coracoid foramen as the bone is broken through the foramen. The foramen when complete would have been small and formed an elongated oval.

4.2.1.3 Coracoid

This bone (BP/1/1669) is also incomplete (plate 13a (ii)), but its general shape is still evident. It is triangular with the proximal end of the bone made up completely of the glenoid facet. The glenoid facet is elongated, almost oblong, and its posterior extent is marked by a thin ridge. Its surface is concavo-convex with the concave surface directed towards the posterior end. The glenoid facet is directed postero-ventrally. The ventral side of the coracoid is damaged.

Wits ETD

4.3 Forelimb

4.3.1 Humerus

In both specimens examined (BP/1/994A & SAM-PK-1073) that have humeral remains only the proximal end of the humerus is preserved (figure 9; plate 15). The head of the humerus is located close to the posterior border of the delto-pectoral crest, and overhangs the dorsal surface of the bone (figure 9a; plate 15a (ii)). Posterior to the head is a narrow, slightly deep groove that extends down the proximal expansion. The head is hemispherical and projects above the dorsal surface so that when viewed from the dorsal border the head extends more posteriorly. At the proximal corner of the posterior border of SAM-PK-1073 is an oval tubercle which has a convex surface. This tubercle extends slightly down the posterior border.

When viewed from the dorsal surface the bone expands in front of the head to form the delto-pectoral crest. The delto-pectoral crest has an arc shape with a concave dorsal surface (figure 9a; plate 15a). It is short and plate-like with the anterior margin directed antero-dorsally. The bone making up the delto-pectoral crest is thin. The distal end of the delto-pectoral crest is twisted towards the biccipital fossa.

Most of the proximal expansions ventral surface is made up by the biccipital fossa (figure 9b; plate 15b). The fossa is antero-posteriorly narrow with the anterior and posterior border approaching each other, making the biccipital fossa deep. In SAM-PK-1073 the biccipital fossa is broad and flat with a slightly concave surface. There is a small, low, round tubercle on the posterior margin just below the thick rounded dorsal border.

4.3.2 Ulna

There are only proximal ends of the ulna preserved in SAM-PK-1073 (figure 10; plate 16). Proximally, the ulna forms a broad, rectangle. The olecranon is low and antero-posteriorly wide with a rounded dorsal surface. It has a more anteriorly directed sigmoidal facet that is triangular with a slightly concave surface towards the anterior border. The sigmoidal facet narrows towards the olecranon (figure 10a; plate 16a). Laterally, there is a thin ridge, close to the anterior border, which extends only a short way down the bone to form the lateral border of the radial articulation. The radial articulation is wide, and in the form of an

Wits ETD

inverted triangle. It has a slightly concave surface that is limited medially and laterally by distinct borders.

Medially, there is a wide concave groove (figure 10b; plate 16b). The groove is located posterior to the medial border of the radial articulation. In medial view the medial border of the radial facet forms the narrow, triangular anterior part of the bone with a rounded tip that is lower than the olecranon.

4.4 Hindlimb

4.4.1 Femur

Both the proximal and distal ends of the femur (BP/1/3518) are antero-posteriorly expanded (figure 11; plate 17). The femur is dorso-ventrally flat with the anterior margin thicker than the posterior figure 11a; plate 17a). The femoral head is located at the anterior corner of the femur. It is oval and is directed antero-dorsally (proximo-anteriorly) with a slightly convex surface. In front of the head on the dorsal surface there is a broad, shallow concave 'groove' that separates it from the greater trochanter. The femoral head project slightly over the dorsal surface (figure 11a; plate 17a).

Along the anterior margin below the head there is a low, elongated oval tubercle (figure 11a; plate 17a) which is the minor trochanter. The minor trochanter does not project onto the anterior border but is directed diagonally towards the posterior border. Posterior to the tubercle is an inverted triangular fossa that is very shallow. The posterior border of the fossa is formed by the greater trochanter.

The greater trochanter is located on the proximo-posterior border of the femur (figure 11a & b; plate 17). It is dorso-ventrally narrow this has been exaggerated in BP/1/3518, and does not extend to the shaft. The short, broad shaft has concave anterior and posterior borders with the posterior border being more concave. The greater trochanter extends from the proximo-posterior 'corner' to the proximal end of the shaft, thus extending down the entire proximal expansion. This gives the proximo-posterior end of the bone a rounded shape. On the dorsal surface, slightly below the greater trochanter, there is a group of

Wits ETD

ridges that form a broad, low ridge that extends diagonally across the shaft to above the intercondylar fossa.

The oval head is separated from the rest of the dorsal border by a narrow, shallow groove and the ventral surface by a broad shallow groove in BP/1/3518, and a slightly narrower and deeper one in BP/1/994E. The dorsally (proximally) articulating surface is very rugose. The greater trochanter is long and dorso-ventrally narrow in the larger individuals (BP/1/3518 & SAM-PK-11262) while it is broad in the smaller individual (BP/1/994E). Its articulating surface is reflected onto the ventral surface in the large individual. Below the greater trochanter there is a wide, oval tubercle with a rugose surface. This tubercle is located on the ventral surface and is at an angle to the posterior margin represents the third trochanter (figure 11b; plate 17b).

At the base of the shaft the bone widens to form the distal end of the femur, which may be slightly exaggerated in BP/1/3518. The posterior part of the distal end is antero-posteriorly wider than the anterior part. Posteriorly the bone shows growth in the postero-ventral direction. At its ventral (distal articulating) end it forms the posterior (ectocondyle) condyle, which does not extend to the posterior margin of the bone. The condyles are at the same level and are separated by a deep, narrow groove.

In both BP/1/3518 & SAM-PK-11262 the condyle of the femur project onto the dorsal surface of the distal end of the femur, and they are raised slightly above the surface. The anterior condyle is larger than the posterior condyle. In dorsal view the surface of the anterior condyle is skewed slightly in the proximal direction. The condyles articulating surface is rounded and directed ventrally. The posterior condyle (ectocondyle) is round and bulbous. The round posterior condyle projects onto the dorsal surface and is raised slightly above the surface. An intercondylar fossa is located slightly above and between the condyles. It is a small and circular fossa that is slightly deep. A smooth ridge marks its distal end.

Ventrally in front of the femoral head is a small, almost circular, shallow fossa. From the distal end of the fossa a narrow, shallow groove passes down the shaft to the proximal end of the distal expansion. A broad, triangular fossa is present on the distal surface above the condyles. Its distal extent is marked by the condyles. On the ventral surface the condyles

Wits ETD

have been flattened in the larger specimen (BP/1/3518) while the small specimen has a small round projection on the ventral surface. There is an oblong tubercle on the postero-ventral 'corner' of the posterior condyle of the larger specimen (BP/1/3518). The surface of the tubercle is slightly concave and faces posteriorly. This probably represents the articulation for the fibula head. On the ventral surface between the condyles is a narrow semi-circular groove with a concave surface in the middle and extends on to the condyles. It is positioned more on the posterior condyle than the anterior one.

4.5 Functional Aspects of the Postcranial Skeleton of Morphotype B

This morphotype unfortunately is made up of isolated elements, therefore only certain elements of the skeleton were available for study. In particular there is no pelvic girdle available for study.

4.5.1 Pectoral Girdle and Forelimb

The scapula of the second morphotype is narrow, long with a straight posterior border and a concave anterior border (figure 8; plate 13). Proximally, the scapula blade is 'bent' slightly anteriorly in relation to the distal end of the scapula. A very narrow scapula spine starts about halfway down the scapula blade, which produces a narrow cleithral groove. It is continuous with the proximal margin of the acromion. The acromion is a broad triangle that is truncated anteriorly with a flat anterior margin. On the distal border of the acromion is a low oval tubercle which is covered by striations that are directed towards the anterior end of the acromion. Along the posterior border below the acromion is an oval tubercle that is raised above the surface of the bone.

Distally, the scapula is narrow with the coracoid articulation directed medially and the articulating surface directed antero-ventrally (plate 13a). The coracoid articulation lies behind the acromion and its lateral surface is concave. Posteriorly, there is a round, laterally expanded glenoid facet. The surface of the glenoid is concavo-convex to almost flat, and is directed ventrally.

WITS ETD

Medially, the surface of the proximal part of the scapula blade is concave (figure 8b; plate 13b). Along the anterior border the acromion has an elongated concave medial surface. At the proximo-posterior corner of this surface is an oval fossa that extends proximally to the distal end of the prespinous area (cleithral groove). On the medial surface of the coracoid articulation in BP/1/994D there is a narrow, deep groove that extends to the distal end of the bone. On BP/1/1669 this groove ends below the coracoid foramen, on the precoracoid.

Only the proximal end of the humerus of this morphotype has been found thus far (figure 9; plate 15). The delto-pectoral crest is sectorial or arc shape. Anteriorly, the border of the delto-pectoral crest is narrow proximally and broad distally. Dorsally, the surface of the delto-pectoral crest is slightly concave. Close to the posterior border is the hemispherical head, which projects more dorsally (figure 9a; plate 15a). In dorsal view there is a wide, shallow groove posterior to the head. It is bordered posteriorly by a sharp, thin ridge that extends down the entire length of the proximal end. Ventrally, the biccipital fossa forms a deep triangle (figure 9b; plate 15b). Posteriorly the border of the biccipital fossa is thick and flattened. Just below the thickened posterior end of the dorsal border is a small, low and round tubercle with a convex surface.

In the ulna the olecranon is antero-posteriorly wide and is very low (figure 10a; plate 16a). Dorsally, the surface of the olecranon is very rugose. The sigmoidal facet is a short triangle surface that ends below the olecranon. Laterally, it forms a thin ridge close to the anterior border, which forms the lateral border of the radial facet. The radial facet is an inverted triangle with a concave surface. The medial border of the radial facet projects in front of the lateral border. Posterior to the ridge formed by the sigmoidal facet is a concave ‘groove’. On the medial surface there is a wide groove close to the posterior border. The proximal part of the posterior border is flattened.

4.5.2 The Glenoid and the Elbow Joint

The glenoid of the second morphotype is made up by the scapula and coracoid (plate 13a). The dorsal part of the coracoid is made up of the glenoid articulation, which is an elongated oval directed postero-ventrally, which narrows in that direction. On the humerus

Wits ETD

the head is directed more dorsally. This would suggest that the humerus was positioned more horizontally than on *K. simocephalus*.

4.5.3 Hindlimb

The femoral head is oval, is directed antero-dorsally, and projects well in front of the anterior border (figure 11; plate 17). Ventrally, the head is surrounded by a groove that ends at the dorsal border. Below the head the ventral surface is slightly concave, and immediately below the head the surface is covered by short, parallel striations. Along the proximo-posterior margin there is a short greater trochanter. Its surface extends from the dorsal border of the femur down the posterior border of the femur. The greater trochanter is at angle of less than 90° to the long axis of the bone. At the distal end of the greater trochanter is another tubercle (Third trochanter), which is oval and long with a convex surface. It is positioned slightly posterior to the greater trochanter. The surface is covered by diagonal, parallel striations.

In dorsal view (figure 11a; plate 17a) there is a large, oval fossa between the femoral head and the greater trochanter. Along the anterior margin, below the head is a low elongated oval tubercle. The shaft of the femur is short, broad and dorso-ventrally flat. Distally, the intercondylar fossa has an irregular shape with the narrowest part between the condyles. In dorsal view the surface of the round anterior condyle is flattened in a proximal direction while the posterior condyle is convex in the ventral direction in the middle of the condyle.

Ventrally, there is a broad, elongated oval fossa between the head and the greater trochanter (figure 11b; plate 17b). Below this there is a shallow groove close to the posterior border. On the distal end of the bone is a wide, triangular fossa, which has a slightly concave surface. Along the anterior margin of the anterior condyle is a small, oval tubercle. The surface of the tubercle is directed obliquely ventrally. Above this the surface is covered by striations that give the bone a roughened appearance.

Wits ETD

CHAPTER FIVE

PRELIMINARY INVESTIGATION OF THE RELATIONSHIP BETWEEN TWO POSTCRANIAL MORPHOTYPES FROM THE *CYNOGNATHUS* ASSEMBLAGE ZONE (SUBZONE B) OF SOUTH AFRICA

5.1 Introduction

Many authors have previously reviewed the relationships of the dicynodonts (e.g. Angielczyk 2001; King 1988; Cluver & King 1983; Keyser & Cruickshank 1979; Cox 1965). The majority of these studies have concentrated on the cranial morphology and how this reflects the relationships of dicynodonts. Recently with an increased interest in the postcranial anatomy of dicynodonts new studies of dicynodonts relationships have included postcranial characters (e.g. Vega- Dias *et al* 2004; Angielczyk 2001; Maisch 2001; Surkov 1998a). Only a few studies have concentrated on the phylogenetic relationships of Triassic dicynodont (Vega-Dias *et al* 2004; Maisch 2001; Cox & Li 1983; Keyser & Cruickshank 1979; King 1988; Cox 1965; Camp 1956).

Recent studies of the relationships of Permian dicynodonts have included certain Triassic dicynodonts although the Triassic dicynodonts were not the focus of the study (e.g. Angielczyk 2001). The result of Angielczyk's analysis suggested that the Triassic dicynodonts (including *Lystrosaurus*) together with the Permian dicynodont *Dicynodon* represent a clade (Angielczyk 2001). Angielczyk (2001) also suggested that the inclusion of postcranial characters would result in more rigorous explanations of the patterns of evolution to be discovered in broader studies of synapsids.

The phylogenetic analysis of Maisch (2001) included 35 characters, including both cranial and postcranial characters. Maisch (2001) concluded that the lystrosaurids represent a basal branch of the larger subgroup of the Pristerodontia, which included *Odontocyclops*, Dicynodontidae, *Dinanomodon* and the Kannemeyeriiformes. The Kannemeyeriiformes represent the remaining Triassic dicynodonts (except *Kombuisia* and *Myosaurus*) and are a divergent group of dicynodonts (Maisch 2001). *Kannemeyeria* and *Wadiasaurus* represented the most pleisomorphic family, the Kannemeyeriidae von Huene 1948 (Maisch

Wits ETD

2001). Maisch (2001) listed the following set of unique derived postcranial characters separated Triassic from the Permian dicynodonts:

1. The pre-acetabular expansion of the ilium is enlarged;
2. The femoral head is distinctly offset;
3. The olecranon is formed by a separate ossification.

Maisch (2001) recognised four clades among the Kannemeyeriiformes, these being the: Shansiodontids, Kannemeyeriids, Stahleckeriids and Dinodontosaurids. These he recognised as families with kannemeyeriids and shansiodontids as basal to a clade formed by the stahleckeriids and dinodontosaurids. This phylogeny is considered to be provisional as primary as more research is required on Triassic dicynodonts (Maisch 2001). Maisch (2001) found that phylogenetic research is hampered by flawed alpha taxonomy, wide geographic distribution (i.e. the world wide dispersion of type specimens) and the lack adequate and detailed descriptions of many important forms.

Vega-Dias *et al* (2004) found that previous phylogenetic investigations (excluding Maisch 2001) of Triassic dicynodonts contained no strict cladistic analysis to support the phylogenetic conclusions. They used Angielczyk (2001) and Maisch (2001) to establish suitable outgroups (Vega-Dias *et al* 2004). Outgroups used in this analysis were *D. trigonocephalus* and *Lystrosaurus* as both of these taxa have skeletal osteologies that are well known, and it has been established by other studies (e.g. Angielczyk 2001) that they are closely related to Triassic Kannemeyeriiformes (Vega-Dias *et al* 2004). The analysis carried out using only postcranial characters provided eight parsimonious trees, while that including the cranial characters only produced a single parsimonious tree, and the analysis including both sets of characters yielded six parsimonious trees (Vega-Dias *et al* 2004).

The comparison mentioned above should be considered with caution because 27 cranial and only 17 postcranial characters were used and the result should be viewed as “not a clear indication that postcranial characters are ‘less valuable’ for phylogenetic analysis in Triassic dicynodonts than cranial ones” (p 152) (Vega-Dias *et al* 2004). In earlier work based on 40 cranial and postcranial characters Vega-Dias (2000) (in Vega-Dias *et al* 2004) had identified two clades: the first included *Jachaleria, Dinodontosaurus, Stahleckeria* and *Angonisaurus* while the second included *Kannemeyeria, Ischigualastia* and *Placerias*. The

Wits ETD

analysis of Vega-Dias *et al* (2004) showed that the Triassic Kannemeyeriiformes consist of two "groupings" (*sensu* Vega-Dias 2004):

1. A paraphyletic assemblage of all basal taxa. Here the Kannemeyeriidae (Maisch 2001) was not reproduced but *Kannemeyeria* and *Wadiasaurus* formed a polytomy with the Shansiodontids, Sinokannemeyeriines, and the *Dinodontosaurus* – stahleckeriid clade.
2. The relationships of the remaining Triassic dicynodonts, the *Dinodontosaurus*-stahleckeriid, clade is completely resolved. According to Vega-Dias (2004) this is as a result of the more detailed primary analysis of these taxa along with there being more specimens available for study. Only *Angonisaurus* is represented by fragmentary material (Vega-Dias 2004).

Vega-Dias *et al* (2004) shows that in recent times the inclusion of postcranial skeletons in the phylogenetic analyses of dicynodonts has possibly allowing for increased resolution on the relationship of dicynodonts. The renewed interest in Triassic dicynodonts (e.g. the present study; Vega-Dias *et al* 2004; Renaut 2000; Vega-Dias 2000 in Vega-Dias *et al* 2004) will go some way to answer King's (1988) concern that no absolute consensus of opinion about Triassic dicynodont relationships could be reached without these first hand studies.

5.2 Results

The methodology followed in the phylogenetic analysis was described in described in the 'materials and methods' chapter (p14 section 2.4). Appendix G contains the list of characters, the data matrix used in the analysis and the resulting tree topologies.

The phylogenetic analysis including both the cranial and postcranial characters produced 3 trees. The tree length is 151 steps with a CI of 0.45, RI of 0.523 and HI of 0.550. Figure 16 represents a strict consensus of the three most parsimonious trees. In the strict consensus tree *K. simocephalus* forms a trichotomy with a clade comprising *Wadiasaurus* and the sinokannemeyeriines and a clade containing *Dinodontosaurus* and the stahleckeriids.

Wits ETD

Morphotype B is placed within the Stahleckeriids and forms a sister group relationship with *Placerias* in a basal position among the stahleckeriids following Vega-Dias *et al* (2004) also found that *Placerias* occupies a basal position amongst the stahleckeriids. In the majority rule (figure 17) the position of *K. simocephalus* forms a sister group to the *Dinodontosaurus* + Stahleckeriidae clade in 67% of the most parsimonious trees.

A decay analysis of the strict consensus shows that these hypothesised relationships are weakly supported. Resolution within most of the Stahleckeriidae relationships is lost at 152 steps (Morphotype B & *Placerias*; *Ischigualastia* + *Jachaleria* & *Stahleckeria* + *Angonisaurus*) while the relationship between *Angonisaurus* and *Stahleckeria* is lost at 153 steps. At 153 steps the sister group relationship of *Dinodontosaurus* to the stahleckeriids and the resolution of the relationships of *Shansiodon* and *Tetragonias* as well as *Wadiasaurus* and the sinokannemeyeriines are lost.

The bootstrap analysis found that the nodes that resolved the positions of *K. simocephalus* and Morphotype B were represented in less than 50% of the trees. In this analysis the relationship between *Shansiodon* and *Tetragonias* (61%), between *Stahleckeria* and *Angonisaurus* (72%), between *Ischigualastia* and *Jachaleria* (66%) is fairly well supported while that of *Parakannemeyeria* and *Sinokannemeyeria* is present in 93% of trees.

In the analysis that included only the postcranial characters there were six most parsimonious trees that had 86 steps. The CI is 0.43, the RI is 0.5 and HI is 0.57. Figure 18 represents the strict consensus of the six trees. *K. simocephalus* forms a polytomy with *Lystrosaurus, Shansiodon, Tetragonias, Wadiasaurus, Parakannemeyeria, Sinokannemeyeria, Angonisaurus* and *Dinodontosaurus* and the Stahleckeriidae. Morphotype B, however, has shifted position among the remaining stahleckeriids. It no longer forms a clade with *Placerias* but rather has a sister group relationship with the *Stahleckeria - Ischigualastia – Jachaleria* clade.

The nodes that resolve the relationships of *K. simocephalus* and Morphotype B were, once again, recovered in less than half the trees of a bootstrap analysis of the matrix containing only postcranial characters. As in the analysis of the cranial and postcranial characters the relationship between *Shansiodon* and *Tetragonias* (60%), between *Stahleckeria* and *Angonisaurus* (74%) and between *Ischigualastia* and *Jachaleria* (66%) are well supported.

WitsETD

The relationship between *Parakannemeyeria* and *Sinokannemeyeria* is again very well supported and occurs in 94% of the trees.

Four most parsimonious trees resulted from the analysis of the cranial and postcranial characters that excluded *Dinodontosaurus* with the shortest tree length being 138 steps. It has a CI of 0.486, a RI of 0.545 and HI of 0.514. Figure 19 shows the strict consensus of the four trees. In the strict consensus *K. simocephalus* forms a trichotomy with *Wadiasaurus*, and a clade containing Sinokannemeyeriinae and Stahleckeriidae. Morphotype B is again positioned within the Stahleckeriidae and forms a sister group relationship with *Placerias*.

The postcranial analysis that excluded *Dinodontosaurus* found three most parsimonious trees with the shortest length of 79 steps (figure 21). It has a CI of 0.456, a RI of 0.511 and a HI of 0.544. *K. simocephalus* forms a polytomy with *Tetragonias* + *Wadiasaurus*, *Angonisaurus*, *Stahleckeria* and a clade containing sinokannemeyeriines and the remaining stahleckeriids. In the majority rule consensus of the three trees (figure 22) *K. simocephalus* forms a sister group to the Morphotype B – *Placerias* clade, however, this relationship is only produced in 67% of the most parsimonious trees.

Morphotype B maintains its sister group relationship with *Placerias* in the postcranial analysis that excluded *Dinodontosaurus* (figure 21). These two taxa form the sister group of the *Ischigualastia – Jachaleria* clade. Their sister group status to the stahleckeriines of Maisch (2001) and the *Ischigualastia – Jachaleria* clade (Vega – Dias *et al* 2004) is only reproduced in 67% of the most parsimonious trees (figure 22).

In order to better understand the results of the phylogenetic analysis a Templeton test was performed. This compared the following two topologies: one of the most parsimonious trees where Morphotype B remains within the stahleckeriids with the shortest tree that nests Morphotype B with *K. simocephalus*. The tree with the artificial grouping was two steps longer. The result was a P value of 0.48 which suggests that there is no significant difference between the two suggested topologies.

Wits ETD

CHAPTER SIX

DISCUSSION

6.1 *Kannemeyeria simocephalus*

6.1.1 Comparative Analysis of the Postcranial Anatomy of *K. simocephalus*

Recent fieldwork has resulted in the recovery of more *Kannemeyeria* specimens from the *Cynognathus* Assemblage Zone (subzone B). This has provided an opportunity to re-examine and re-evaluate the postcranial anatomy of *K. simocephalus*. At least one specimen is fairly complete and is associated with cranial material that has been confidently assigned to *Kannemeyeria simocephalus*. This specimen (BP/1/5624) along with previous descriptions, (e.g. Pearson 1924b; Cruickshank 1975) was used to provide a better understanding of the postcranial anatomy of *K. simocephalus*. Another result of this particular project was an evaluation of all postcranial material assigned to *Kannemeyeria*.

In the current project as well as in the description by Pearson (1924b) the vertebrae are disarticulated, and the order in which they occur cannot be determined with any certainty. By comparison with the figures in Pearson (1924b) the vertebrae described from SAM-PK-3017 are most likely from the dorsal region of the vertebral column. The axis has a tripartite articulation along the anterior border which actually represents the centrum of the atlas. The rib facet along the anterior margin of the centrum shows the same structure as that described in *Zambiasaurus* (Cox 1969).

Pearson (fig. 22, p 833, 1924b) (Plate 18) and Cruickshank (1975) described the scapula blade of *K. simocephalus* as long and narrow and this has resulted in both Camp (1956) and Surkov (1998b) recognising this as a characteristic of *Kannemeyeria*. An examination of the scapulae of BP/1/5624, BP/1/6160 and ELM1 (plate 1) has shown that *K. simocephalus*, however, has a broad blade, with those of BP/1/5624 and BP/1/6160 broader than that of ELM 1. After a careful examination of photographs of the scapula (R3740) illustrated by Pearson (1924b) it was noted that this particular scapula blade does not conform with the features that identify the scapula of *K. simocephalus*.

Wits ETD

On BP/1/5624 (plate 1) the prespinous fossa is presented by broad, deep groove, which is bordered by the scapula spine posteriorly and the anterior border anteriorly. The fossa is very narrow in the two smaller individuals (BP/1/6160 & ELM 1; plate 1) where the scapula spine is less prominent. It must also be noted that Cruickshank (1975) considered that the small prespinous fossa seen in *Kannemeyeria* was an advance over the condition seen in other Triassic dicynodonts. In lateral view the scapula spine is continuous with the proximal border of the acromion process. The acromion of *K. simocephalus* is a narrow triangle with a slightly flattened anterior end (plate 1).

BP/1/6104 and ELM 1 (Plate 1a) show that scapula of *K. simocephalus* has a wide, flared distal end. In front of the glenoid in both specimens the distal end of the scapula projects ventrally. This ventral projection ends as a thick, round tubercle. The glenoid facet of *Kannemeyeria* is described as large, facing almost entirely backward with only a small part facing laterally (Cruickshank 1975), however, an examination of the glenoid of *K. simocephalus* showed that it does not face laterally but is rather expanded laterally. ELM 1 is the only specimen of *K. simocephalus* with a complete glenoid that is unobstructed. In this specimen the glenoid is circular with a concave surface, and that faces postero-ventrally (plate 1b).

Both Pearson (1924b) and Cruickshank (1975) have not described the medial surface of the scapula in any detail. Pearson (1924b) figured the medial surface of the scapula (figure 21, p832), which shows a groove at the distal end of the scapula that extends from the coracoid foramen. Observations of BP/1/5624 (plate 2) show the medial surface of the scapula of *K. simocephalus* to be concave, with a shallow subscapula fossa. Medially, the acromion is concave and is separated from the rest of the bone by a low ridge that is the anterior margin, which becomes flattened ventrally. At the proximo-posterior corner of the acromion's medial surface is a horseshoe-shaped tubercle (plate 2). Thus far this structure has not been described in any other Triassic dicynodonts. On the coracoid plate articulation of the scapula of *K. simocephalus* is a broad, shallow groove that extends to the coracoid foramen, which is elliptical. The coracoid foramen is located on the precoracoid of most of the Triassic dicynodonts at varying distances from the dorsal border, which articulates with the distal end of the scapula, however, the precoracoid foramen is located between the scapula and precoracoid in *Ischigualastia* (Cox 1965). A scapula has been preserved with a

Wits ETD

notch on the antero-distal end which suggests that the coracoid foramen may also occur between the scapula and precoracoid in *Wadiasaurus* (Bandyopadhyay 1988).

Pearson (1924b) found that the head of the humerus of *Kannemeyeria* faced dorsally and anteriorly, and that it extends to the proximal end of the bone. She also noted that the proximal and distal ends are at an angle to each other (Pearson 1924b). In the specimens examined so far the humeral head is located close to the posterior extent of the dorsal border of the delto-pectoral crest. The head forms an inverted triangle, is convex and is directed antero-dorsally. Cruickshank (1975) described the distal condyles of *Kannemeyeria* as "weakly ossified". After careful study it was found that in the two smaller individuals that the condyles were not as distinct as that of the larger individual. In the large individual the condyles are well-defined and "clearly demarcated". Cruickshank (1975) also found that the proportions of the humerus were very different from that figured by Pearson (1924b), however, recent examination of photographs of the material described by Pearson has shown that the humerus described is similar to that of BP/1/6160 and ELM 1 (plate 4). Cruickshank (1975) did not elaborate on the features that were different, but suggested that the differences were due to crushing suffered by the specimen he was describing.

Surkov (1998b) considered that large Triassic dicynodonts (*Dinodontosaurus* and *Placerias*) had massive limbs and hemispherical humeral heads and that the ectepicondyle extended far distally. *K. simocephalus*, although large, has an inverted triangular head and the ectepicondyle does not extend far distally.

As noted by Pearson (1924b) *K. simocephalus* has a well ossified olecranon. The ulna of BP/1/6160 shows a groove along the medial surface that extends from below the olecranon to the distal end. Like the specimens described by Pearson (1924b) and Cruickshank (1975), the ulna of *K. simocephalus* (BP/1/5624) does not have a separate ossification for the olecranon. Cruickshank (1975) described the ulna of ELM 1 as antero-posteriorly flattened, however, a recent examination of this specimen suggests that this may not be the case. The broad proximal end of the ulna may well be the actual shape of the bone.

It has been noted that there are a number of differences between the ulnae of BP/1/5624 and BP/1/6160, and ELM 1 (plate 5). The radial facet of ELM 1 is narrower than that of

Wits ETD

BP/1/5624 and BP/1/6160 and the laterally projecting ridge on the lateral surface of the ulna is also located further anteriorly in ELM 1 than in BP/1/5624 and BP/1/6160. Also the shape of the olecranon of ELM 1 is round and wide, whereas the olecranon of BP/1/5624 and BP/1/6160 are triangular or wedge shaped. Both BP/1/5624 and BP/1/6160 are associated with skulls that have been identified as *K. simocephalus*. The ulna of ELM 1 is distinctly different form that of BP/1/5624 and BP/1/6160.

There are also differences between the radii BP/1/6160 (plate 6) and ELM 1 (plate 32). The radius of BP/1/5624 was not considered for all comparisons as it has suffered some damage. The ends of the radius (BP/1/6160) of *K. simocephalus* are expanded forming narrow articulating surfaces both proximally and distally. This is different from that of ELM 1, which does not have greatly expanded ends, and which has the proximal and distal articulating surfaces almost round and wide. On the proximal expansion of the radius facing more posteriorly is the ulna articulation. In ELM 1 the ulna articulation is proximo-distally narrow and triangular, while in both BP/1/5624 and BP/1/6160 the ulna articulation forms a narrow rectangle, with both having a convex surface. The variation of the form of the radii of BP/1/6160 and ELM 1 has led to the radius of ELM 1 being considered of uncertain affinity.

ELM 1 (plate 32) has the only complete pelvic girdle. The anterior process of the ilium extends far in front of the acetabulum and is dorso-ventrally wide with a hook shaped anterior end. This specimen agrees with the character described by Camp (1956). The anterior process is higher than the posterior one, which is close to the acetabulum. A comparison of Pearson's (1924b, fig 29, p841) illustration of the ilium with that of ELM 1 shows that the anterior process of the ilium illustrated by Pearson is slightly dorso-ventrally wider, and antero-posteriorly shorter than that of ELM 1. The posterior process of the illustrated ilium (Pearson 1924b) is narrower and would probably have ended in a sharp point. The projected shape of the ilium in BP/1/5624, even though this particular specimen is missing the dorsal part of the ilial blade, resembles that of the ilium illustrated in Pearson (1924b). Although this shape is similar to that of ELM 1, it is also different, in that the anterior process of ELM 1 is narrower and longer than that of the British Museum specimen (BMNHR 3761) is figured by Pearson (1924b). In ELM 1 the concavity of the anterior process or hook shape of the anterior process, is much greater. ELM 1 has a broad, ventrally directed posterior process that has a flattened posterior border and narrows to

Wits ETD

form a sharp point at its ventral end. Both Camp (1956) and Surkov (1998b) describe the acetabulum as facing ventrally, however, in ELM 1 and BP/1/5624 the acetabulum faces more laterally. As a result of the difference in the morphology of ELM1 when compared with BMNHR361 and BP/1/5624, the pelvic girdle of ELM 1 is therefore considered to be of uncertain affinity.

Pearson (1924b, fig 34 & 35, p848) concluded that although the femur showed an exaggerated flattening it was a naturally flat, broad bone. An examination of the femora of other specimens of *K. simocephalus* show that the femur figured by Pearson (1924b, fig 34 &35, p848) does not resemble any of the femora assigned to *K. simocephalus* (plate 20). The shape of the femur illustrated by Pearson (1924b) may not be as exaggerated as suggested by Pearson (1924b). The femur of *K. simocephalus* (plate 8) has a narrow proximal and distal expansion with the greater trochanter more or less parallel to the long axis of the bone. In all specimens examined the head of the femur is continuous with the greater trochanter. The head of the femur of *K. simocephalus* is round which agrees with features Surkov (1998b) found to characterise the Middle to Late Triassic dicynodonts. In *K. simocephalus* the femoral head is surrounded on the ventral surface by a narrow, shallow groove that extends onto the dorsal surface. The femur of *K. simocephalus* does not have a third trochanter and there is no distinct neck.

In *Lystrosaurus* the dorsal border of the scapula is convex in the middle, whereas all other Triassic dicynodonts have antero-posteriorly expanded dorsal borders. *Placerias, Ischigualastia* and *Dinodontosaurus* have flat dorsal borders, while in *Placerias* and *Ischigualastia* the anterior border is lower than the posterior border. The dorsal border in *Kannemeyeria* is expanded antero-posteriorly with a convex surface.

Lystrosaurus have a straight rectangular scapula blade with straight anterior and posterior borders, but a thick posterior border. *Kannemeyeria* and *Sinokannemeyeria* have straight, tall blades, however, the blade of *Kannemeyeria* is wide while *Sinokannemeyeria* has a narrow blade. *Wadiasaurus* has a slightly curved anterior border, but also a narrow blade, whilst *Parakannemeyeria* also has a slightly convex blade with a straight, thick posterior border. The scapula blade of *Ischigualastia* and *Dinodontosaurus* has short, broad scapula blades but in *Dinodontosaurus* and *D. trigonocephalus* is not constricted above the acromion. The upper blade of *Ischigualastia*, like that of *Robertia, Cistecephalus* and

Wits ETD

Diictodon, is inclined posteriorly. *Tetragonias* also has a broad blade but its upper blade is directed anteriorly.

An elongated scapula spine is present on the lateral surface of the scapula of *Placerias*, *Kannemeyeria* and *Wadiasaurus*. A low scapula spine that is not prominent and does not project far anteriorly occurs in *Parakannemeyeria*, *Ischigualastia*, *Tetragonias*, *Zambiasaurus* and *Rhinodicynodon* while a scapula spine is absent in *Dinodontosaurus*.

The clavicle facet of the medial surface of the acromion of *Eodicynodon* is limited posteriorly by a triangular sheet of bone, however, the other descriptions of the Permian dicynodonts do not mention such a structure on the medial surface of the acromion process. In *Kannemeyeria* there is a facet on the proximo-posterior corner of the medial surface of the acromion. It varies from triangular in the large specimen (BP/1/5624) to round and oval in the small specimen.

The shape of the acromion process varies among the Triassic dicynodonts. It is short and directed anteriorly in *Placerias*, while a rectangular acromion process that is directed antero-laterally occurs in *Angonisaurus*, *Sinokannemeyeria* and *Dinodontosaurus*. A triangular acromion process occurs in *Wadiasaurus, Kannemeyeria, Parakannemeyeria*, *Rhinodicynodon*, *Tetragonias* and probably also in *Zambiasaurus*, however the acromion process is either absent or vestigial in *Ischigualastia*.

On the medial surface of the distal end of the scapula there is a groove on the precoracoid articulation (Pearson 1924; own obs BP/1/5624 & BP/1/6160). According to Pearson (1924b) this is related to the precoracoid foramen. In the drawings of *Ischigualastia* (figure 6 p468 Cox 1965) there is a short groove on the medial surface of the distal end of the scapula and the same groove is described in *Wadiasaurus*. In *Kingoria* and *Ischigualastia* the precoracoid foramen is located between the distal end of the scapula and the proximal end of the precoracoid.

Lystrosaurus has no olecranon developed (Young 1935) but this is contradicted and has been described as moderately developed (Ray & Chinsamy 2003). *Kannemeyeria* has a low narrow olecranon that is part of the ulna and does not show any signs of a suture contact. The remaining Triassic dicynodonts *Sinokannemeyeria, Parakannemeyeria,*

Wits ETD

Wadiasaurus and *Placerias* all have separately ossified olecranons except that in *Wadiasaurus* and *Sinokannemeyeria* the olecranon is fused to the rest of the ulna. In *Ischigualastia* and *Dinodontosaurus* the separately ossified olecranon is joined to the rest of the bone by a cartilaginous epiphysis.

The fan-shaped iliac blade of *Lystrosaurus* has two to five notches on the dorsal border. The dorsal border of the ilium of *Kannemeyeria* is either smooth or irregular while the dorsal border of *Sinokannemeyeria* is also indented. *Ischigualastia* has a dorso-ventrally expanded anterior blade but constricted dorso-ventrally posteriorly while *Dinodontosaurus* is thick anteriorly and notched two-thirds back from the anterior process. *Uralokannemeyeria* is antero-posteriorly expanded giving the iliac blade a fan-shape with two notches dorsally and oval foramen. *Wadiasaurus* differs from the other Triassic dicynodonts in that it has a small anterior process is higher than the posterior process. In all the Triassic dicynodont the anterior process is higher than the posterior process and the anterior part of the blade.

Lystrosaurus, Kannemeyeria and *Sinokannemeyeria* also have the dorsal border of the iliac facet interrupted by a groove or incision. In *Kannemeyeria* the groove divides the acetabular facet into two separate articular facets for the femur and in *Sinokannemeyeria* the incision occurs in the middle of the facet.

In *Kannemeyeria* the femoral head is continuous with major trochanter but in *Sinokannemeyeria* it is separated from the trochanter major (greater trochanter) by a weak groove. In *Dinodontosaurus* has the head of the femur is not offset from the rest of the bone, however, in *Ischigualastia* the femoral head is offset medially from the shaft and there is a distinct hollow on the edge of the trochanter major. In *Wadiasaurus* the head of the femur is demarcated by a rim and the trochanter major is continuous with the head while in *Placerias* the head is offset from the shaft by an incipient neck. The femur of most of the dicynodont taxa is dorso-ventrally flattened.

The femoral head of *Kannemeyeria* like that of the Triassic dicynodonts, is round and inflected medially so that it overhangs the ventral surface. *Kannemeyeria* like other Triassic dicynodonts, except for *Lystrosaurus*, have an incipient neck. The femoral head of

Wits ETD

Kannemeyeria, unlike the other Triassic dicynodonts, is continuous with the greater trochanter.

This study has raised questions about the identification of material as *K. simocephalus*. BP/1/5624 and BP/1/6160 have both been assigned to *K. simocephalus* because they are both associated with skull that have been identified as *K. simocephalus*. Elements of skeletons assigned to *K. simocephalus*, in particular ELM 1 and some material, in particular the scapula, femora and ulna described by Pearson (1924b), were found to differ significantly from that of the skeletons which have been accepted as *K. simocephalus*.

6.1. 2 Diagnosis of *Kannemeyeria simocephalus*

It must also be noted that at this time *K. lophorhinus* is poorly described therefore it was not included in the comparison. *Eodicynodon* is used as the outgroup taxon to determine the polarity of the character states of *K. simocephalus*. Its position as a basal dicynodont made it the most appropriate. Comparison with *Eodicynodon* was used to determine the pleisomorphic state of characters for *K. simocephalus*. As *K. lophorhinus* was not included in the comparative analysis the synapomorphic characters unite *K. simocephalus* with other Triassic dicynodonts.

The postcranial skeleton of *K. simocephalus* was analysed using both Permian and Triassic dicynodont postcranial anatomy. Most of the comparisons were done using literature, especially those of the Triassic dicynodonts where most of the material is housed in international institutions. The majority of the comparative analysis was based on literature, it as still possible to identify a unique suite of pleisomorphic, apomorphic and autapomorphic characters.

It is possible to add the following postcranial characters to the current specific cranial diagnosis (p114-115, Renaut 2000) so that the full diagnosis is:

K. simocephalus differs from the remaining Kannemeyeriiformes by retaining the following pleisomorphic characters: Scapula has straight anterior and posterior border. Glenoid lower than coracoid articulation. Round glenoid articulation. Olecranon fused to

WitsETD

shaft. Supra-acetabular notch present on ilium. Pubis and ischium are fused. Oblong obturator foramen. Straight femoral shaft. Femoral head continuous with greater trochanter. No third trochanter.

The Kannemeyeriiforme dicynodonts are share the following synapomorphic characters which sets them apart from other dicynodonts: Antero-posteriorly expanded dorsal scapula border. Scapula spine present. Triangular acromion. Distal end of scapula flared. Distal scapula projects in front of scapula spine. Triangular olecranon. Anterior process of ilium is wide and posterior process is narrow. Anterior process well in front of acetabulum. Supra-acetabular notch present. Femur has concave posterior border. Femoral head is medially inflected. Narrow greater trochanter.

When compared with other Kannemeyeriiforme dicynodonts *K. simocephalus* has the following autapomorphic characters: At the proximo-posterior corner of the medial surface of the acromion is a horse-shoe shaped tubercle. The ventral articulating surface of the posterior condyle of the femur is lower than the anterior. The greater trochanter is at 90° to the long axis of the femur. Anterior border of the femur is almost straight.

K. simocephalus shares a number of characters with the Permian and Triassic dicynodonts, however, the greater number of characters shared with the Triassic dicynodonts provides evidence for it being more closely related to Triassic dicynodonts. The presence of certain autapomorphic characters may proves useful in the future for identifying isolated postcranial elements to at least the generic level.

Wits ETD

6.2 Morphotype B

6.2.1 Comparison with *K. simocephalus*

During the re-examination of the postcranial skeleton of *K. simocephalus*, material assigned to this genus, and unidentified material, from the *Cynognathus* Assemblage Zone (subzone B) in South Africa was re-examined. A number of isolated elements showed gross morphology that is significantly different from that of *K. simocephalus* as typified by BP/1/5624 and BP/1/6160.

The following discussion highlights the main differences. The scapula of Morphotype B is more robust than that of *K. simocephalus*, and has a more concave anterior border (plate 21a (i)). Dorsally, the border is not as greatly expanded in Morphotype B and the proximo-anterior corner is round. This is different from *K. simocephalus* which has an expanded dorsal border of the scapula. The proximal half of the scapula blade is angled anteriorly to the distal half of the bone (plate 21 a (ii)). Distally on the posterior border above the glenoid is an oval tubercle for the origin of the triceps muscle, whereas in *K. simocephalus* this tubercle is round. The glenoid facet of the scapula is round and directed ventrally in Morphotype B while in *K. simocephalus* the glenoid is oval and directed postero-ventrally. Anteriorly, along the distal end of the scapula the coracoid articulation of Morphotype B is directed antero-ventrally in BP/1/994D while in the larger BP/1/1669 the coracoid articulation is directed more ventrally than anteriorly. In *K. simocephalus* the coracoid articulation is directed ventrally (plate 21).

Proximally on the humerus the delto-pectoral crest of BP/1/994A is arc or sectorial shaped, while the delto-pectoral crest of *K. simocephalus* is rectangular and at 90° to the shaft (plate 22). In *K. simocephalus* the head forms an inverted triangle that has a convex surface and is directed antero-dorsally, while that of BP/1/994A is hemispherical or elongated oval with a convex surface that is directed dorsally. On the ventral surface the biccipital fossa is triangular in BP/1/994A, while in *K. simocephalus* it is rectangular (plate 22b).

When compared with *K. simocephalus* the ulna of Morphotype B (SAM-PK-1073) has a lower and wider olecranon and it projects further anteriorly to meet the proximal end of the sigmoidal facet, and the radial facet is smaller. The groove posterior to the lateral projection of the sigmoidal facet is wider in Morphotype B (SAM-PK-1073) than *K. simocephalus* (BP/1/5624) (plate 23). In Morphotype B (SAM-PK-1073) the sigmoidal facet is shorter, narrower and does not extend to the proximal end of the bone. On the medial surface the groove is broader in Morphotype B (SAM-PK-1073).

The femur of BP/1/3518 has more widely expanded proximal and distal ends when compared with *K. simocephalus* (plate 24). In Morphotype B the femoral head is oval and directed antero-dorsally while that of *K. simocephalus* is round and is medially inflected (plate 24b). Both femoral head are surrounded by shallow grooves on the ventral surface. The greater trochanter of Morphotype B (BP/1/3518 & SAM-PK-11262) is shorter and

Wits ETD

dorso-ventrally thinner than that of *K. simocephalus* (plate 24a). Below the greater trochanter in the second morphotype, there is a tubercle that forms a narrow, elongated oval with a flattened surface. The shaft of this new morphotype is shorter and more dorso-ventrally flattened than that of *K. simocephalus* and its posterior border is more concave.

Unlike the condyles of *K. simocephalus*, the femoral condyles articulating surfaces of Morphotype B end at the same level ventrally, and the anterior condyle's dorsal surface is flattened in the proximal direction and is square (plate 24a). Although the anterior condyle of *K. simocephalus* is slightly flat in the proximal direction it still retains a round shape, and the posterior condyle is slightly lower that the anterior one. When compared with *K. simocephalus* the intercondylar fossa of this specimen is shallower and has an irregular shape (plate 24a). On the ventral surface the groove between the condyles is narrower and shallower than that of *K. simocephalus* and is positioned more on the surface of the posterior condyle.

After close examination it has been noted that some of the elements of ELM 1 (plate 32a) and some of the elements described by Pearson (1924b) (plate 18; plate 19; plate 20) do not belong to *K. simocephalus*. A comparison of the drawing of the scapula and femur of the *Kannemeyeria* specimen that was mounted at the time (Pearson 1924b), showed clear resemblance to Morphotype B. On comparing the form of the ulna and radius of ELM 1 with that with accepted *K. simocephalus* forms, it was found that the ulna rather resembled that of Morphotype B (SAM-PK-1073). The radius is significantly different from that of *K. simocephalus* studied, and at this time it is considered that it is possible that it belongs to Morphotype B.

More recently the material described by Pearson (1924b) has been re-examined by way of photographs (provided by Dr P. J. Hancox). The scapula (BMNHR3762; figure 22 p833 Pearson 1924b) has a narrow blade with a concave anterior margin and the proximal half of the blade is at an angle to the distal half of the scapula blade (plate 18). Antero-dorsally the dorsal border of the scapula is rounded. The glenoid is round, expanded laterally and the coracoid articulation is directed more medially. On the medial surface of the acromion there is an elongated oval, shallow fossa at the proximo-posterior corner (plate 18). The presence of these features on the scapula has led to the conclusion that this material does

Wits ETD

not conform with the accepted anatomy of the scapula of *K. simocephalus* as described here but rather they conforms to the description of Morphotype B above.

The ulna has also been re-examined using photographs (provided by Dr P. J. Hancox). Pearson (1924b figure 33 p847) has reconstructed the olecranon and the distal end of the ulna (BMNHR 3762a figure 33 p847); however, a review of the photographs (plate 19) at shows that the proximal end of the bone is the same as that of Morphotype B (SAM-PK-1073). Distally, the ulna resembles the distal end of the ulna of ELM 1. This has led to the conclusion that this ulna does not correspond to the known anatomy of the ulna of *K. simocephalus*, but rather matches that of the new morphotype.

The femur figured in Pearson (1924b; figure 34 BMNHR3740) has also been re-examined using photographs (provided by P. J. Hancox). The proximal and distal ends of the femur are widely expanded antero-posteriorly (plate 20). This femur (R3740) has a dorso-ventrally flat shaft and the femoral head is oval and directed antero-dorsally. In this specimen the head of the femur is not as flattened as that of Morphotype B (BP/1/3518) therefore it shows the slight medial inflected more clearly. The distal condyles end at the same level ventrally and the dorsal surface of anterior condyle is flattened in the proximal direction (plate 20). The antero-dorsal direction of the articulating surface of the head and the flat shaft as well as the distal articulating condyles end at the same level are all features that are the same as seen in Morphotype B (BP/1/3518), therefore this material could be included in the new morphotype rather than in *K. simocephalus*.

A comparison of the pelvic girdle of ELM 1 with that of the BMNHR3761 shows a number of differences. The British Museum specimen forms the basis of the description of the pelvic girdle for *K. simocephalus* (plate 7b; 7c). Anteriorly, the process of the R3761 is short, wide and located higher than the posterior process (plate 7b), while in ELM 1 the anterior process is dorso-ventrally narrow, elongated and hook shaped (plate 32b). The posterior process is small in both specimens and is located lower than the anterior process. In ELM 1 the acetabulum is directed more ventrally, and the supra-acetabular notch is located in the middle of the supra-acetabular ridge. At the level of the articulation of the ilium with the ischium there is another groove. In *K. simocephalus* there is no groove between the ischium and the ilium articulation. At this point dorsally directed articulating surface of the femoral head of Morphotype B suggests that it may well be possible that the

WITS ETD

pelvic girdle belongs to Morphotype B. Due to the lack of additional material it will therefore be considered to be of uncertain affinity until such time more material becomes available.

The pubo-ischiadic plate of ELM 1 is larger than that of *K. simocephalus*. In their gross morphology these two pubo-ischiadic plates look very similar, however, in ELM 1 the posterior border is more flared, and is directed more posteriorly than in *K. simocephalus*, while in *K. simocephalus* the tubercle on the postero-ventral border of the ischium is more prominent than in ELM 1. The pubis of ELM 1 is smaller and the pubic tubercle in ELM 1 is also smaller and directed more anteriorly. In ELM 1 the pubis and ischium are closer together and the concave surface between the ischium and the pubis is only visible in the *K. simocephalus*. At this time it remains speculative but the shape of the acetabulum suggests that it is more suited to an articulation that involves the femur of Morphotype B; however, this material will be designated of uncertain affinity until more postcranial material is available for study.

In mammals in order to determine if postcranial material belongs to a different species a large sample size is studied and a range of variation is determined for a specific species using a modern reference (Brink pers comm.). Unfortunately, the current sample size of *K. simocephalus* and Morphotype B is very small. This makes it difficult to determine the exact taxonomic relationship of these two morphotypes of the *Cynognathus* B zone. The resulted of the analysis of the postcranial material from the B zone has also brought to the fore the need for more extensive collecting. This collecting needs to be done in the context of stringent taphonomic records. It is also become necessary to re-examine other isolated and fragmentary cranial remains that were previously assigned to *K. simocephalus* (in foreign institutions). It is therefore difficult at this time state with any confidence whether or not Morphotype B is a species of *Kannemeyeria*.

Morphotype B is represented only by postcranial elements at this time because thus far the cranial material that does exist has been identified as *Kannemeyeria simocephalus*. The lack of cranial material has made it difficult to determine if this material does belong to a new (unknown) or known taxon other than *K. simocephalus*. Based on the fact that over 200 *K. simocephalus* skull have been collected from *Cynognathus* Assemblage Zone and as yet there has been no significant variation found in the skull morphology to suggest the

Wits ETD

presence of more than one species of *Kannemeyeria* in South Africa. Renaut (2000) did recognise a '*Kannemeyeria*-morphotype' that would have been an ecological generalist. This would suggest that the skull morphology would allow this animal to exploit a wide range of habitat and niches within the habitats (Renaut 2000). It does suggest that the variation if it does exit in the cranial morphology may well be of the nature that it could have been accepted to be within the range of variation.

6.2.2 Comparison with other African Triassic dicynodonts

6.2.2.1 *Zambiasaurus*

A comparison with *Zambiasaurus* showed that the postcranial morphology of certain elements of Morphotype B showed some resemblance to those of *Zambiasaurus*. It must, however, be remembered that the specimen of *Zambiasaurus* that is used in this comparison is a juvenile. The following is a discussion of the comparison of the postcranial morphology of Morphotype B and *Zambiasaurus*.

The scapula blade of *Zambiasaurus* is much narrower than that of Morphotype B (plate 25). In both Morphotype B and *Zambiasaurus* the coracoid articulation is directed antero-ventrally and the glenoid faces ventrally (plate 25a). In *Zambiasaurus* the tubercle for the origin of the scapula head of the triceps muscle is reduced when compared with Morphotype B (plate 25a). On the medial surface of the scapula of *Zambiasaurus* there appears to be neither, neither a tubercle nor the fossa presents (plate 25b). Medially it appears that the coracoid articulation is slightly longer in *Zambiasaurus* and that is directed more ventrally while in Morphotype B it is directed more anteriorly (plate 25b). The groove on the medial surface of the distal end of the scapula is wider, shallower and closer to the glenoid in *Zambiasaurus*.

The proximal end of the humerus of Morphotype B is similar to that of *Zambiasaurus* in that the head of the humerus is located more posteriorly, and is an elongated oval with its convex articulating surface, directed dorsally (plate 26a). The humerus of *Zambiasaurus* the delto-pectoral crest is arc or sectorial shaped which is the same as Morphotype B. In both Morphotype B and *Zambiasaurus* the biccipital fossa is triangular (plate 26b). The olecranon of Morphotype B is wider than that of *Zambiasaurus* (plate 27), which is almost

Wits ETD

triangular/wedge-shaped. In *Zambiasaurus* the sigmoidal facet is directed more anteriorly than that of Morphotype B (plate 27).

The femora of Morphotype B and *Zambiasaurus* are structurally different from each other. *Zambiasaurus* has a narrower femur with a longer shaft. The distal condyles are less well developed in *Zambiasaurus* and are not distinct. The greater trochanter is parallel to the long axis of the femur in *Zambiasaurus*, whereas in Morphotype B it is short and at an angle to the long axis of the bone.

In Morphotype B the femoral head is better developed and distinct (plate 28). It is also clearly medially inflected in Morphotype B whereas in *Zambiasaurus* the head is not distinct and it is not clear if it is medially inflected. The poor development of the femoral head and articulating condyles in *Zambiasaurus* can be attributed to this specimen being a juvenile.

6.2.2.2 *Angonisaurus*

Angonisaurus is the only other large dicynodont known from the *Cynognathus* Assemblage Zone. At present it has a stratigraphic range above that of *Kannemeyeria simocephalus* with no known overlap. Most of the material assigned to this taxon is incomplete (Cox & Li 1983) and fragmentary (BP/1/5531) (Hancox & Rubidge 1995).

A comparison with Morphotype B shows that *Angonisaurus* has a wider scapula blade (Plate 29). The acromion process of Morphotype B is smaller and more truncated than that of *Angonisaurus*, which has a rectangular, wide acromion. Ventrally the coracoid articulation is directed more ventrally in *Angonisaurus*. In Morphotype B and Angonisaurus the glenoid is directed ventrally. The groove on the medial surface of the distal end of the scapula is wider and shallower in *Angonisaurus* (plate 29b).

Morphotype B has a narrower proximal humeral expansion than that of *Angonisaurus* (plate 30a). The articulating surface of the humeral head in both Morphotype B and *Angonisaurus* is directed dorsally, however, in *Angonisaurus* the head is positioned closer to the middle of the dorsal border (plate 30a). The head of the humerus of *Angonisaurus* is more prominent and projects higher over the dorsal surface of the humerus than that of

Wits ETD

Morphotype B. In *Angonisaurus* the delto-pectoral crest is probably triangular and long (plate 30a). In *Angonisaurus* the delto-pectoral crest is long and is about half the length of the bone, whereas in Morphotype B the delto-pectoral crest is short. In Morphotype B the delto-pectoral crest would probably be at an acute angle to the shaft of the humerus as it has an arc shape. Although the delto-pectoral crest is at an angle to the shaft of the humerus, it is more obtuse than that of Morphotype B.

The olecranon of the ulna of Morphotype B is broad while that of *Angonisaurus* is narrow and wedge shaped (plate 31). Proximally, the ulna is narrower and longer in *Angonisaurus*. In *Angonisaurus* the distal end of the olecranon projects slightly over the sigmoidal facet. The sigmoidal facet is narrower and more concave in *Angonisaurus* than in Morphotype B.

6.2.3 Comparison with New World Stahleckeriids

The scapula blade of Morphotype B and *Placerias* is narrow while that of *Ischigualastia, Stahleckeria* and *Jachaleria*. In *Stahleckeria* and *Jachaleria* the scapula blade appears almost fan-shape proximally. Morphotype B has a better developed scapula spine that *Ischigualastia* where it is represented by a ridge and none is described for *Jachaleria*, however, the scapula spine is better developed in *Placerias* and *Stahleckeria*. The acromion is present and well developed in Morphotype B, *Placerias* and *Stahleckeria* but is more prominent in Morphotype B whereas in *Jachaleria* it is reduced to a knob and is absent in *Ischigualastia*. The acromion is directed more laterally and is narrower in *Stahleckeria*. In morphotype B the scapula glenoid facet is narrower and smaller than that of *Placerias*, *Stahleckeria, Ischigualastia* and *Jachaleria*. Like in Morphotype B the glenoid is directed ventrally in *Stahleckeria*. The coracoid foramen is located within the precoracoid below the scapula border in Morphotype B, *Placerias* and *Stahleckeria* while it is located between the precoracoid and scapula in *Ischigualastia* and *Jachaleria*.

The humerus of Morphotype B is more gracile than that of the stahleckeriids. In Morphotype B the proximal expansion is wedge –shaped whereas in *Placerias, Ischigualastia* and *Stahleckeria* it is rectangular and more robust. The humeral head is raised above the dorsal surface in Morphotype B, *Placerias, Ischigualastia* and *Stahleckeria*. It is located closer to the posterior border of the proximal expansion in

Wits ETD

Morphotype B and *Stahleckeria* and closer to the anterior border in *Placerias* and *Ischigualastia*. The delto-pectoral crest is short and directed more dorsally in Morphotype B and *Placerias* while it is long and directed more anteriorly in *Stahleckeria* and *Ischigualastia*. In Morphotype B and *Placerias* the delto-pectoral crest is at an angle (less than 90°) to the long axis of the bone and is at 90° to the long axis of the bone in *Ischigualastia* and *Stahleckeria*.

In Morphotype B the olecranon is low and wide while it is elongated, narrow and separately ossified in *Placerias, Ischigualastia* and *Jachaleria;* however, in *Stahleckeria* the olecranon is triangular, broad and robust. The sigmoidal facet is longer and has a more concave surface in *Placerias, Ischigualastia, Stahleckeria* and *Jachaleria* than in Morphotype B. *Jachaleria* has a more elongated and more concave radial facet than Morphotype B while *Placerias* has a smaller and more concave radial facet than Morphotype B.

The femur of *Stahleckeria* and *Ischigualastia* is more robust than that of Morphotype B, *Placerias* and *Jachaleria*. In Morphotype B the femoral head is oval while it is round in *Placerias, Stahleckeria* and *Ischigualastia*. The femoral head is separated from the rest of the bone by an incipient neck in *Placerias* and a distinct neck in *Ischigualastia* while the head is separated from the greater trochanter by a groove in Morphotype B and *Stahleckeria*. In *Jachaleria* the femoral head is continuous with the greater trochanter. The femoral head is located well above the greater trochanter in *Placerias, Stahleckeria* and *Ischigualastia* while in Morphotype B they are at the same level. In Morphotype B, *Placerias* and *Jachaleria* the greater trochanter is long and narrow but it is short and wide in *Stahleckeria* and *Ischigualastia*. The shaft of the femur is narrower and straighter in *Placerias* and *Stahleckeria* than Morphotype B. In *Ischigualastia* the shaft is narrower than in Morphotype B but the posterior border is as concave as in Morphotype B.

The above comparison although preliminary at this time (because it is based solely on photos and literature) shows that Morphotype B does share certain features of the postcranial skeleton with various members of the stahleckeriids. This again raises questions about the possibility of a stahleckeriid in subzone B of the *Cynognathus* Assemblage Zone. These preliminary results once again places emphasis on the need to re-

Wits ETD

examine material previous assigned to *K. simocephalus* and for more directed field work with respect to Morphotype B.

6.3 Comparative Functional Anatomy

6.3.1 Comparative Functional Morphology

The glenoid of *K. simocephalus* and Morphotype B is made up of the scapula and coracoid. In *K. simocephalus* the glenoid facet of the scapula is directed postero-ventrally and the concave surface of the coracoid facet is short with the articulating surface directed slightly laterally. The head of the humerus is directed anteriorly and slightly dorsally. This would suggest that the humerus was in a fairly horizontal position, and that the delto-pectoral crest would be directed medially. In Morphotype B the glenoid facet of the scapula is expanded laterally and directed ventrally, and the coracoid facet is longer and directed ventro-laterally. The humeral head of this morphotype is directed dorsally and is hemispherical. It is probable that the humerus of Morphotype B was in a more upright position, which would have caused the forelimb to be closer to the saggital plane. This more upright position of the humerus would place the delto-pectoral crest in a more anterior facing position.

On the proximo-posterior corner of the medial surface of the acromion of *K. simocephalus* there is a tubercle. To date this tubercle has not been noted in any other Triassic dicynodonts. In BP/1/5624 the tubercle surface is rugose and the shape of the tubercle is different when compared with that of BP/1/6160. The distortion of the surface of the tubercle of BP/1/5624 could have been caused by a violent removal of the ligament that may have attached there. This tubercle is possibly the insertion for a ligament that would have functioned to stabilise the clavicle articulation thereby stabilising the pectoral girdle. This may suggest that the pectoral girdle of *K. simocephalus* required greater stability. In the same position in Morphotype B there is a shallow, broad oval fossa. The surface is smooth and covered by long parallel striations. This would indicate that this was an attachment site for a muscle tendon. As a result of the limb being closer to the saggital plane this muscle possibly had been converted to function like a ligament. The proximal half of the scapula blade is angled anteriorly to the distal half of the bone and it is likely

WitsETD

that this allowed forces from the humerus to be dispersed along the scapula, and may well be related to the upright position of the humerus.

An examination of some skeletal material belonging to ELM 1 is considered to be of uncertain affinity; however, it is possible that these elements could belong to the Morphotype B. The acetabulum of *K. simocephalus* faces laterally and the medially inflected head of the femur would suggest that it is held in a more upright position. This would place the hindlimb more under the body and would allow the hindlimb to produce a more effective propulsive stroke during locomotion. It was noted during a comparison of the pelvic girdle of ELM 1 with other specimens of *K. simocephalus* that it does not conform to features of the pelvic girdle of *K. simocephalus*. The acetabulum of ELM 1 faces ventrally and the antero-dorsal facing femoral head would suggest that this particular pelvic girdle belongs to the second morphotype. This would allow the femur to take an upright position; however, it may not have been as close to the body as in *K. simocephalus*. The supra-acetabular notch is wider in the ELM 1 specimen than in *K. simocephalus*. It is possible that this would provide a groove for the passage of a ligament from above the supra-acetabular ridge to the head of the femur. In both *K. simocephalus* and Morphotype B it would most likely have functioned to stabilise the acetabular joint and maintain the position of the femur, thereby preventing dislocation of the joint.

6.3.2 Comparative Muscle Architecture of *K. simocephalus* and Morphotype B

6.3.2.1 Pectoral Girdle and Forelimb

In mammals the muscles of the pectoral girdle attach the forelimb to the body so that the trunk hangs suspended between the two forelimbs (domesticated equids and bovids) (Bezuidenhout *et al*. 1996). These muscles also assist in the movement of the head, neck and trunk when the forelimb bears weight (Bezuidenhout *et al*. 1996). As there is no evidence of bony attachment of the pectoral girdle and forelimb in therapsids, the muscles of the pectoral girdle must have fulfilled a similar role.

The trapezius muscle in mammals (domesticated equids and bovids) consists of two parts: a cranial and thoracic part (Bezuidenhout *et al.* 1996). In mammals (domesticated equids

Wits ETD

and bovids) the cranial part inserts onto the length of the scapula spine, and the thoracic part inserts on the proximal third of the scapula spine (Bezuidenhout *et al.* 1996), while in reptiles the anterior part inserts along the cranial margin of the suprascapula cartilage and the distal (dorsal) half of the clavicle (Jenkins & Goslow 1983). The posterior part inserts on the cranial half, on the lateral surface of the suprascapula cartilage (Jenkins & Goslow 1983). In *Kannemeyeria* the scapula spine extends to the proximal border of the acromion. The acromion is narrow, which makes the spine longer. In *K. simocephalus* this provides sufficient area for the insertion of the trapezius muscle (figure 12). In Morphotype B the scapula spine starts only halfway down the blade and the acromion is wider which makes the spine shorter (figure 12). This provides much less area for the insertion of the trapezius muscle. It is therefore possible that this muscle was smaller in the second morphotype.

In reptiles the latissimus dorsi muscle originates by aponeurosis that attaches to the spinous process and interspinuous ligament of the eighth cervical vertebra to the third lumbar vertebra as well as the muscles and ribs on the lateral surface of the thorax (Jenkins & Goslow 1983). It inserts on the linear sulcus (dorsal humerus between the proximal and middle third) (Jenkins & Goslow 1983). Bezuidenhout *et al.* (1996) show that in mammals (domesticated equids and bovids) the latissimus dorsi originates on the thoraco-lumbar fascia by aponeurosis and the last three ribs. This muscle inserts on the *tuberculum teres major* and fascia on the medial side on the *M. triceps brachii caput longus* (Bezuidenhout *et al.* 1996). The insertion of the latissimus dorsi muscle is along the posterior border of the humerus in Permian dicynodonts and in Triassic dicynodonts, it inserted on a tubercle on the posterior border of the humerus (King 1981b; Walter 1986). Approximately a third of the way down from the dorsal border on the posterior border of the humerus of *K. simocephalus* is a posterior projecting oval tubercle (figure 13). In Morphotype B this tubercle is located closer to the dorsal border of the humerus and is small round (figure 13). The variation in the position and size of this tubercle would suggest that it is possible the latissimus dorsi muscle was slightly larger in *K. simocephalus* than in Morphotype B.

The pectoralis muscle in mammals (domesticated equids and bovids) consists of three parts. The *M. pectoralis descendens* which originates on the manubrium sterni, the second part, the transversus originates ventrally on the sternum from the *manubrium sterni* to the third costal cartilage and the third part the profundus which originates on the ventral midline on the sternum (major part) and the abdominal fascia (minor part) (Bezuidenhout

et al. 1996). The first two parts insert on the *crista tuberculi majoris* of the humerus while the major part of the profundus inserts on the *tuberculum minus* of the humerus as well as the by aponeurosis on the *tuberculum majus* and the minor part blends with the fascia on the medial aspect of the brachium (Bezuidenhout *et al*. 1996). In reptiles the pectoralis muscle is also divided into three parts: the anterior part originates on the interclavicle, the posterior margin of the proximal half of the lateral process and the lateral margin anterior half of the medial process, and it inserts on the apex of the delto-pectoral crest (Jenkins & Goslow 1983). The middle part of the muscle originates on the posterior half of the medial process of the interclavicle (sternum in the midline and the sternocostal cartilage of the second and third thoracic ribs) and it inserts across the entire lateral surface of the delto-pectoral crest (Jenkins & Goslow 1983). The posterior part originates in the midline along the *linea alba* and from the thoracolumbar fascia at the level of lumbar vertebrae three and four and it inserts on the distal margin of the delto-pectoral crest (Jenkins & Goslow 1983). In the Triassic dicynodonts the pectoralis muscle inserts on the delto-pectoral crest which is homologous with the *crista ventralis* in salamanders (Walter 1986). In *D. trigonocephalus* the muscle originated on the ventral surface of the interclavicle and sternum (King 1981b). Defauw (1986) cited the median ridges and adjacent fossae on the interclavicle and sternum as origin sites for the pectoralis muscle in Permian dicynodonts. The ventral surface of the delto-pectoral crest was the insertion site for this muscle (King 1981b; Defauw 1986).

Unfortunately, no interclavicle or sternum is preserved for Morphotype B. Only the interclavicle is preserved for *K. simocephalus* and on its ventral surface there are two tubercles anteriorly situated and bordered medially by wide grooves. In *K. simocephalus* these would provide ample area for the origin of the pectoralis muscle. *M. pectoralis* would have inserted on the ventral surface of the delto-pectoral crest of *K. simocephalus* (figure 13) and Morphotype B (figure 13). The delto-pectoral crest of *K. simocephalus* is longer than that of Morphotype B, which again suggests that the pectoralis muscle was of a more substantial size in *K. simocephalus*.

The levator scapulae muscle is made up of two parts in reptiles: the dorsal part, which originates on the lateral process of the atlas to the fourth cervical vertebrae, and the aponeurosis covering the epaxial muscle, inserts on the lateral surface of the suprascapula adjacent to the anterior margin via aponeurosis (Jenkins & Goslow 1983). Its ventral part

Wits ETD

originates via the same atlantal tendon of the dorsal part, and it inserts by fibres on the anterior border of the scapula and the dorsal third of the clavicle (Jenkins & Goslow 1983). Romer (1922) noted that this muscle was actually part of the serratus anterior muscle. In Triassic dicynodonts the serratus anterior muscle inserts on the proximo-posterior corner of the scapula blade on the lateral and medial surfaces (Walter 1986). The serratus muscle inserts on the dorsal part of the medial surface of the scapula blade (Defauw 1986). On the scapula of *K. simocephalus* the dorsal border is expanded antero-posteriorly with both ends slightly blunt (figure 12), while the anterior margin of Morphotype B is rounded anteriorly (figure 12). In Morphotype B the blunt posterior border is slightly thicker than the anterior part of the dorsal border, while in *K. simocephalus* the posterior border is slightly thickened. These areas are not very large and would suggest that the serratus muscle in both animals was not very large.

The deltoideus muscle in mammals (domesticated equids and bovids) originates from the scapula spine below the *M. infraspinatus* by a broad aponeurosis and the acromion part of the scapula, while it inserts on the deltoid tubercle of the humerus (Bezuidenhout *et al*. 1996). Its clavicle part has become part of the *M. brachiocephalus* (Bezuidenhout *et al*. 1996). In reptiles the deltoideus muscle is made up of two parts, the scapula part and the clavicular part (Jenkins & Goslow 1983). The smaller dorsal head of the clavicle part originates from the dorsal surface of the interclavicle while the larger ventral head originates from the ventral surface of the proximal third of the clavicle and the ventral surface of the interclavicle at the junction of the median and transverse processes (Jenkins & Goslow 1983). Both parts insert on the antero-dorsal surface of the proximal end of the humerus between the head and the delto-pectoral crest (Jenkins & Goslow 1983).

The scapula part of the deltoideus originates from a narrow linear area that extends from the lateral surface of the suprascapula and scapula to the dorsal (distal) end of the clavicle and inserts on the antero-dorsal surface of the proximal end of the humerus (Jenkins & Goslow 1983). The deltoideus muscle originated on the lateral surface of the scapula and on the clavicle of *D. trigonocephalus*, and had the same origin in the Triassic dicynodonts (King 1981b; Walter 1986). Defauw (1986) in her study of African dicynodonts had the origin of the deltoideus muscle along the cranial border of the scapula blade, and included the suprascapula cartilage.

Wits ETD

In Triassic dicynodonts the deltoideus muscle inserted on the dorsal surface of the delto-pectoral crest (Walter 1986), however, in *D. trigonocephalus* the deltoideus muscle inserted on the proximal end of the delto-pectoral crest (King 1981b). Defauw (1986) situated the insertion of the deltoideus muscle antero-laterally on the proximal part of the delto-pectoral crest. The lateral surface of the scapulae of *K. simocephalus* and Morphotype B is concave posterior to the posterior margin of the scapula spine (figure 12). The fossae end half way down the spine and the one on the scapula of Morphotype B is narrower and shorter than that of *K. simocephalus*. It would suggest that in both *K. simocephalus* and Morphotype B the deltoideus muscle is a broad, well developed muscle.

In mammals (domestic bovids and equids) the teres minor muscle originates from the infraglenoid tuberculum and the distal caudal margin of the scapula (Bezuidenhout *et al.* 1996). The scapulo-humeralis anterior, which is equivalent to the teres minor muscle, has two heads in reptiles (Jenkins & Goslow 1983). One head originates from the antero-lateral surface and anterior margin of the scapula and the second head from the lateral and dorsal margin of the coracoid cartilage and the coracoid itself (Jenkins & Goslow 1983). Walter (1986) shows that in Triassic dicynodonts the origin of the scapulo-humeralis anterior muscle would have been on the lateral surface of the scapula in front of the origin of the scapula head of the triceps. The origin of this muscle in *D. trigonocephalus* was also in a fossa in front of the triceps origin on the scapula (King 1981b). In Morphotype B and *K. simocephalus* there is a narrow fossa in front of the triceps origin (figure 12). This would have provided sufficient space for a tendon of origin for the scapulo-humeralis anterior.

The teres minor muscle inserts on the teres minor tuberculum on the *Linea m. tricipitis* of the humerus (domesticated equids and bovids) (Bezuidenhout *et al.* 1996) while in reptiles both heads of the scapulo-humeralis converge to insert on the dorso-medial surface of the humerus proximal to the insertion of latissimus dorsi (Jenkins & Goslow 1983). In *D. trigonocephalus* the scapulo-humeralis anterior muscle would have inserted in the fossa on the antero-dorsal proximal surface of the humerus (King 1981b) while in the Triassic dicynodonts the insertion was in front of the head on the dorsal surface above the dorsal extent of the delto-pectoral crest (Walter 1986). In front of the humeral head the surface above the dorsal border of the delto-pectoral crest is a concave surface in both *K. simocephalus* and Morphotype B, which would have been the area for insertion for the scapulo-humeralis muscle (figure 13).

Wits ETD

The subscapular muscle in mammals (domesticated equids and bovids) originates on the subscapula fossa and inserts on the *tuberculum minor* (Bezuidenhout *et al.* 1996). In reptiles the equivalent muscle is the scapulo-humeralis posterior, which originates on the posterior half of the lateral surface of the scapula and suprascapula, and inserts on the dorsal surface of the lesser tubercle (Jenkins & Goslow 1983). Both heads converge to insert on the dorso-medial surface of the humerus proximal to the insertion of latissimus dorsi (Jenkins & Goslow 1983). Defauw (1986) referred to her reconstruction of the muscle in *Lystrosaurus*, which she reconstructed as originating the flat lower half of the scapula blade (Defauw 1981). Above he origin of the scapula head of the triceps in *K. simocephalus* the posterior margin of the scapula is flattened, which provides ample space for the origin of the scapulo-humeralis posterior muscle (figure 12). On the second morphotype, the surface above the scapula head of the triceps the posterior border is not as flat as that of *K. simocephalus* (figure 12). The surface would be sufficient for an area of origin for scapulo-humeralis posterior muscle. The posterior corner of the dorsal border of the humerus is flattened and thick providing an area of insertion for the posterior scapulo-humeralis muscle. In Morphotype B the proximo-posterior corner when viewed ventrally is flattened slightly antero-posteriorly and forms a rounded, thick area for the insertion of the scapulo-humeralis posterior muscle.

In mammals (domesticated equids and bovids) the triceps muscle is made up of four heads: the long head, which originates from the infraglenoid tubercle and the caudal margin of the scapula, the lateral head that originates on the *Linea m. tricipitis* of the humerus, the medial head from the *crista tuberculi minoris* of the humerus and the accessory head from the caudal surface of the humeral neck (Bezuidenhout *et al*. 1996). All the heads of the muscle insert on the olecranon of the ulna (domesticated equids and bovids) (Bezuidenhout *et al*. 1996). In retiles the triceps comprises three heads: the lateral head originates from the entire antero-dorsal surface of the humeral shaft, the long head (scapula) has two origins: a posterior one from the caudal border of the cranio-dorsal ligament and the postero-lateral surface of the scapula and an anterior origin from the caudal margin of the sternoscapula ligament and the latissimus dorsi (Jenkins & Goslow 1983). The medial head's origin is on the entire dorso-medial surface of the humerus and along with the other heads of the triceps it inserts on the olecranon (Jenkins & Goslow 1983).

Wits ETD

In *K. simocephalus* (round tubercle) and Morphotype B (oval tubercle) there is a tubercle along the posterior border of the scapula for the origin of the scapula head of the triceps (figure 12). On the humerus of *K. simocephalus* there is a broad fossa in front of the posterior border for the origin of the medial head, and the lateral head could originate from the tubercle on the dorsal surface of the posterior border of the humeral shaft (figure 13). Due to the only the proximal end of the humerus being preserved in Morphotype B, only the possible origin of the medial head of the triceps can be ascertained. This is a narrow fossa in front of the posterior border (figure 13). These muscles all have a single insertion site, the olecranon of the ulna, however, the olecranon of *K. simocephalus* is a narrow triangle, and that of Morphotype B is antero-posteriorly broad and very low (plate 5a; plate 16a).

The coracobrachialis and biceps muscles originated along the ventral border of the coracoid plate and the coracobrachialis muscle inserted in the biccipital fossa and distal end of the delto-pectoral crest (Walter 1986). The biccipital fossa of *K. simocephalus* is large, shallow and rectangular, while that of Morphotype B forms a narrow, deep triangle (figure 13).

The extensors would have originated on the ectepicondyle and the flexors on the entepicondyle (Walter 1986). The entepicondyle of *K. simocephalus* is flared and thickened towards the ventral end and provides the area for the origin of the flexors. In *K. simocephalus* the ectepicondyle is also flared but is thin, providing ample area for the origin of the extensors (figure 13).

Defauw (1986) showed that the deltoideus, pectoralis, supracoracoideus, scapulo-humeralis anterior and posterior, latissimus dorsi and coracobrachialis muscles are all single joint muscles of the glenohumeral joint. With the exception of the pectoralis and latissimus dorsi muscles the remaining muscles act to stabilise the joint (Defauw 1986). Defauw (1986) also suggests that the glenohumeral joint was stabilised by a cruciate ligament.

Wits ETD

6.3.2.2 The Pelvic Girdle and Hindlimb

The ilio-femoralis muscle originated on the lateral surface of the ilium blade in Triassic dicynodonts and inserted on the greater trochanter (Walter 1986). Yuhe (1983) applied the mammalian terminology to the muscle and showed that the origin of the gluteus muscle was divided into sections the: gluteus maximus from the dorsal fascia and dorsolateral ilium; gluteus medius from the middle of the ilium and the gluteus minimus from the upper part of the ilium. The insertion was divided into two sections: the greater trochanter and the third trochanter (Yuhe 1983). The ilio-femoralis muscle originates on the ilium in reptiles and inserts on the upper surface of the femur (Cluver 1978). In mammals (domesticated equids and bovids) the gluteus muscle is divided in three: the superficial gluteus muscle originates on the sacrum and *Crista iliaca* and inserts on the fourth trochanter of the femur, the middle gluteus muscle originates on the internal surface of the facies gluteus of the ilium and inserts on the major trochanter while the deep gluteus originates on the *spina ischiadica* and the ilium shaft, and inserts on the major trochanter (Bezuidenhout *et al*. 1996). *M. ilio-femoralis* originated on the lateral surface of the ilium blade of *Kannemeyeria* and as in *Cistecephalus* (Cluver 1978) this muscle inserts on the greater trochanter (figure 15; figure 11).

The ilio-femoralis muscle would have originated most likely as a single muscle mass on the lateral surface of the ilium blade in *K. simocephalus* (figure 14), and the presence of only a greater trochanter on the femur would suggest that there was only a single insertion site for this muscle. In Morphotype B the situation may have been different as the presence of the greater trochanter and a third trochanter suggests that the ilio-femoralis (or gluteus muscle in this case) was divided into possible insertions (figure 15).

In mammals (domesticated equids and bovids) the obturator internus muscle originates on the dorsal surface of the ischium and pubis, on the periphery of the obturator foramen and the medial ilium shaft (Bezuidenhout *et al*. 1996). The ischio-trochanteric muscle (obturator internus) in *Cistecephalus* originated from the medial surface of the ischium and inserted on the femoral head (Cluver 1978), which was most likely the case in *K. simocephalus* as well. In mammals (domesticated equids and bovids) originates on the ventral surface of the pubis and ischium and the *Tendo symphysialis* and inserts on the *Facies aspera* (Bezuidenhout *et al*. 1996). The adductor muscle had its origin on the pubo-ischiadic plate and its insertion on the ventral surface of the femur (Cluver 1978). The

Wits ETD

muscle more than likely had its origin on the pubo-ischiadic plate in *K. simocephalus* and its insertion on the ventral surface was probably in the fossa in front of the head of the femur (figure 14; figure 15).

M. ambiens (*M. quadratus femoris*) originates on the ventral surface of the ischium in mammals (domesticated equids and bovids) and inserts distal to the *Fossa trochanterica* (Bezuidenhout *et al*. 1996). In Triassic dicynodonts the *M. ambiens* originated on the pubic tubercle and the area above it (Walter 1986). The pubic tubercle of *K. simocephalus* is round and the surface is covered by ridges which would have provided enough area for the origin the ambiens muscle (figure 14). Walter (1986) and Defauw (1986) reconstructed the adductors of the femur as originating on the ventral edge of the pubo-ischiadic plate. The pubo-ischio femoralis muscle originated on the lateral surface of the pubo-ischiadic plate above the adductor muscles (Defauw 1986). On the dorsal surface of the femur Defauw (1986) placed the origin of the femoro-tibialis muscle in the fossa between the greater trochanter and the head. In *Lystrosaurus*, *Oudenodon* and *Kingoria* the origin of the femoro-tibialis muscle extends down the shaft of the femur and onto the ventral surface of the shaft. In *K. simocephalus* there is a broad groove on the femur shaft and this would suggest that the origin of the femoro-tibialis muscle may have also have extended down the shaft (figure 15). In Morphotype B there is a groove that extends from the fossa between the head and the greater trochanter towards the anterior border, however, it is very narrow and may not be sufficient for an expanded origin of the femoro-tibialis muscle (figure 15).

The *Fossa extensoria femoris* is the origin for the digital extensors in mammals (domesticated equids and bovids) and it inserts extensor process of P3 (digit III) in horses and on the medial extensor process of P2 (digit III) and lateral extensor process P2 (digit III) in bovids (Bezuidenhout *et al*. 1996). Defauw (1986) has placed the origin of the digital extensor above the posterior condyle of the femur. In both Morphotype B and *K. simocephalus* there is a groove above the posterior condyle that extends up the shaft. This area would have provided a suitable area for the origin of the digital extensor (figure 15).

M. gastrocnemius originates on the lateral and medial supracondylar tubercle of the femur in mammals (domesticated equids and bovids) and inserts on the *Tuber calcanei* (Bezuidenhout *et al*. 1996). The gastrocnemius muscle was positioned above and between the femoral condyles in *Oudenodon* and *Lystrosaurus* and with an origin above each of the

Wits ETD

condyles in *Kingoria* (Defauw 1986). In *K. simocephalus* there is a fossa between the condyles on the ventral surface, which would have provided a suitable area for the origin of the gastrocnemius muscle. On the distal ventral surface of the femur of Morphotype B there is a broad, semi-circular fossa between the condyles. This fossa is positioned lower than that of *K. simocephalus* and it would have been the site for the origin of the gastrocnemius muscle. Most of the muscle of the pelvic girdle and hindlimb also act in most instances to stabilise the acetabulofemoral joint. Some of the muscles act to extend and flex the hips and knee joints.

6.4 Phylogenetics

6.4.1 Analysis of the relationships of *K. simocephalus* and Morphotype B

This current analysis is a preliminary investigation into the relationship of the two postcranial morphotypes found in the *Cynognathus* Assemblage Zone (subzone B) of South Africa. The preliminary results would tend to support the analysis of the gross morphology which has suggested that the two morphs are significantly different from each other.

Fifty-six characters were included in the analysis. A potential character was excluded from the analysis. It concerns the presence of a tubercle at the proximo-posterior corner of the medial surface of the acromion (seen in *K. simocephalus*) and an elongated fossa in the same position (in Morphotype B). After consulting the literature of other Triassic dicynodonts it was found that this part of the scapula was not described and could only be considered indeterminate in all other taxa. Therefore this character was removed from the analysis because the coding would provide no information.

As in the analysis of Vega-Dias *et al* (2004) a number of taxa have not been considered in this study due to the lack of information about their postcranial anatomy, viz. *Vinceria*, *Rhinodicynodon, Rhadiodromus, Rechnisaurus* and *Sangusaurus*. In the initial analysis which included both cranial and postcranial characters *K. simocephalus* form a polytomy with *Wadiasaurus* and the sinokannemeyeriines of Maisch (2001). The sister group of *Shansiodon-Tetragonias* was reproduced but in this analysis it does not form part of the

Wits ETD

polytomy with *K. simocephalus* as in Vega-Dias *et al* (2004). In this analysis the family Kannemeyeriidae was not reproduced as in Vega-Dias *et al* (2004). *K. simocephalus* is positioned among the basal Triassic dicynodonts.

The current analysis reproduced the Stahleckeriidae of Maisch (2001) which includes *Stahleckeria, Angonisaurus, Ischigualastia, Jachaleria* and *Placerias*. Morphotype B forms a sister group relationship with *Placerias*, which places Morphotype B within the Stahleckeriidae. The *Placerias* – Morphotype B clade is currently in a basal position among the stahleckeriids. Morphotype B and *Placerias* form the sister group to the Stahleckeriinae of Maisch (2001) and the *Ischigualastia* – *Jachaleria* clade of Vega-Dias *et al* (2004).

The relationships of *K. simocephalus* are not resolved in the most parsimonious trees, which may be an indication that some of the characters being used are not as informative as previously thought. Resolution of the relationships of Morphotype B is also lost relatively easily in the decay and bootstrap analyses. The weak support of the relationships of Morphotype B is probably due to the fact that there is no cranial material currently known for this taxon.

This analysis has shown that *K. simocephalus* and Morphotype B fall into two distant positions on the cladogram. *K. simocephalus* is located among *Wadiasaurus, Sinokannemeyeria, Parakannemeyeria, Shansiodon* and *Tetragonias*. Morphotype B is located with *Stahleckeria, Placerias, Angonisaurus, Ischigualastia* and *Jachaleria*. These taxa together form the family Stahleckeriidae of Maisch (2001). The current position of Morphotype B suggests that it is a stahleckeriid. In 67% of the most parsimonious trees *K. simocephalus* forms the sister group to *Dinodontosaurus*- stahleckeriid clade. The *Placerias* – Morphotype B clade is reproduced in 100% of the most parsimonious trees.

The postcranial analysis showed *K. simocephalus* forming a polytomy with a number of the Triassic dicynodonts. These include *Wadiasaurus, Sinokannemeyeria, Parakannemeyeria, Shansiodon, Tetragonias, Angonisaurus* and *Dinodontosaurus*. The postcranial anatomy of *K. simocephalus* is well-known, therefore the polytomy is probably as a result of the lack of knowledge of the postcranial anatomy of the remaining taxa. Morphotype B remains within the Stahleckeriidae. It is positioned as the sister group of

Wits ETD

Stahleckeria and *Ischigualastia – Jachaleria* and not *Placerias*. *Angonisaurus* does not retain its position among the Stahleckeriidae in this analysis because there is very little postcranial material available. The material that is available for study from the *Cynognathus* Zone of South Africa is also fragmentary.

In the analysis that included both cranial and postcranial characters the CI (0.45) and RI (0.523) indices are lower than that of Vega-Dias *et al* (2004) (0.48 & 0.58 respectively). The consistency index of the postcranial analysis is 0.43. In this study the consistency index is lower than that of the analysis that included both cranial and postcranial characters. This would again suggest a lot of homoplasy amongst the Triassic dicynodonts. The presence of homoplasy among the Triassic dicynodonts has been considered the main reason for there being so few postcranial characters that can distinguish the different taxa from each other (Vega- Dias *et al* 2004) and that the uniformity of the postcranial anatomy of Triassic dicynodonts makes it difficult to identify diagnostic characters that are useful in a phylogenetic analysis (Vega-Dias *et* al 2004). This analysis of the postcranial anatomy of *K. simocephalus* has, however, shown that the postcranial anatomies of the different taxa are able to produce characters that are informative in phylogenetic analyses. It also brings to the fore the urgent need to generate interest in the study of the postcranial anatomy of Triassic dicynodonts (as stated in Vega-Dias *et al* (2004)). In the current phylogenetic analysis as in Vega-Dias *et al* (2004) there is more resolution in the relationships of the South American Triassic dicynodonts as they all have been studied in much greater detail and according Vega-Dias *et al* (2004) they also have greater numbers of specimens.

Analyses were also performed which excluded the problematic taxon *Dinodontosaurus*. In the analysis that included both the postcranial and cranial characters *Kannemeyeria* and *Wadiasaurus* forms a polytomy with the sinokannemeyeriines of Maisch (2001) and the stahleckeriids. A possible explanation for the changing position of *K. simocephalus* between the analysis that included and excluded the South American taxon *Dinodontosaurus* may well consist of more than one taxon. *Dinodontosaurus* is possibly the reason that the position of *K. simocephalus* changes among the Triassic dicynodonts.

Morphotype B forms a polytomy with *Placerias* and the Stahleckeriinae of Maisch (2001). It would appear from the analysis that the presence or absents of *Dinodontosaurus* has no

Wits ETD

effect on the family Stahleckeriidae of Maisch (2001). It also seems to have had little effect on the relationship of Morphotype B among the stahleckeriids.

In the postcranial character analysis that excludes *Dinodontosaurus*, *K. simocephalus* forms a polytomy with *Angonisaurus, Stahleckeria* and *Wadiasaurus* and *Tetragonias* and a new clade consisting of the sinokannemeyeriines (of Maisch 2001) and the remaining stahleckeriids (including Morphotype B). *Stahleckeria* may have formed part of this polytomy as a result of its relationship with *Angonisaurus*, which has very little postcranial known and that material is also fragmentary.

The sister group relationship of Morphotype B with *Placerias* is also retained in the postcranial analysis. In the majority rule tree *K. simocephalus* forms the sister group of Morphotype B + *Placerias*. Once again the relationship between Morphotype B and *Placerias* is maintained. The position of *K. simocephalus* as the sister group to Morphotype B – *Placerias* is weakly supported while once again the relationship between Morphotype B and *Placerias* is well supported.

The consistency index (≈ 0.49) of the analysis (cranial & postcranial characters) is higher than that of the initial analysis (0.423) and that of Vega-Dias *et al* (2004), however its retention index of ≈ 0.55 is lower than that of Vega-Dias *et al* (2004) but higher than that in this study's initial analysis. In the postcranial analysis the CI is 0.46 and the RI is 0.51 which are both higher than the initial than the initial postcranial analysis. These figures again suggest a high degree of homoplasy among the postcranial anatomy of the Triassic Kannemeyeriiformes (Maisch 2001).

It is also noticeable that most of the African and the South American Kannemeyeriiformes (Maisch 2001) are more closely related with the exception of *Tetragonias*. *Tetragonias* forms the Shansiodontidae (of Maisch 2001) with *Shansiodon*. The Asian Kannemeyeriiformes (Maisch 2001) tend to form a grouping of their own. The Dinodontsauridae was not reproduced in this current analysis, which suggests that the relationships within the family are very weak as suggested by Vega- Dias *et al* (2004). In this analysis the evolutionary lines of *Kannemeyeria* and *Placerias* have remained distinct as suggested by Cruickshank (1972).

Wits ETD

Based on the unexpected result of the phylogenetic analysis a Templeton test was performed in order to determine how significant the result actually was. One of the most parsimonious trees was compared with an artificial one that nested *K. simocephalus* and Morphotype B together. The P value was ≈ 0.48 which suggests that these two hypotheses are not significantly different. This implies that the hypothesis that places Morphotype B among the stahleckeriids is not very well supported, however, it must be noted that currently there is no known cranial material attributed to Morphotype B.

6.4.2 Palaeobiogeography Implications

The relationships established in the phylogenetic analysis have interesting biogeographic implications. *K. simocephalus* from the *Cynognathus* Assemblage Zone (subzone B) of South Africa forms a polytomy with *Wadiasaurus* from India and, *Sinokannemeyeria* and *Parakannemeyeria* from China. It has been suggested by Renaut (2000) that the Asian and Russian kannemeyeriids could be accommodated within the *Kannemeyeria*. In order for this to be proved or disproved requires a reinvestigation of the Asian and Russian kannemeyeriids. If these animals can be accommodated within *Kannemeyeria*, this would give *Kannemeyeria* a wider geographic distribution not only geographically but temporally as well.

An interesting result of the phylogenetic analysis was that Morphotype B nested within the Stahleckeriidae. Morphotype B from the *Cynognathus* Assemblage Zone (subzone B) of South Africa forms a clade with *Placerias* from North America which is considered a highly advanced form of stahleckeriid. Camp (1956) considered *Placerias* as having diverged from the South American stahleckeriids to follow a separate evolutionary path. Previously, the only stahleckeriid known from Africa was *Angonisaurus* from East Africa (Cox & Li 1983) and more recently from South Africa (Hancox & Rubidge 1995). In the phylogenetic analysis *Angonisaurus* forms a clade with *Stahleckeria* from South America. In both instances the African stahleckeriids form relationships with 'new world' stahleckeriids.

It has been suggested by Vega-Dias *et al* (2004) that stahleckeriids possibly originated in Africa and underwent an initial adaptive radiation here before moving into the Americas.

WitsETD

The presence of Morphotype B in the *Cynognathus* Assemblage Zone of South Africa makes this the earliest occurrence of the Stahleckeriidae. It would also lend support to the theory that stahleckeriids originated in Africa (Morphotype B) underwent an initial radiation in Africa represented by *Angonisaurus* from South Africa and East Africa (Tanzania) as well as *Moghreberia,* sometime synonymised with *Placerias* (Vega-Dias *et al* 2004), from Morocco. This would have provided the stahleckeriids with an ideal route into the Americas.

6.5 Possible Identification of Morphotype B

Currently, due to recent work on the cranial morphology of *Kannemeyeria*, two species of *Kannemeyeria* are recognised in southern Africa, viz. *K. simocephalus* and *K. lophorhinus*. These two species are geographically and temporally separated and *K. simocephalus* is the only species known from South Africa.

There are three possible solutions to the identification of Morphotype B. First, Morphotype B could be a species of *Kannemeyeria* and included among the known sample of *Kannemeyeria* skulls from South Africa are skulls of Morphotype B. This is conjecture as there is currently no positively associated cranial material for Morphotype B. According to Renaut (2000) *Kannemeyeria* has a generalist cranial morphology therefore in this conjecture the driving evolutionary force would be changing the postcranial anatomy faster than the cranial morphology. This therefore does not preclude the inclusion of Morphotype B in *Kannemeyeria*.

In particular the more dorsally directed humeral articulating surface and the ventrally directed glenoid along with the antero-dorsally directed femoral head would imply that there may be improvement in the locomotor apparatus of this animal. This would have allowed Morphotype B to move more freely in its habitat. If Morphotype B is a species of *Kannemeyeria* then it is possible to presume that it also would have had a generalist cranial morphology, which would allow it to exploit a food source different to that *K. simocephalus*. The ability to move more freely in the habitat along with the ability of Morphotype B to possibly exploit different food sources would imply niche partitioning between the two morphotypes in the *Cynognathus* Assemblage Zone (subzone B).

WITS ETD

In order to determine if this is actually the case it will require a re-investigation of the localities where the two morphotypes co-occur. This will include identifying and excavating new specimens of both morphotypes. Importance will have to be placed on finding associated skulls and postcranial skeletons of both morphotypes.

Secondly, a tuskless *Kannemeyeria* has been described by Renaut *et al* (in press), which is isolated and has no associated with postcranial material. It is possible that the postcranial material denoted as Morphotype B may belong to this tuskless species. The position of this particular specimen among Triassic dicynodonts is not completely known, however, this is the most intriguing possibility as the tusks of most stahleckeriids have either been greatly reduced (e.g. *Placerias*) or are completely absent as in the stahleckeriines (e.g. *Ischigualastia)* (Vega – Dias *et al* 2004). It is also intriguing as Maisch (2001) also suggested that the stahleckeriid ancestor would have had a cranial morphology that represented an evolutionary phase similar to that of *Kannemeyeria*. If this postcranial morphology is found associated with cranial morphology then it does raise the question of a possible stahleckeriid ancestor. In order to determine if this is possible more field work will be required to investigate the locality where this skull was found.

The third possibility for identifying Morphotype B stems from the preliminary results of the phylogenetic analysis, which suggests that Morphotype B is positioned within the stahleckeriids. The result of the phylogenetic analysis suggests that a kannemeyeriid co-occurs with a stahleckeriid in the *Cynognathus* Assemblage Zone (subzone B) in South Africa. The co-occurrence of a stahleckeriid in the *Cynognathus* Assemblage Zone (subzone B) would make it the earliest occurrence of a stahleckeriid. In order to verify or negate this possibility, again more field work is required to locate a skull associated with postcranial material currently assigned to Morphotype B. Currently, Morphotype B is known from a limited number of localities. More fieldwork will be required to determine if Morphotype B is present at other localities in the *Cynognathus* Assemblage Zone (subzone B) of South Africa.

Wits ETD

CHAPTER SEVEN

CONCLUSION

The main aim of this project was to provide a detailed description of the postcranial skeleton of *K. simocephalus*. During the course of the study material assigned to *K. simocephalus* in South African institutions was re-examined. The material was compared with BP/1/5624, which has a skull and associated postcranial material positively identified as *K. simocephalus* (Renaut 2000). This comparison has raised questions about the identification of large postcranial material from the *Cynognathus* Assemblage Zone (subzone B) belonging only to *K. simocephalus*.

An examination of the postcranial skeleton of *K. simocephalus* also led to the identification characters that diagnose it. The presence of a tubercle on the medial surface of the scapula, the greater trochanter of the femur is parallel to the long axis of the bone and the articulating surface of the posterior condyle is lower than that of the anterior one. These features will allow at least some material to be identified either as *K. simocephalus* or to be removed from this taxon.

After a careful examination of the material assigned to *Kannemeyeria* it was found that some of the postcranial material was were different from what is currently understood to be *K. simocephalus*. The following are some of the more notable differences between this material and *Kannemeyeria simocephalus*. Proximally, the scapula blade is angled anteriorly in relation to the distal end. The acromion process forms a broad triangle in BP/1/994D and on the proximo-posterior corner of the medial surface of the acromion is an elongated fossa. On the humerus of this morph the delto-pectoral crest is arc shaped. The femora of this morph are dorso-ventrally flat with expanded proximal and distal ends. The oval head of the femur is directed antero-dorsally, and is continuous with the greater trochanter (trochanter major). At the distal end of the greater trochanter is an elongated oval third trochanter. Based on these differences this material is referred to as Morphotype B.

To date the most complete description of *K. simocephalus* is that of Pearson (1924b). During the course of this study some of this material was re-examined using photographs. The scapula, ulna and femora were found to be different from *Kannemeyeria*

Wits ETD

simocephalus, but rather resemble Morphotype B. This suggests that Pearson (1924b) was dealing with a mixed specimen. A re-examination of ELM 1 (considered the most complete *Kannemeyeria* specimen) found that it is also possibly a mixed specimen.

This would make BP/1/5624 the most complete *K. simocephalus* specimen currently known and thus makes it a suitable candidate for a referred type for the postcranial anatomy of *K. simocephalus*. This must be considered with caution because although the material is fairly complete more than one individual was identified as part of BP/1/5624.

Most of the material belonging to the new morph occurs as isolated elements. Some of the material has been found associated with material identified as *K. simocephalus*. At this juncture one cannot say for certain if this postcranial material is actually associated with the *K. simocephalus* skulls or is just mixed in with the postcranial material. This is a distinct possibility as all the material collected in the past that belonged to medium to large dicynodonts from the *Cynognathus* Assemblage Zone (subzone B) of South Africa was assigned to *K. simocephalus*. Even if the material identified as Morphotype B was collected separately it was most likely included in bulk lots under one catalogue number with *K. simocephalus*. Currently the specimen from Winnaarsbaken, particularly BP/1/994 and BP/1/3518 have no associated cranial material which precludes this material from being included in any taxon, known or new. It has therefore been concluded at this time to refer to this material as Morphotype B of the *Cynognathus* Assemblage Zone (subzone B) of South Africa. This material shows that *K. simocephalus* was not the only medium to large dicynodont in the *Cynognathus* B zone. The material of Morphotype B shows some similarities to *Zambiasaurus*, however, it must be noted that the *Zambiasaurus* material is that of a juvenile. Morphotype B has been shown to be significantly different from *Angonisaurus*; however, a preliminary comparison with the remaining members of the Stahleckeriidae shows that Morphotype B shares a number of postcranial morphological characteristics with them. Based on the photographs available it does appear to share a number of characteristics with *Placerias* in particular.

Morphotype B is currently only known from a limited number of localities and has been found as isolated elements associated with *K. simocephalus*. Based on information from collections both morphotypes occur in the same bone beds. This suggests that these morphs neither spatially nor temporally separated. The lack of cranial material for this second

Wits ETD

morphotype is somewhat puzzling as over the years over 200 hundred *Kannemeyeria* skulls have been collected from the *Cynognathus* Assemblage Zone (Subzone B). *Kannemeyeria* cranial morphology has been studied in great detail and so far there has been no identification of different cranial morphology. Recently, however, another possible candidate has come to the fore, a tuskless *Kannemeyeria* specimen described by Renaut *at al* (in press).

The morphs are sufficiently different from each so as to suggest that a phylogenetic analysis may shed some light on their relationship with each other and to other Triassic dicynodonts. It also provided an opportunity to determine if postcranial characters would be of use in a phylogenetic analysis.

The nature of the study of postcranial characters in the phylogenetic analysis of taxa is such that in many cases one has to rely upon literature in order to code for characters. A large number of the descriptions are not sufficiently detailed and lack photographic plates made it difficult to provide a complete analysis. In this particular analysis a number of taxa were removed particularly because of the paucity of information about their postcranial anatomy. It has again brought to the fore the need for more detailed studies of the postcranial skeletons of various dicynodonts.

The current analysis, however, has proved to be of value in some respects. In the case of *K. simocephalus* it relationship among the basal Kannemeyeriiformes appears to be less stable. It forms part of the basal array with the sinokannemeyeriines (of Maisch 2001) and *Wadiasaurus*, however, with the removal of *Dinodontosaurus* the sinokannemeyeriines are removed from this array and cluster with the stahleckeriids. In the analysis that excludes *Dinodontosaurus K. simocephalus* forms a sister group relationship with Morphotype B – *Placerias*.

Morphotype B forms a sister group relationship with *Placerias*, within the Stahleckeriidae (of Maisch 2001). Even though the decay and bootstrap analyses show that its relationship within the Stahleckeriidae is very weak, it is most likely that Morphotype B is a Stahleckeriid. The absence of cranial material for Morphotype B may be the reason for its weakly supported relationship within the Stahleckeriidae (of Maisch 2001).

Wits ETD

The analysis of the postcranial characters corroborated the position of Morphotype B within the Stahleckeriidae (of Maisch 2001). Morphotype B also retained its position within the Stahleckeriidae with the removal of the cranial characters although its sister group relationship with *Placerias* is dissolved in favour of a closer relationship to stahleckeriines. In both analyses Morphotype B – *Placerias* have a basal position among the Stahleckeriids. It leads to the conclusion that Morphotype B, although currently only existing of postcranial material, is a stahleckeriid. This preliminary result suggests that *K. simocephalus* and Morphotype B represent two different taxa, a kannemeyeriid and a stahleckeriid, that co-occur in the *Cynognathus* Assemblage Zone (subzone B). Although the Templeton test showed no significant difference, which suggests that the position Morphotype B among the stahleckeriids is not well supported. This however must be taken in the context as there is no cranial material for Morphotype B and it is possible that when found the cranial material will strengthen its relationship among the stahleckeriids.

It has been suggested by Vega-Dias *et al* (2004) that stahleckeriids may have evolved in Africa during the Middle Triassic based on the presence of *Angonisaurus* in the Middle Triassic of the Manda Formation and that their initial radiation occurred in Africa. The presence of this stahleckeriid in the *Cynognathus* Assemblage Zone (B zone) would make this the earliest occurrence of the Stahleckeriidae and supports Vega – Dias *et al* (2004) suggestion.

Based on the area for attachment of muscles it suggests that Morphotype B was a more lightly built animal than *K. simocephalus*. Most notably difference is the olecranon of Morphotype B is wide with a large area for the insertion of the triceps muscle, which is responsible for the flexion of the shoulder joint and extension of the elbow. This could be seen as evidence that the shoulder and elbow joints were being used regularly. The dorsally directed articulating surface of the humerus implies that it was held in a more upright positioned. Although these only two aspects of the functional morphology they imply that Morphotype B was capable of efficient locomotion. *K. simocephalus*, however, the humeral articulation is directed more anteriorly and this would suggest that the humerus was positioned more horizontally and the narrow olecranon suggests that the triceps muscle was not very large in *K. simocephalus* and that there was no great flexion of the shoulder joint and extension of the elbow. This implies that it is probable that *K. simocephalus* had a less efficient locomotor apparatus.

Wits ETD

The femoral head of Morphotype B is directed more antero-dorsally, which suggests that the hindlimb like that of *K. simocephalus* was in an upright position. This supports a more upright posture of both the forelimb and hindlimb of Morphotype B, which would allow this animal to walk long distances and use its habitat more efficiently. When a more complete skeleton of Morphotype B is known, it may shed more light on whether or not the locomotor apparatus was actually more efficient.

It can be tentatively concluded from the above comparison that it highly likely that *K. simocephalus* and Morphotype B exploited different micro-habitats (niches) within a particular larger habitat. This study would suggest that the postcranial skeleton probably played a deciding role in the survival, migration and evolution of *Kannemeyeria* and Morphotype B.

This study has also made it necessary to review what is currently known about cranial material assigned to *K. simocephalus*, especially fragmentary material. This review will have to take into consideration differences that have been accepted possible individual variation. Another step forward from this point would be to undertake fieldwork that would reinvestigate known localities where *K. simocephalus* and Morphotype B has been found and those where no Morphotype B material know. This also provides an opportunity to explore new localities. More field work will provide opportunities to better understand the relationship between the two postcranial morphotypes, especially if well-preserved, articulated skeletons that include skulls can be found.

The results of the preliminary phylogenetic analysis also re-iterated the need for re-investigating the postcranial anatomy of Triassic dicynodonts in order to better understand the relationships within the group but also in order to better understand their evolution, biogeography and functional anatomy. This especially evident among the African Triassic dicynodonts where a number of genera have not had any postcranial material described.

Wits ETD

CHAPTER EIGHT

REFERENCES

Angielczyk, K. D. 2001. Preliminary phylogenetic analysis & stratigraphic congruency of the dicynodont anomodonts (Synapsida: Therapsida). *Palaeontologia Africana* **37**, 53-79.

Bandyopadhyay, S. 1988. A kannemeyeriid dicynodont from the Middle Triassic Yerrapalli Formation. *Philosophical Transactions of the Royal Society, London, B* **320**, 185-233.

Bandyopadhyay, S. 1989. The mammal-like reptile *Rechnisaurus* from the Triassic of India. *Palaeontology* **32**(2), 305-312

Barbarena, M. C., Araújo, D. C., Lavina, E. L. 1985. Late Permian and Triassic tetrapods of Southern Brazil. *National Geographic Review* **Winter 1985**, 5-20

Barry, T. H. 1974. A new dicynodont ancestor from the Upper Ecca (Lower Middle Permian) of South Africa. *Annals of the South African Museum* **64**, 117-136.

Battail, B., Dejax, J., Richir, P., Taquet, P. & M. Veran. 1995. New data on the continental Upper Permian in the area of Luang-Prabang, Laos. *Journal of Geology* **5-6** (Ser. B): 11-15.

Bezuidenhout, A. J., Groenewald, H. B., Hornsveld, M. & Turner, P. H. (1996) *Veterinary Anatomy: A study and dissection guide*. Vol. **1.**

Bonaparte, J. F. 1966. Una nueva "fauna" Triásica de Argentina (Therapsida: Cynodontia Dicynodontia) consideraciones filogenéticas y paleobiogeográficas. *Ameghiniana* **4**(8), 243-293.

Brink, A. S. 1952. The manus of *Cistecephalus*. *South African Journal of Science* **49**, 13-15.

Broom, R. 1899. On two new species of dicynodonts. *Annals of the South African Museum* **1**, 452-456.

Broom, R. 1903. On the structure of the shoulder girdle in *Lystrosaurus*. *Annals of the South African Museum* **4**, 139-141.

Broom, R. 1937. A further contribution to our knowledge of the fossil reptiles of the Karroo. *Proceedings of the Zoological Society, Series B* **1937**, 299-318.

Bryant, H. N. & Seymour, K. L. 1990. Observation and Comments on the reliability of muscle reconstruction in fossil vertebrates. *Journal of Morphology* **206**: 109-117.

Camp, C. L. 1956. *Triassic Dicynodont Reptiles*. Part 2. Triassic Dicynodonts compared. *Memoirs of the University of California* **13**(4), 305-348.

Wits ETD

Camp, C. L. & Welles, S. P. 1956. *Triassic Dicynodont Reptiles*. Part 1. The North American genus *Placerias*. *Memoirs of the University of California* **13**(4), 255-304.

Cheng, Z. 1980. *Mesozoic stratigraphy and paleontology of the Shaanxi-Gansu-Ningxia Basin*. *Vertebrate fossils. Beijing: Publishing House of Geology Beijing*, 115-188.

Chinsamy, A & Rubidge, B. S. 1993. Dicynodont (Therapsida) bone histology: phylogenetic and physiological implications. *Palaeontologia Africana* 30, 97-102.

Cluver, M. A. 1978. The skeleton of the mammal-like reptile *Cistecephalus*. *Annals of the South African Museum* **76**(5), 213-245.

Cluver, M. A. & King, G. M. 1983. A reassessment of the relationships of Permian dicynodontia (Reptilia, Therapsida) and a new classification of dicynodonts. *Annals of the South African Museum* **91**(3), 195-273.

Courtenay-Latimer, M. 1948. *Kannemeyeria wilsoni* Broom; How it came to the East London Museum. **In:** du Toit, A.L. (ed.), *Special publications of the Royal Society of South Africa. The Robert Broom Commemorative Volume*, 107-109. Cape Town, Royal Society of South Africa.

Cox, C. B. 1959. On the anatomy of a new dicynodont genus with evidence of the position of the tympanum. *Proceedings of the Zoological Society, London* **132**, 321-367.

Cox, C. B. 1965. New Triassic dicynodonts from South America, their origins and relationships. *Philosophical Transactions of the Royal Society, London, Series B* **248**(753), 457-516.

Cox, C. B. 1969. Two new dicynodonts from the Triassic N'tawere Formation, Zambia. *Bulletin of the British Museum (Natural Museum) Geology* **17**(6), 255-294.

Cox, C. B. 1972. A new digging dicynodont from the Upper Permian of Tanzania. **In:** Joysey, K. A. & Kemp, T. S. (Eds), *Studies in Vertebrate Evolution*, 173-189. Edinburgh, Oliver & Boyd.

Cox, C. B. 1998. The jaw function and adaptive radiation of the dicynodont mammal-like reptiles of the Karoo Basin of South Africa. *Zoological Journal of the Linnaean Society* **122**, 349-284.

Crozier, E. A. 1970. Preliminary report on two Triassic dicynodonts from Zambia. *Palaeontologia africana* **13**, 39-45.

Cruickshank, A. R. I. 1965. On a specimen of the anomodont reptile *Kannemeyeria latifrons* (Broom) from the Manda Formation of Tanganyika, Tanzania. *Proceedings of the Linnaean Society, London* **176**(2), 149-157.

WitsETD

Cruickshank, A. R. I. 1967. A new dicynodont genus from the Manda Formation of Tanzania (Tanganyika). *Journal of Zoology, London* **153**, 163-208.

Cruickshank, A. R. I. 1970. Taxonomy of the Triassic anomodont genus *Kannemeyeria*. *Palaeontologia Africana* **13**, 47-55.

Cruickshank, A. R. I. 1972. A note on the genus *Proplacerias* Cruickshank 1970. *Palaeontologia Africana* **14**, 17.

Cruickshank, A. R. I. 1975. The skeleton of the Triassic anomodont *Kannemeyeria wilsoni* Broom. *Palaeontologia Africana* **18**, 137-142.

Cruickshank, A. R. I. 1986. Biostratigraphy and classification of a new Triassic dicynodont from East Africa. *Modern Geology* **10**, 121-131.

Danilov, A. I. 1971. A new dicynodont from the Middle Triassic of southern CisUralia. *Paleontolgical Journal* **5**, 265-268.

Danilov, A. I. 1973. Remains of the postcranial skeleton of *Uralokannemeyeria* (Dicynodontia). *Paleontolgical Journal* **1973**(2), 128-131.

Defauw, S. L. 1986. *The Appendicular Skeleton of African Dicynodonts.* PhD Thesis. Wayne State University, Detroit, Michigan.

Groenewald, G. H. 1991. Burrow casts from the *Lystrosaurus-Procolophon* Assemblage zone, Karoo sequence, South Africa. *Koedoe* **34(1)**: 13-22.

Hancox, P. J. 1998. *A stratigraphic, sedimentological and palaeoenvironmental synthesis of the Beaufort-Molteno contact in the Karoo Basin*. Unpublished PhD thesis, University of the Witwatersrand, Johannesburg.

Hancox, P. J. 2000. The Continental Triassic of South Africa. *Zbl. Geol. Paläont.* **1(11-12),** 1285-1324.

Hancox, P. J., Shishkin, M. A., Rubidge, B. S. & Kitching, J. W. 1995. A threefold subdivision of the *Cynognathus* Assemblage Zone (Beaufort Group, South Africa) and its palaeogeographical implications. *South African Journal of Science* **91**, 143-144.

Hancox, P. J. and Rubidge, B. S. 1995. The first specimen of the Middle Triassic dicynodont *Angonisaurus* from the Karoo of South Africa: implications for the dating and biostratigraphy of the *Cynognathus* Assemblage Zone, Upper Beaufort. *South African Journal of Science* **92**, 391-392.

Haughton, S. H. 1915. On the skull of the genus *Kannemeyeria*. *Annals of the South African Museum* **12**, 91-97.

Haughton, S. H. 1917. Descriptive catalogue of the Anomodontia, with special reference to examples in the South African Museum. *Annals of the South African Museum* **12**, 172.

Wits ETD

Jäeckel, O. 1911. Die Wirbeltiere. *Eine Ubersicht über die fossilen und lebenden Foramen*. Berlin.

Jenkins, F. A. & Goslow, G. E. jr. 1983. The functional anatomy of the shoulder of the Savannah monitor lizard (*Varanus exanthematicus*). *Journal of Morphology* **175**, 195-216.

Keyser, A. W. 1973. A new Triassic vertebrate fauna from South West Africa. *Palaeontologia africana* **16**, 1-15.

Keyser, A. W. 1974. Evolutionary trends in Triassic Dicynodontia (Reptilia Therapsida). *Palaeontologia africana* **17**, 57-68.

Keyser, A. W. 1977. A new dicynodont genus and its bearing on the origin of the Gondwana Triassic dicynodontia. **In:** Laskar, B. & Raja Rao, C.C. (eds), *Fourth International Gondwana Symposium*: papers **vol. 1**, 184-198. Delhi, Hindustan Publishing Corporation.

Keyser, A. W. & Cruickshank, A. R. I. 1979. The origins and classification of the Triassic dicynodonts. *Transactions of the Geological Society of South Africa* **82**, 81-108.

Keyser, A. W. & Smith, R. M. H. 1979. Vertebrate biozonation of the Beaufort Group with special reference to the western Karoo Basin. *Annals of the Geological Survey of South Africa* **12**, 69-72.

King, G. M. 1981a. The postcranial skeleton of *Robertia broomiana*, an early dicynodont (Reptilia, Therapsida) from the South African Karoo. *Annals of the South African Museum* **84**(5), 203-231.

King, G. M. 1981b. The functional anatomy of a Permian dicynodont. *Philosophical Transactions of the Royal Society, B, Biological Sciences* **291**(1050), 243-322.

King, G. M. 1985. The postcranial skeleton of *Kingoria nowacki* (von Huene) (Therapsida: Dicynodontia). *Zoological Journal of the Linnaean Society* **84**, 263-289.

King, G. M. 1988. Anomodontia. *Encyclopedia of Paleoherpetology* **17C**, 64-171.

King, G. M. 1990a. The Dicynodonts: A study in Palaeobiology. 233pp. Chapman & Hall, London.

King, G. M. 1990b. Life and Death in the Permo-Triassic: the fortunes of the dicynodont mammal-like reptiles. *Sidney Haughton Memorial Lecture* **3**, 1-17. Cape Town, Royal Society of South Africa.

King, G. M. 1990c. Dicynodonts and the end Permian event. *Palaeontologia Africana* **27**, 31-39.

King, G. M. 1991. The aquatic *Lystrosaurus*: a palaeontological myth. *Historical Biology* **4**, 285-321.

Wits ETD

King, G. M. 1992. Palaeobiogeography of Permian Anomodonts. *Terra Nova* **4**, 633-640.

King, G. M. & Cluver, M. A. 1991. The aquatic *Lystrosaurus*: an alternative lifestyle. *Historical Biology* **4**, 323-341.

King, G. M. 1993. Species longevity and generic diversity of the dicynodont mammal-like retiles. *Palaeogeography, Palaeoclimatology, Palaeoecology* **102**, 321-332.

Kitching, J. W. 1977. On the distribution of the Karoo vertebrate fauna with special reference to certain genera, and the bearing of this on the zoning of the Beaufort Beds. *Bernard Price Institute for Palaeontological Research Memoir No.* **1**.

Kitching, J. W. 1995. Biostratigraphy of the *Cynognathus* Assemblage Zone. **In**: Rubidge, B. S. (ed), *Biostratigraphy of the Beaufort Group (Karoo Supergroup)*, 40-45.

Lucas, S. G. 1998. Global Triassic tetrapod biostratigraphy and biochronology. *Palaeogeography, Palaeoclimatology, Palaeoecology* **143**, 347-384.

Lucas, S. G. & Wild, R. 1995. A Middle Triassic dicynodont from Germany and the biochronology of Triassic dicynodonts. *Stuttgarter Beitr. Naturk., B*, **220**, 1-16.

Lucas, S. G. & Harris, S. K. 1996. Taxonomic and biochronological significance of specimens of the Triassic dicynodont *Dinodontosaurus* Romer 1943 in the Tübingen collection. *Paläont. Z.* **70**, 603-622.

Maisch, M. A. 2001. Observations on Karoo and Gondwana vertebrates. Part 2: A new skull-reconstruction of *Stahleckeria potens* von Huene, 1935 (Dicynodontia, Middle Triassic) and a reconsideration of kannemeyeriiform phylogeny. *Neues Jahrbuch für Geologie und Paläontologie Monatschefte* **2000**, 15-28.

Mazin, J. M., King, G. M. 1991. The first dicynodont from the Later Permian of Malagasy. *Palaeontology* **34**(4), 837-842.

Modesto, S., Rubidge, B., Visser, I & Welman, J. 2003. A new dicynodont from the Upper Permian of South Africa. *Palaeontology* **46**(1), 211-223.

Pearson, H. S. 1924a. The skull of the dicynodont reptile *Kannemeyeria*. *Proceedings of the Zoological Society* **1924**, 793-825.

Pearson, H. S.1924b. A dicynodont reptile reconstructed. *Proceedings of the Zoological Society* **1924**, 827-855.

Ray, S. 2001. Small Permian dicynodonts from India. *Paleontological Research* **5**(3), 177-191.

Ray, S, Chinsamy, A & Bandyopadhyay, S. 2002. An assessment of *Lystrosaurus murrayi* osteohistology. *Abstracts*: 11. 8th International Symposium on Mesozoic Ecosystems, Cape Town, South Africa.

Wits ETD

Ray, S. & Chisamy, A. 2003. Functional aspects of the postcranial anatomy of the Permian dicynodont *Diictodon* and their ecological implications. *Palaeontology* **46**(1), 151-183.

Roy-Chowdhury, T. 1970. Two new dicynodonts from the Triassic Yerrapalli Formation of Central India. *Palaeontology* **13**(1), 132-144.

Renaut, A. J. 2000. *A re-evaluation of the cranial morphology and taxonomy of Triassic dicynodont genus Kannemeyeria*. Unpublished PhD thesis. University of the Witwatersrand, Pp 394.

Renaut, A. J. & Hancox, P. J. 2001. Cranial description and taxonomic re-evaluation of *Kannemeyeria argentinensis* (Therapsida: Dicynodontia). *Palaeontologia africana* **37**, 81-91.

Renaut, A. J., Hancox, P. J., & Welman, J. (In Press). A tuskless specimen of the Triassic dicynodont *Kannemeyeria* (Synapsida: Therapsida). *South African Journal of Science*

Romer, A. S. (1922) The locomotor apparatus of certain primitive and mammal-like reptiles. *Bull. Am. Mus. Nat. Hist.* **46**(10), 517-606.

Rubidge, B. S. 1984. The cranial morphology and palaeoenvironment of *Eodicynodon* Barry (Therapsida: Dicynodontia). *Narvorsinge van die Nasionale Museum, Bloemfontein* **4**(14), 325-402.

Rubidge, B. S. 1985. The first record of a complete snout of the primitive dicynodont *Eodicynodon Oosthuizeni*, Barry 1974 (Therapsida: Dicynodontia). *Narvorsinge van die Nasionale Museum, Bloemfontein* **4**(17), 501-509.

Rubidge, B. S. 1987. South Africa's oldest land-living reptiles from the Ecca-Beaufort transition in the southern Karoo. *South African Journal of Science* **83**, 165-166.

Rubidge, B. S. 1990a. A new vertebrate biozone at the base of the Beaufort Group, Karoo sequence (South Africa). *Palaeontologia Africa* **27**, 17-20.

Rubidge, B. S. 1990b. Redescription of the cranial morphology of *Eodicynodon oosthuizeni* (Therapsida: Dicynodontia). *Narvorsinge van die Nasionale Museum, Bloemfontein* **7**(1), 1-41.

Rubidge, B. S.; King, G. M. & Hancox, P. J. 1994. The postcranial skeleton of the earliest dicynodont synapsid *Eodicynodon* from the Upper Permian of South Africa. *Palaeontology* **37**(2), 397-408.

Rubidge, B. S. & Sidor, C. A. 2001. Evolutionary patterns among Permo –Triassic therapsids. *Annual Review of Ecology & Systematics* **32**b, 449-480.

WitsETD

Seeley, H. G. 1908. On the fossil reptile with a trunk from the Upper Karoo rocks of Cape colony. *Reports of the British Association for the Advancement of Science* **78**, 713.

Shishkin, M. A., Rubidge, B. S., Hancox, P. J. 1995. Vertebrate biozonation of the Upper Beaufort series of South Africa- A new look on correlation of the Triassic biotic events in Euramerica and southern Gondwana. **In**: (eds) Sun, A-L. and Wang, Y., *Sixth symposium on Mesozoic terrestrial ecosystem and biota, Short Papers*, 39-41.

Sun, A-L. 1960. On a new genus of kannemeyerids from Ningwu, Shansi. *Vertebrata Palasiatica* **4**(2), 67-81.

Sun, A-L. 1963. The Chinese kannemeyerids. *Palaeontologica Sinica* **17**, 73-109.

Surkov, M. V. 1998a. Morphological features of the postcranial skeleton in anomodonts reflecting the evolutionary development of the group. *Paleontological Journal* **32**(6), 620-623.

Surkov, M. V. 1998b. The postcranial skeleton of *Rhinodicynodon gracile* Kalandadze, 1970 (Dicynodontia). *Paleontological Journal* **32**(4), 402-409.

Vega-Dias, C. & Schultz, C. L. 2004. Postcranial material of *Jachaleria candelariensis* Araújo and Gonzaga 1980 (Therapsida, Dicynodontia), Upper Triassic of Rio Grande do Sul, Brazil. *Paleobios* **24**(1), 7-31.

Vega-Dias, C., Maisch, M. A. & Schultz, C. L. 2004. A new phylogenetic analysis of Triassic dicynodonts (Therapsida) and the systematic position of *Jachaleria candelariensis* from the Upper Triassic of Brazil. *Neues Jahrbuch für Geologie und Paläontologie Monatschefte Abhandlungen* **231**(1):145-166.

Walter, L. R. 1986. The limb posture of kannemeyeriid dicynodonts: functional and ecological consideration. **In:** Padian, K. (ed.), *The Beginning of the Age of Dinosaurs*: *Faunal change across the Triassic – Jurassic boundary*. Cambridge, Cambridge University Press.

Watson, D. M. S. 1912. The skeleton of *Lystrosaurus*. *Records of the Albany Museum* **2**(4), 287-295.

Watson, D. M. S. 1913. The limbs of *Lystrosaurus*. *Geological Magazine (5th series)* **10**, 256-258.

Weithofer, A. 1888. Uber einen nueun dicynodonten (*D. simocephalus*) aus der Karoo formation Südafrikas. *Annln. Naturk. Mus. Wein.* **3**: 1-4.

Yeh, H-K. 1959. New dicynodont from *Sinokannemeyeria*-fauna from Shansi. Vertebrata Palasiatica **3**(1): 187-204.

Wits ETD

Young, C. C. 1935. On two skeletons of dicynodontia from Sinkiang. *Bulletin of the Geological Society of China* **14**(4), 483-517.

Young, C. C. 1937. On the Triassic dicynodonts from Shansi. *Bulletin of the Geological Society of China* **17**, 393-411.

Yuhe, L. 1983. Restoration of the pelvic muscles of *Lystrosaurus*. *Vertebrata Palasiatica* **21(4)**, 328-40.

Wits ETD

APPENDIX A

FIGURES AND PLATES OF *K. SIMOCEPHALUS*

Wits ETD

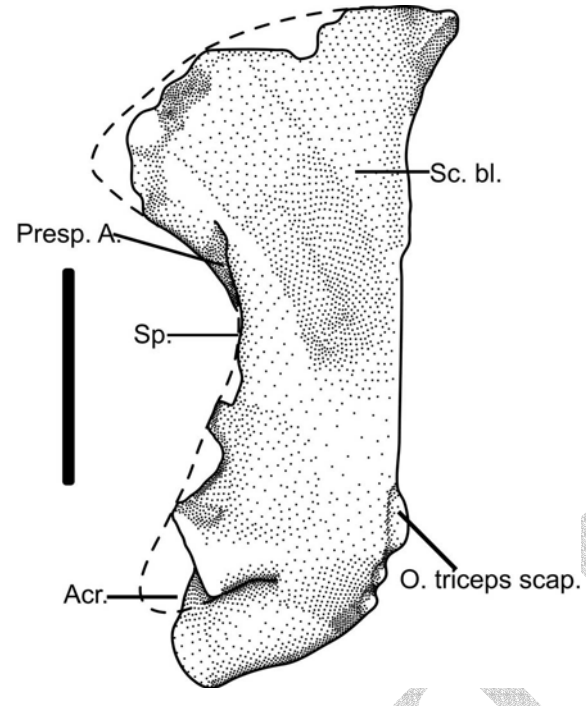

a)

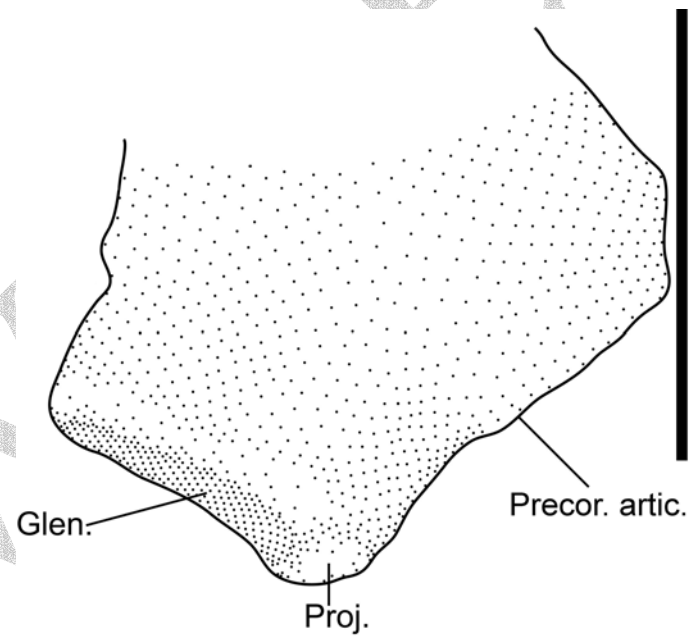

b)

Figure 1 Lateral view of the scapula of *Kannemeyeria simocephalus* showing: a) scapula blade of the left scapula of BP/1/5624;
b) Distal end of the right scapula of BP/1/6104 showing the glenoid and the coracoid articulation. Scale bar = 10 cm

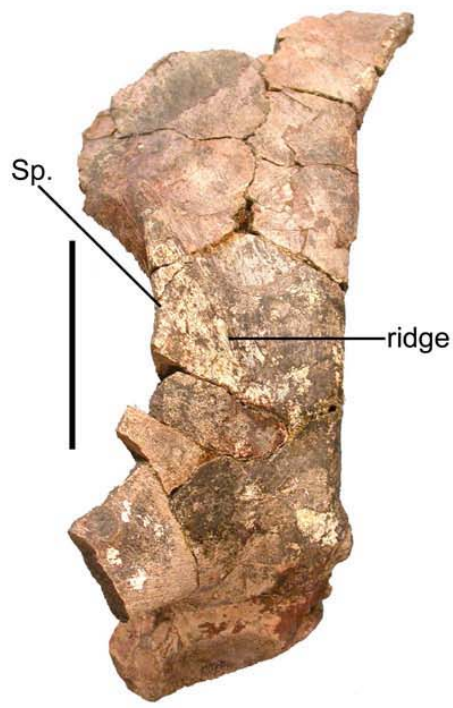

a) i BP/1/5624

b) ii BP/1/6160

a) iii ELM 1

b) BP/1/6104

Plate 1 Lateral view of the scapula of *Kannemeyeria simocephalus* showing the left scapula in various states of preservation in a) i-ii and the distal end of the left scapula of BP/1/6104 in b).

Scale bar = 10 cm

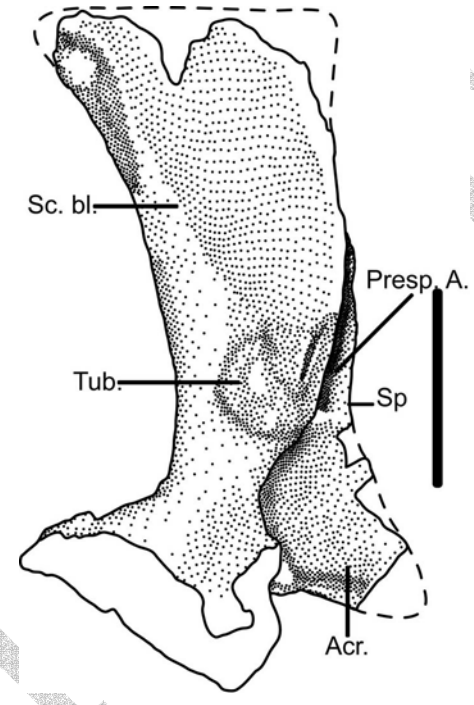

Wits ETD

Figure 2 Medial view of the left scapula of *K. simocephalus* (BP/1/5624) showing the prominent tubercle on the porixmo-posterior corner of the acromion.
Scale bar = 10 cm

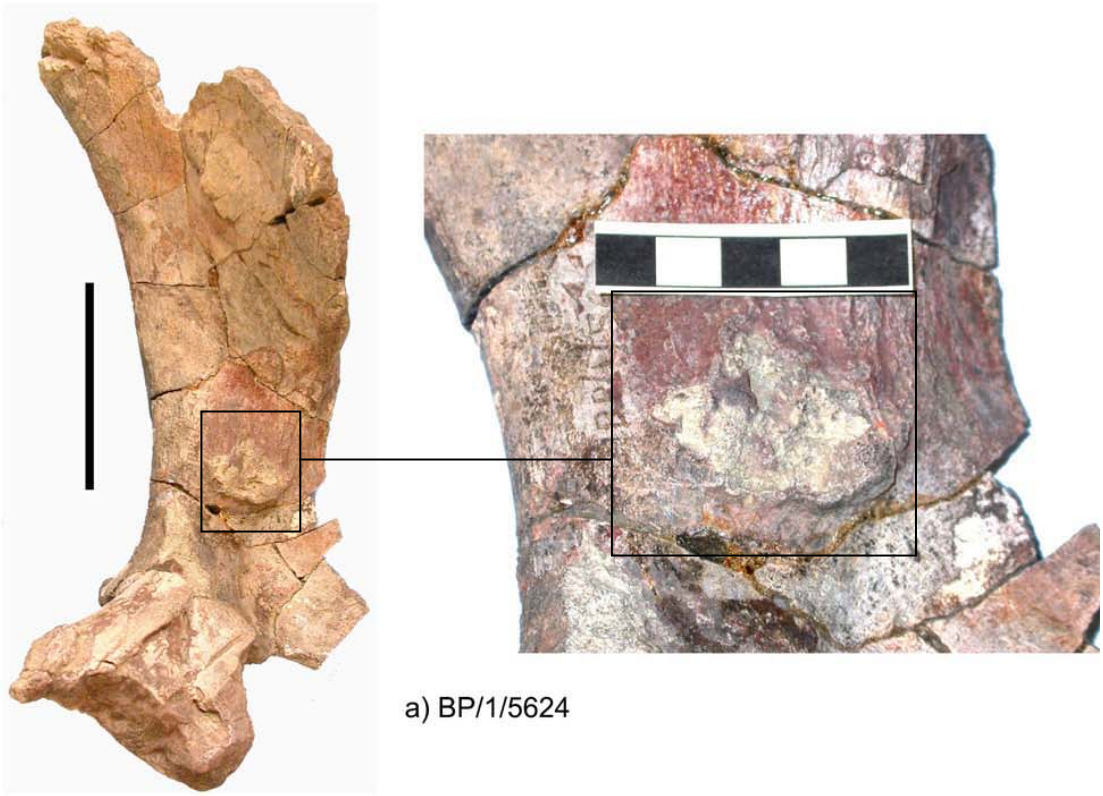

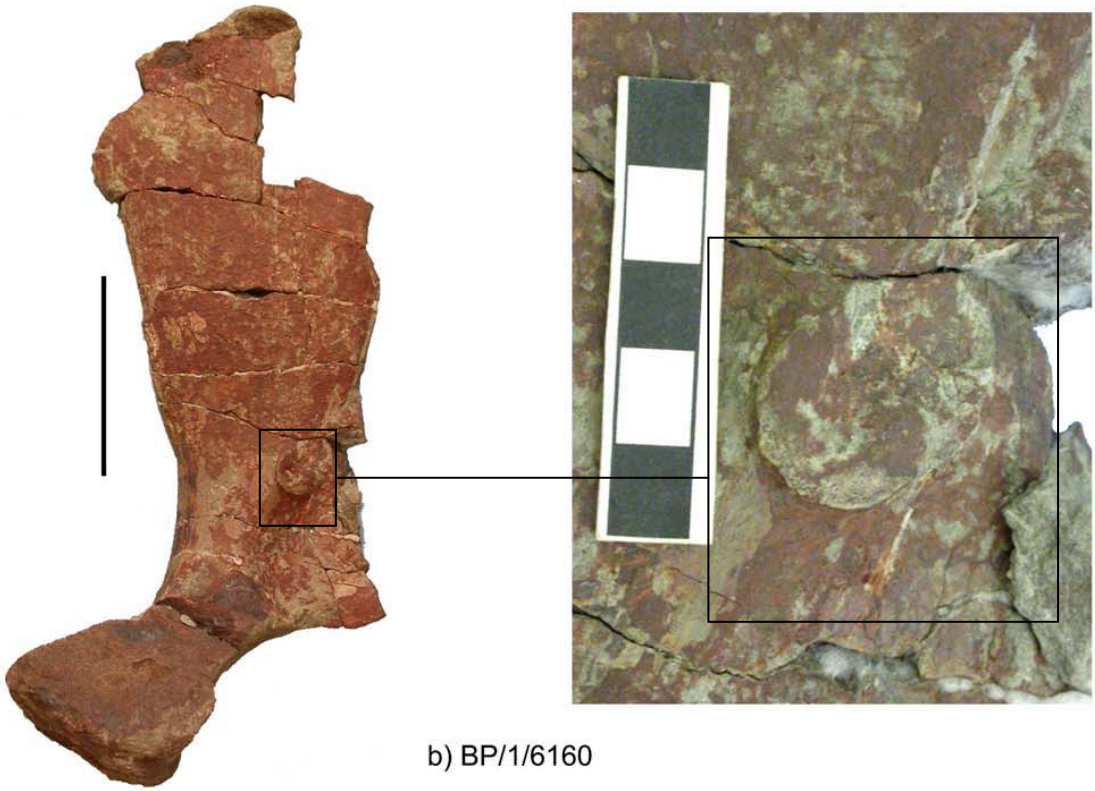

Plate 2 Medial view of the left scapula of *K. simocephalus* showing the tubercle on the proximo-posterior corner of the acromion of BP/1/5624 and BP/1/6160.

Scale bar = 10 cm; insert scale bar = 5 cm

a) ELM 1

b) ELM 1

c) ELM 1

Plate 3 a) Lateral view of the right glenoid of *K. simocephalus* (ELM 1) showing its postero-ventrally directed articulating surface; b) Dorsal view of the interclavicle of *K. simocephalus* (ELM 1) showing damage along the distal end and along the lateral side; c) Lateral view of the left clavicle of *K. simocephalus*. Scale bar = 10 cm

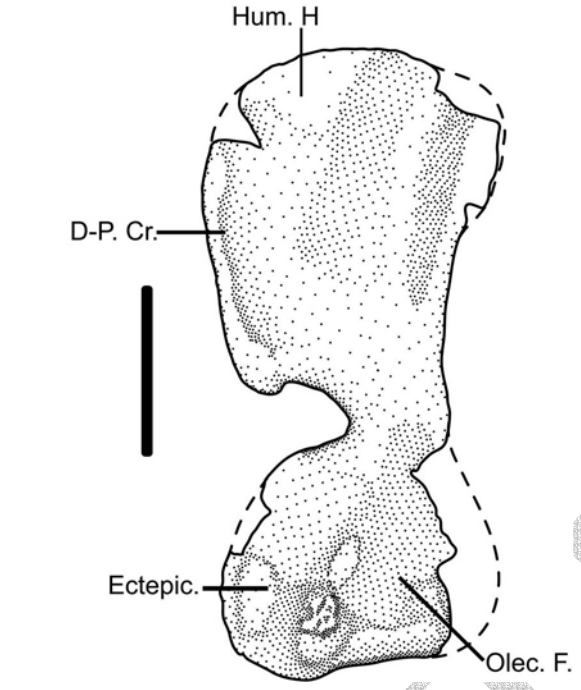

a)

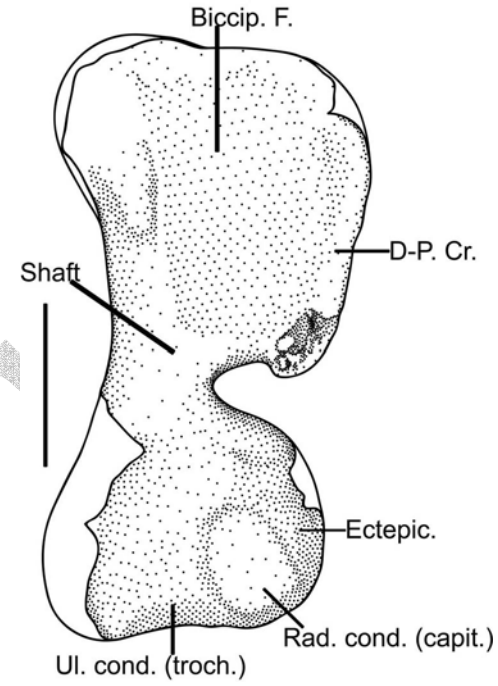

b)

Figure 3 The left humerus of the small specimen (BP/1/6160) of *K. simocephalus* shown in dorsal view (a) and the ventral view (b), both showing the large proximal expansion and well developed delto-pectoral crest.

Scale bar = 10 cm

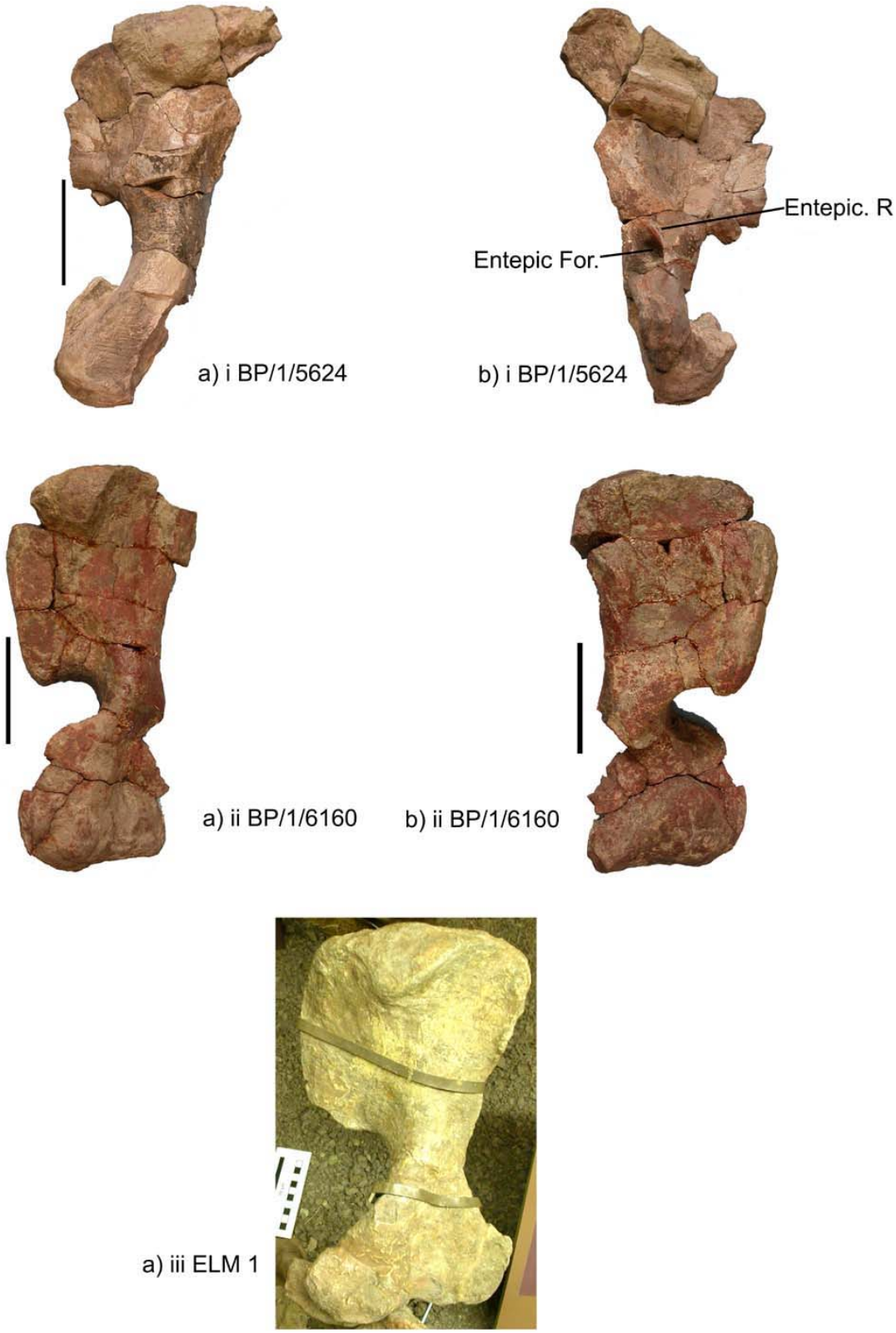

Plate 4 Humerus of *K. simocephalus* showing variation in the form of the left bone in three individuals studied a) i-iii shows the dorsal view of BP/1/5624, BP/1/6160, ELM1 respectively, and b) i-ii shows the ventral view of BP/1/5624 and BP/1/6160. Scale bar = 10 cm

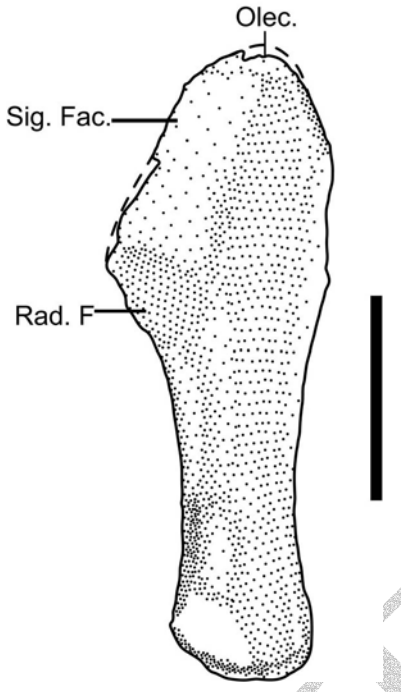

a)

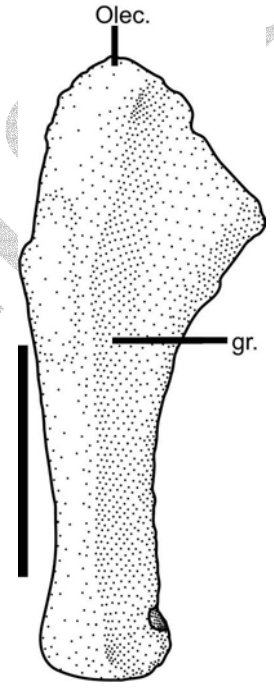

b)

Figure 4 Left ulna of *K. simocephalus* showing the narrow, triangular and low olecranon in a) lateral view of BP/1/5624 and b) medial view BP/1/6160.

Scale bar = 10 cm

Wits ETD

Plate 5 Ulna of *K. simocephalus* showing the low olecranon and the variation in form between the left one of the larger individual [a)i BP/1/5624] and the smaller individual [a) ii BP/1/6160] and b) shows the medial view. Scale bar = 10 cm

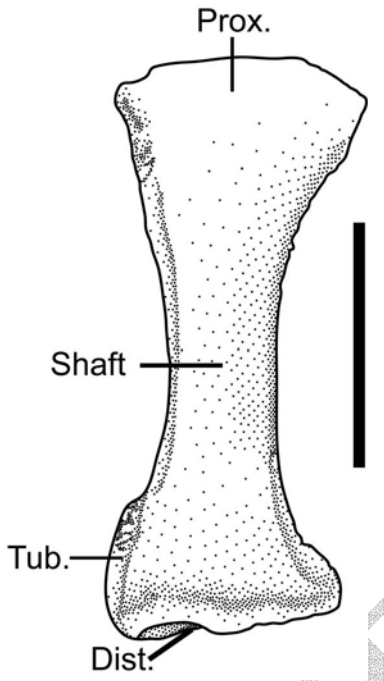

a)

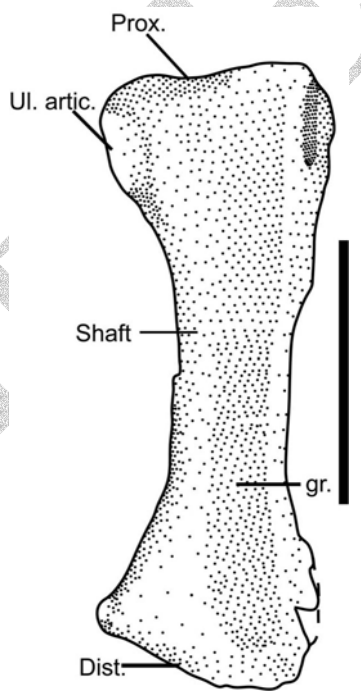

b)

Figure 5 Right radius of *K. simocephalus* showing a well developed tubercle above the distal end in a) anterior view (BP/1/5624 and the well developed ulna articulation in b) posterior view (BP/1/6160).

Scale bar = 10 cm

Wits ETD

a) i BP/1/5624

a) ii BP/1/6160

b) BP/1/6160

Plate 6 Radius of *K. simocephalus* showing the well developed tubercle above the distal end in anterior view a)i BP/1/5624 and the well developed ulna articulation in anterior view a) ii BP/1/6160 and posterior view b) BP/1/6160.

Scale bar = 10 cm

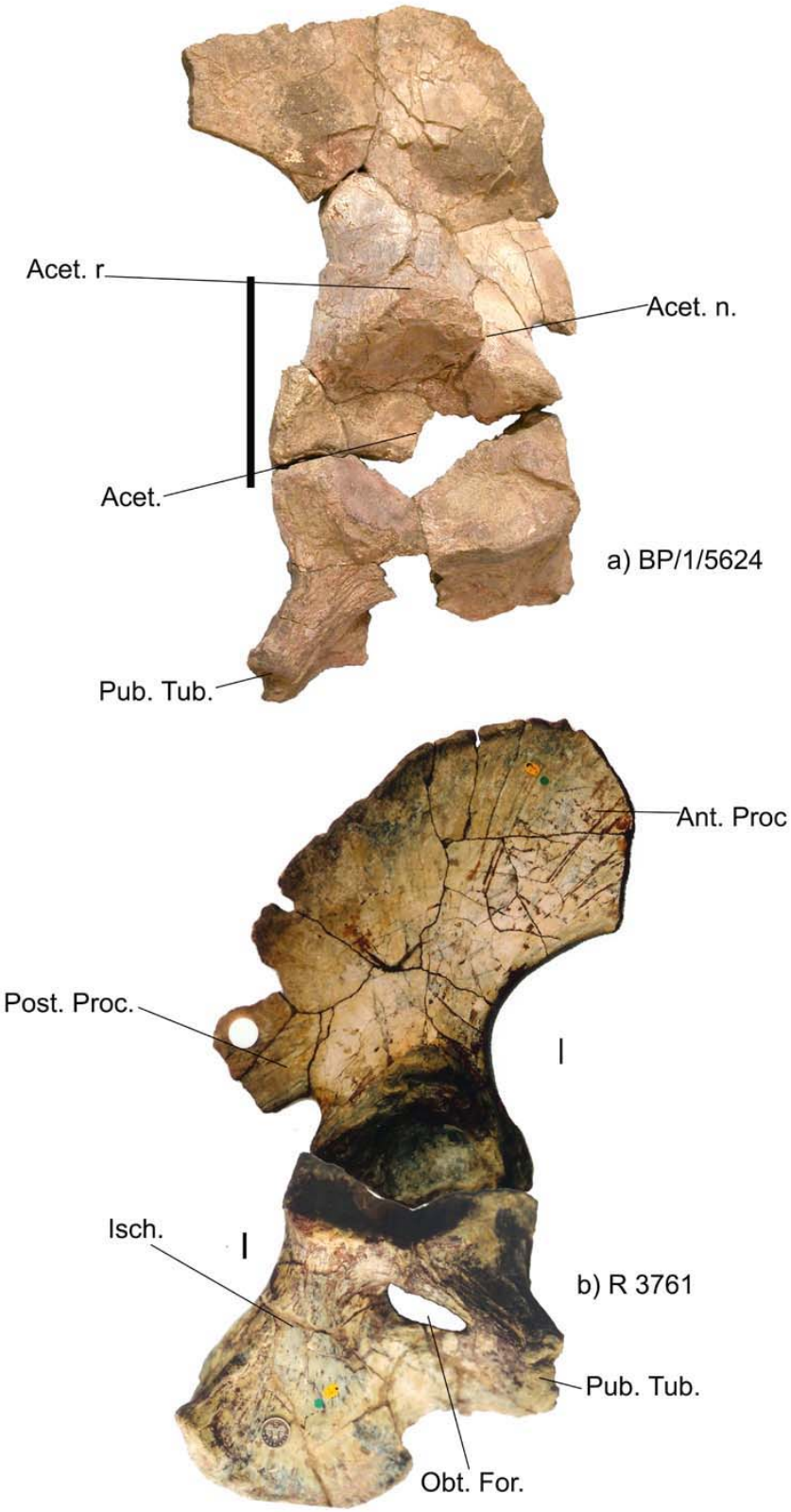

Plate 7 Lateral view of the right and left pelvic girdles of *K. simocephalus* incomplete in a) BP/1/5624 and fairly complete in b) R 3761 showing an elongated oval obturator foramen.

Scale bar = 10 cm; coin = 17mm

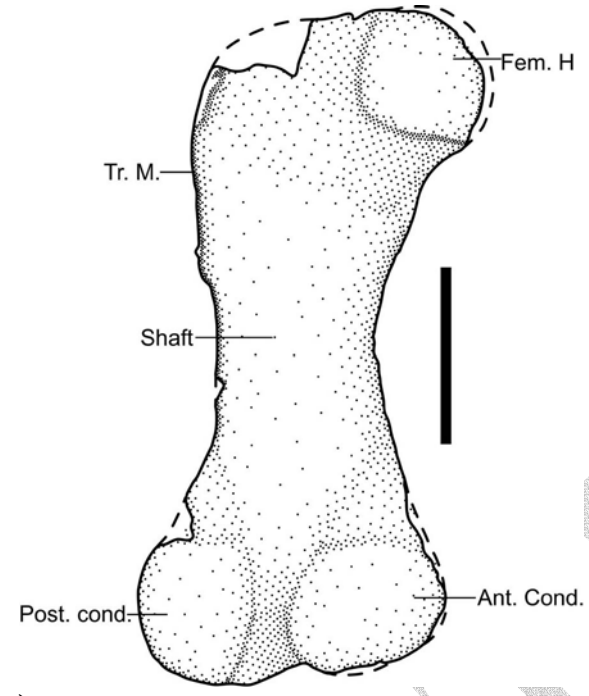

a)

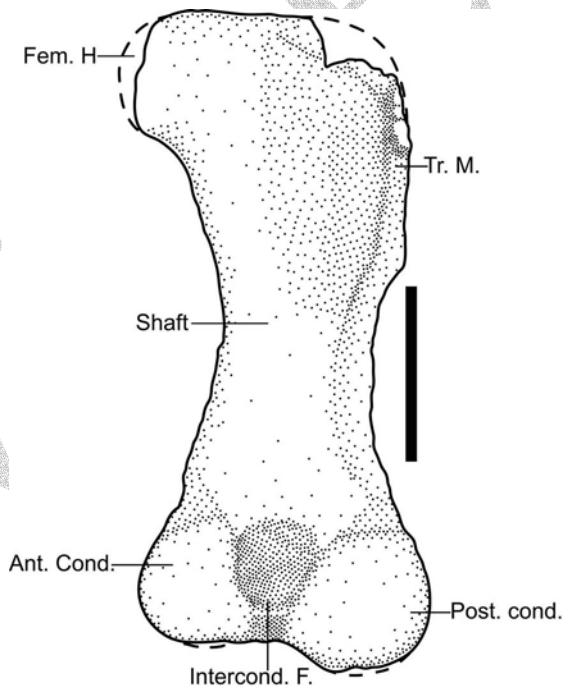

b)

Figure 6 Left femur of *K. simocephalus* (BP/1/5624) showing the medially inflected head in a) ventral view and the narrow greater trochanter and straight shaft in b) dorsal view. Scale bar = 10 cm

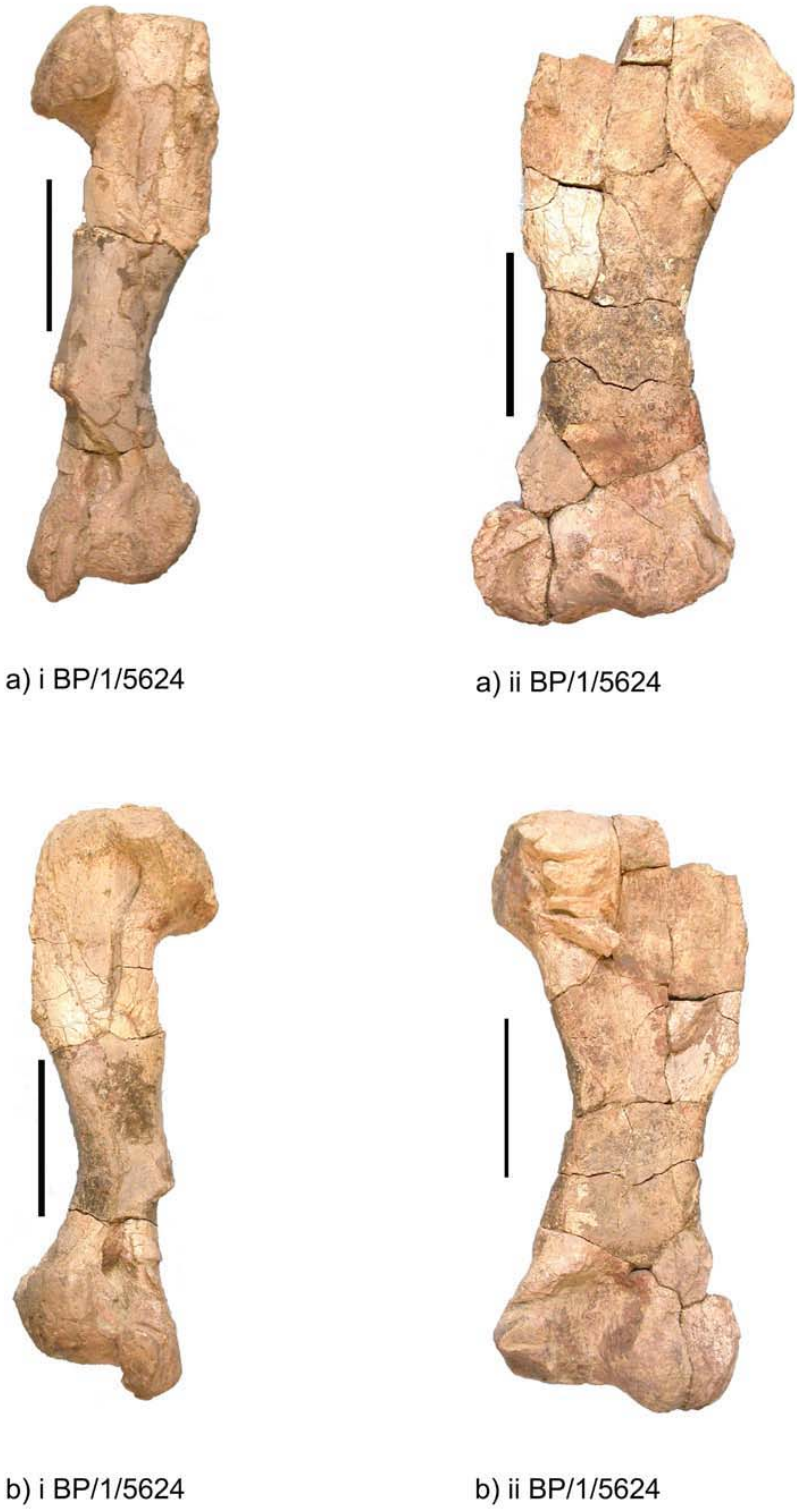

Plate 8 Femora of *K. simocephalus* showing different types of distortion in right (a (i) & b (i)) and left (a (i) & b (ii)) viewed in a) ventral view and b) dorsal view.

Scale bar = 10 cm

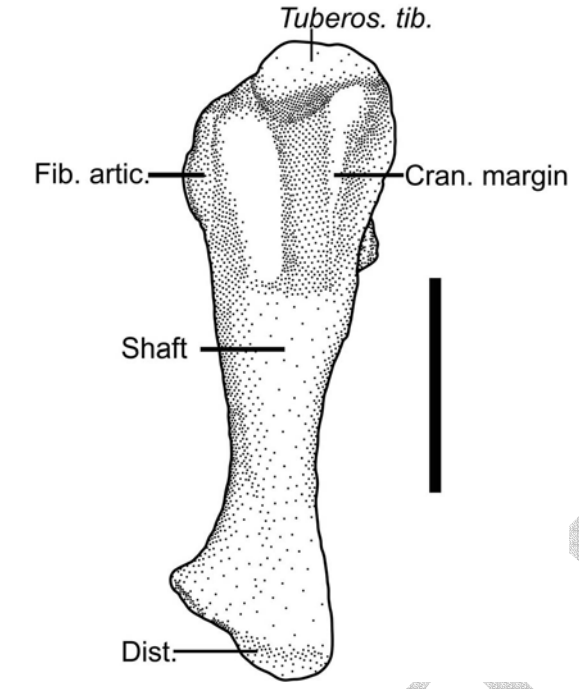

a)

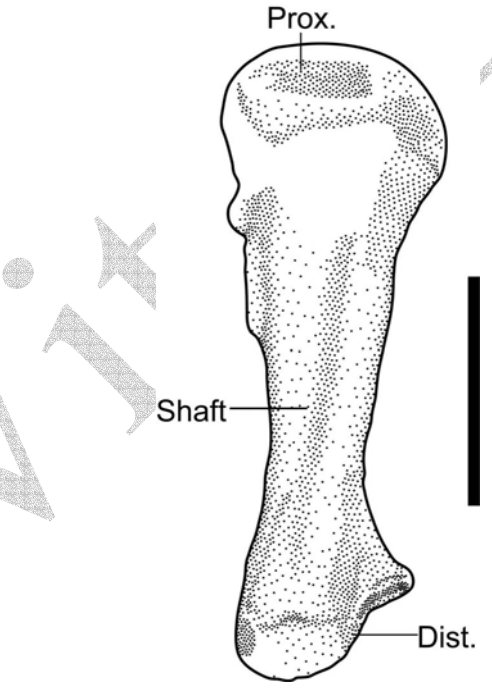

b)

Figure 7 Right tibia of *K. simocephalus* showing a prominent tibial tuberosity and cranial margin in anterior view (a) and a shallow groove that extends down the length of the shaft in posterior view (b).

Scale bar = 10 cm

Withheld

a) BP/1/5624

b) ELM 1

c) ELM1

Plate 9 a) Tibia of *K. simocephalus* (BP/1/5624) showing a prominent tibial tuberosity. b & c) Shows the thin right and left fibula of *K. simocephalus* (ELM 1).
Scale bar = 10 cm

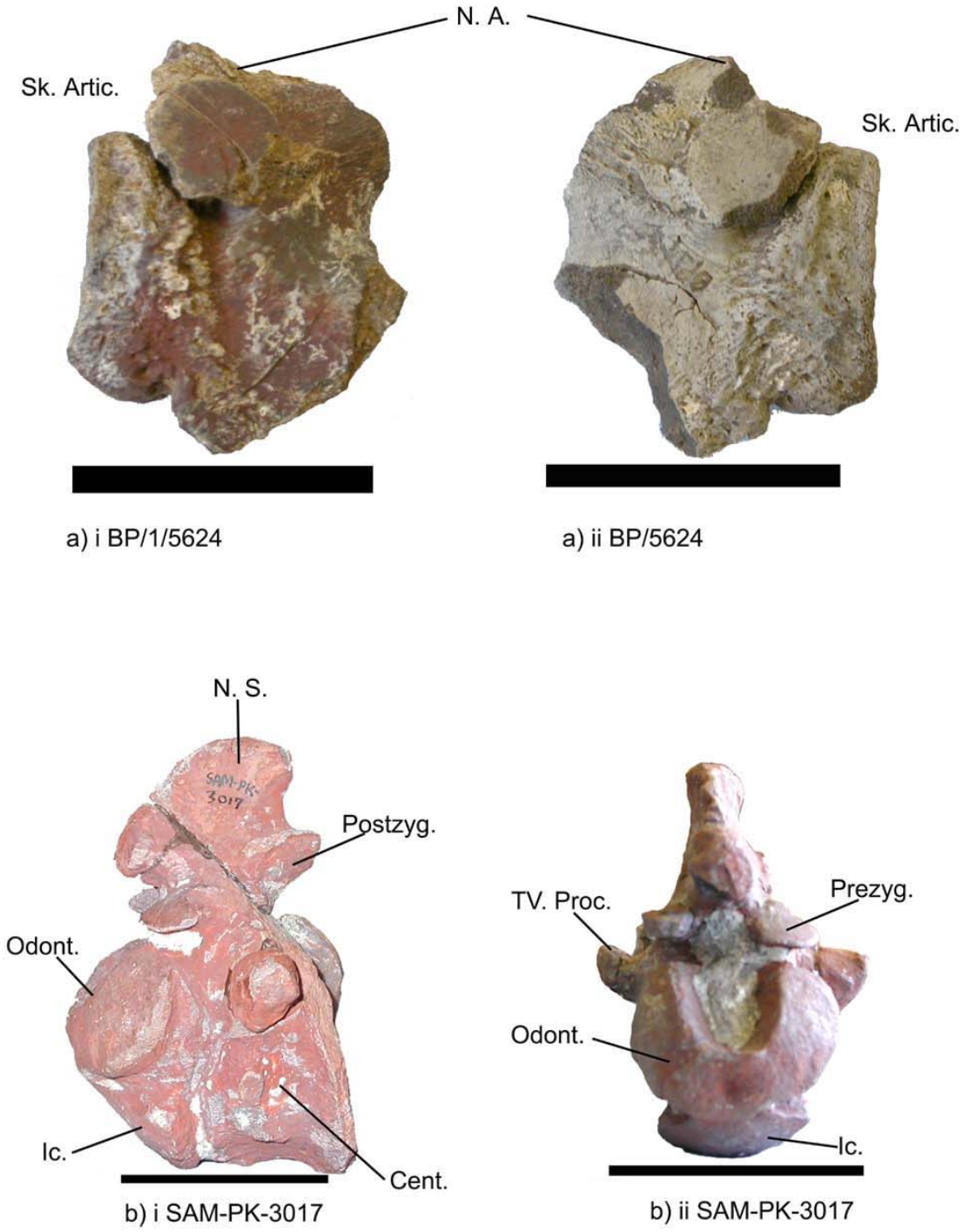

Plate 10 The atlas-axis complex of *K. simocephalus* showing the lateral view of the atlas (a (i) left; a(ii) right) and the lateral view of the axis in (b(i)) and anterior view in b(ii). Scale bar = 5 cm

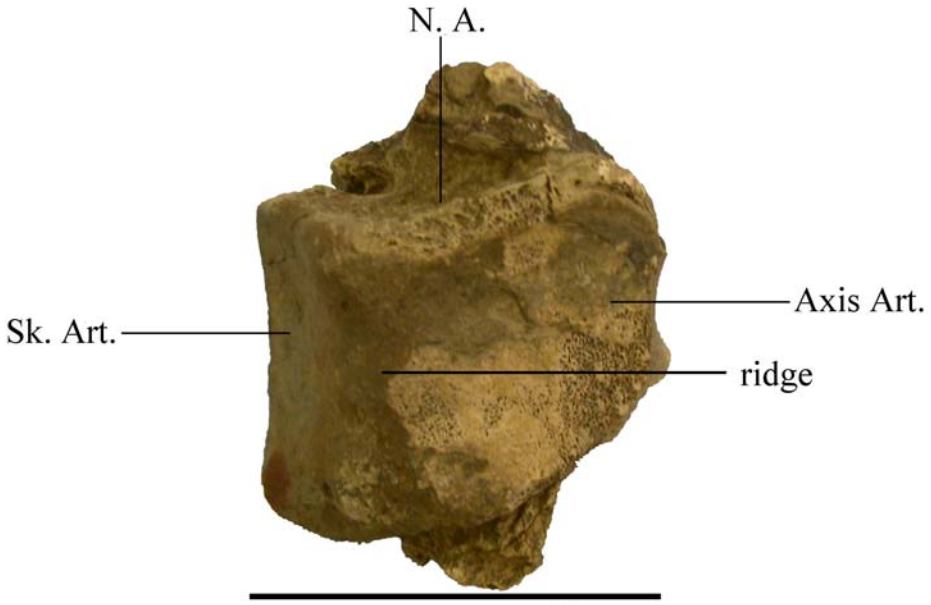

a) BP/1/5624

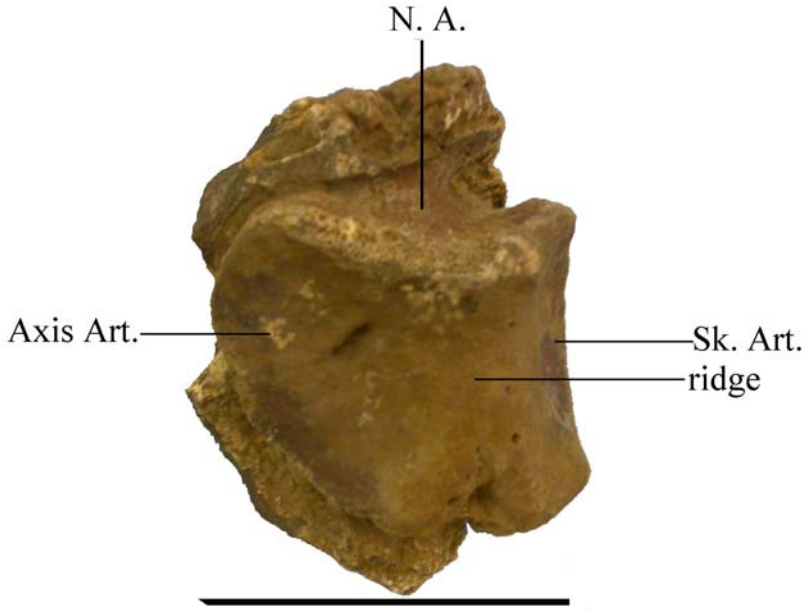

b) BP/1/5624

Plate 11 Medial view of the Atlas of *K. simocephalus* a) right half; b) left half

Scale = 5 cm

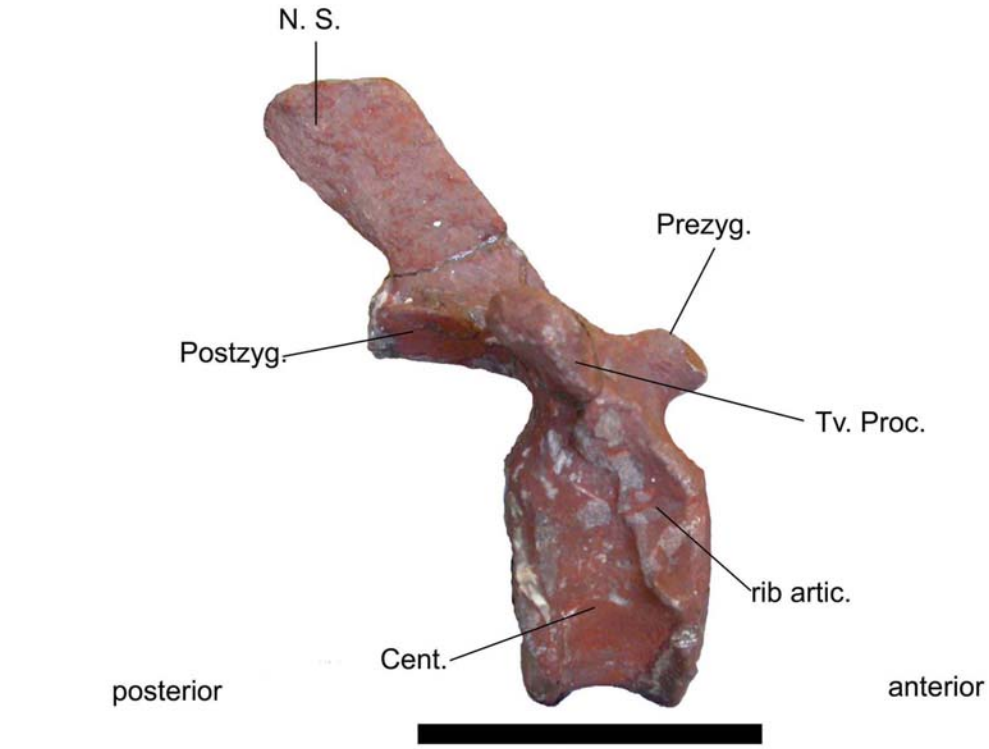

a) SAM-PK-3017

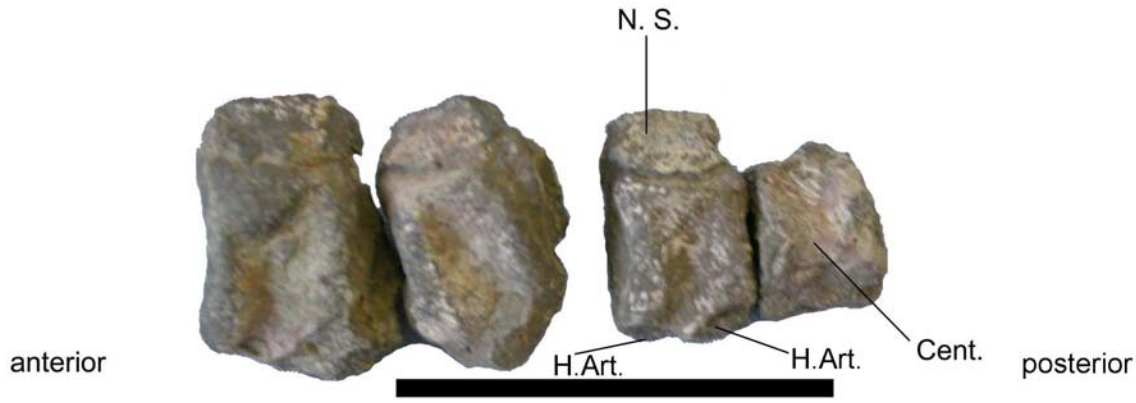

b) BP/1/5624

Plate 12 a) Lateral view of a possible dorsal vertebrae of *K. simocephalus* (SAM-pk-3017) showing a posteriorly inclined neural spine and a prominent rib articulation on the centrum; while b) shows lateral view of four Caudal vertebrae showing a decrease in size in the posterior direction. Scale bar = 5 cm

APPENDIX B

FIGURES AND PLATES OF MORPHOTYPE B

Wits ETD

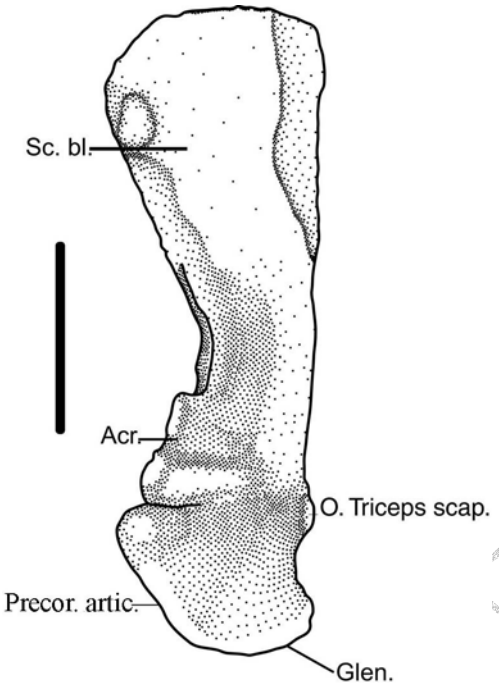

a)

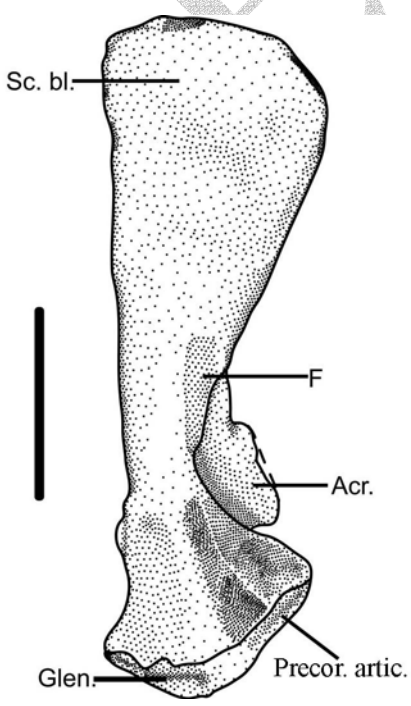

b)

Figure 8 Left scapula of Morphotype B (BP/1/994D) in a) lateral view and b) medial view showing a fossa at the proximo-posterior corner of the acromion.

Scale bar = 10 cm

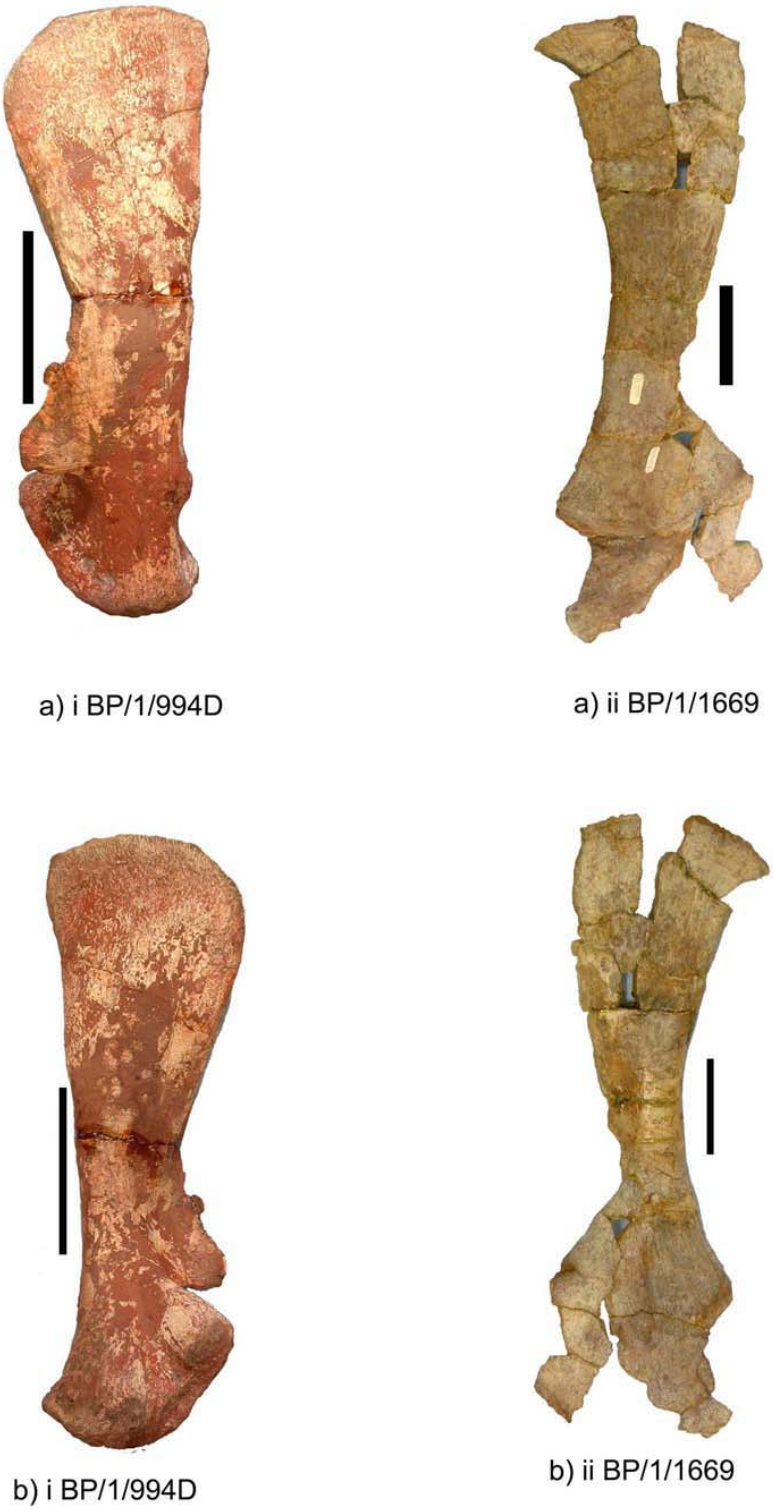

Plate 13 Left (BP/1/994D) and right (BP/1/1669) scapula of Morphotype B showing that BP/1/1669 is much larger in a) lateral view and b) medial view.

Scale bar = 10 cm

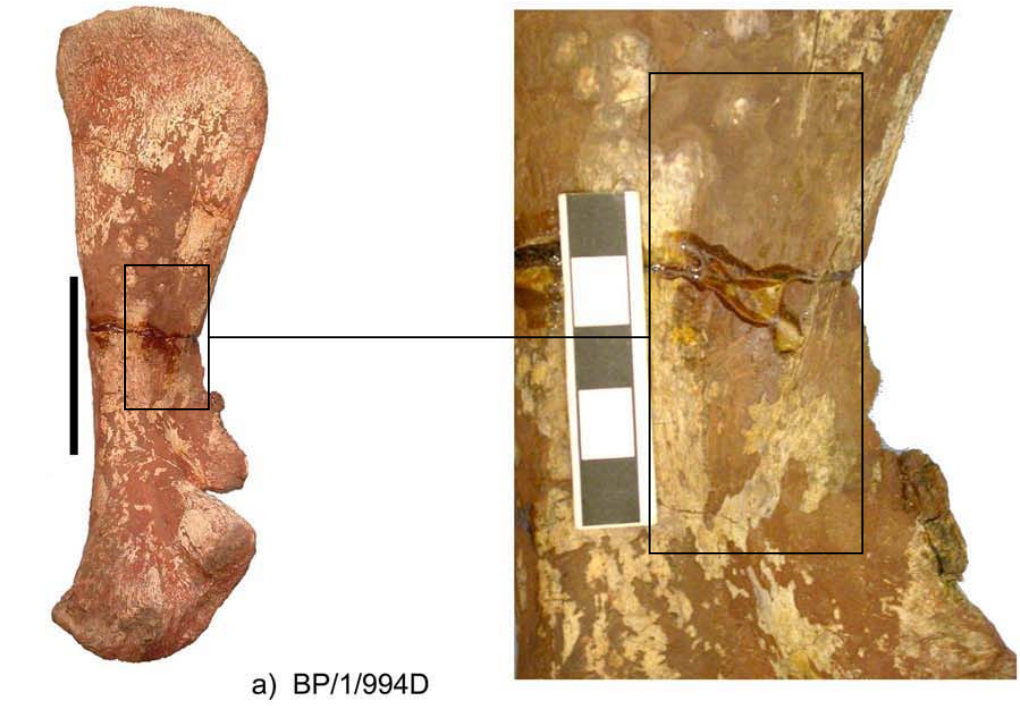

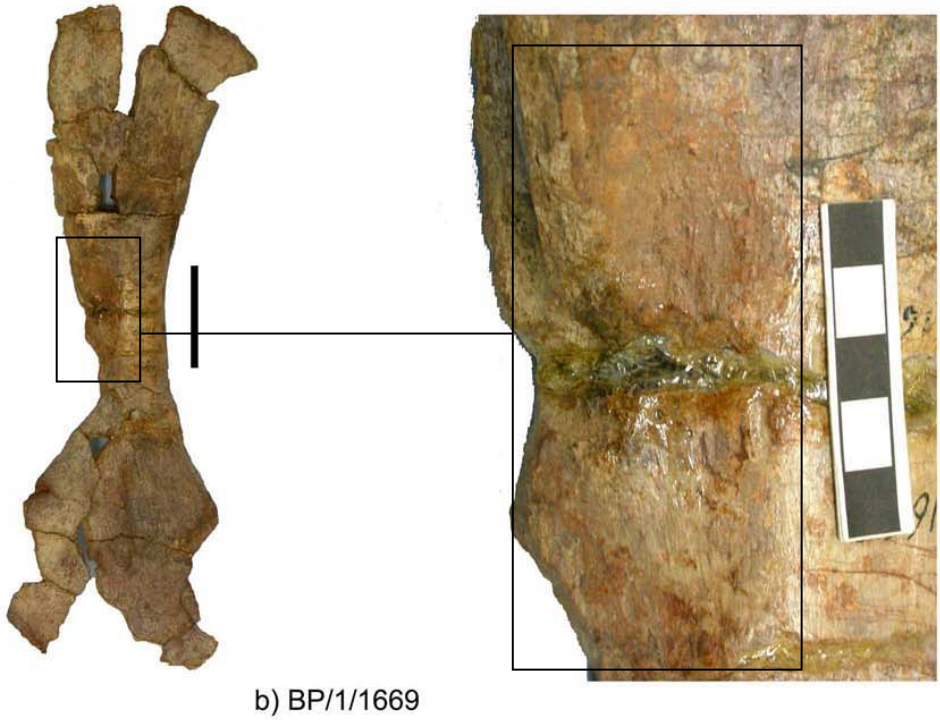

Plate 14 Medial view of the left [a) BP/1/994D] and right [b) BP/1/1669] scapula of Morphotype B showing the fossa at the proximo-posterior corner of the acromion.
Scale bar = 10 cm

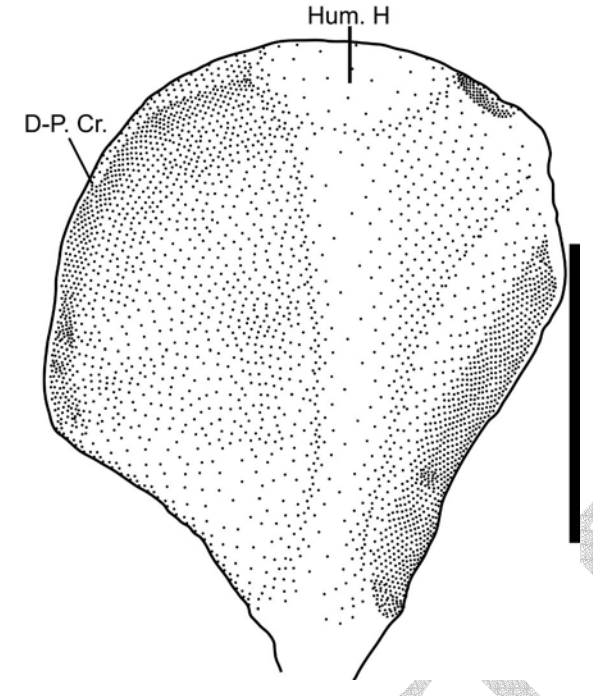

a)

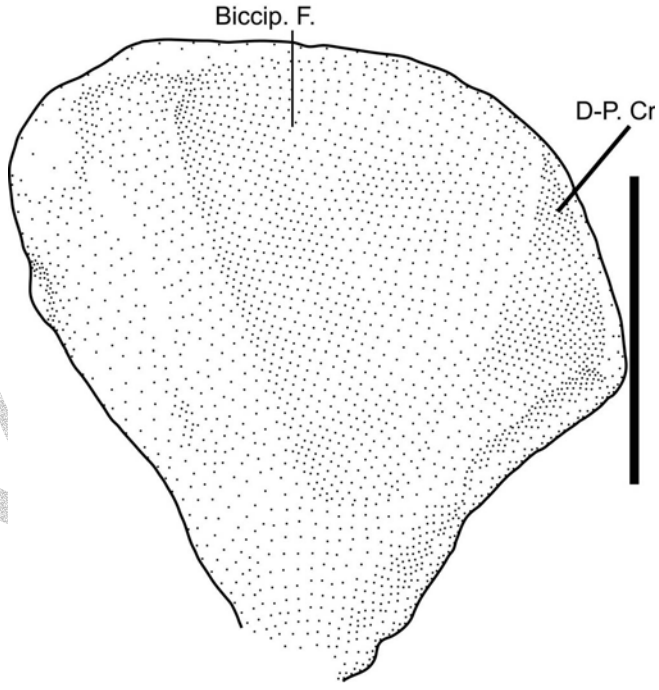

b)

Figure 9 Proximal expansion of the humerus of Morphotype B (BP/1/994A) showing an arc shaped delto-pectoral crest in a) dorsal view and the medial direction of the delto-pectoral crest in b) ventral view.

Scale bar = 10 cm

a) i BP/1/1994A

a) ii SAM-PK-1073

b) BP1/1994A

Plate 15 Proximal end of the left humerus of Morphotype B showing the arc shaped delto-pectoral crest in a) i-ii dorsal view [i. BP/1/994a; ii SAM-PK-1073] and that it is slightly medially directed in b) ventral view (BP/1/994A).

Scale bar = 10 cm

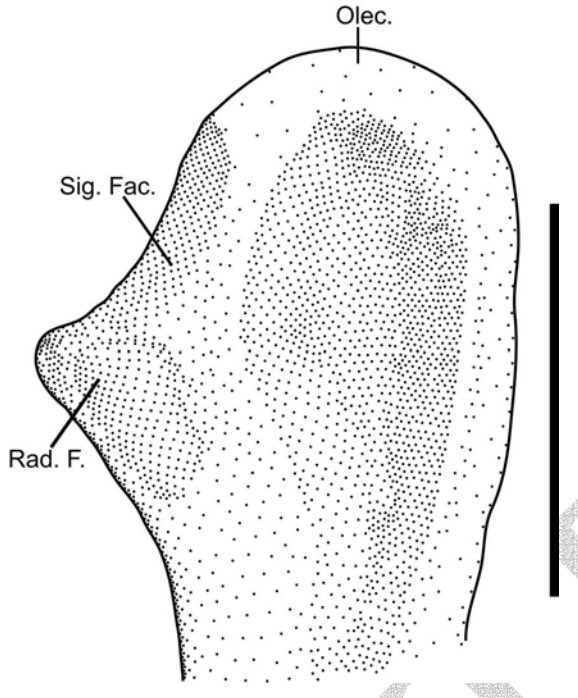

a)

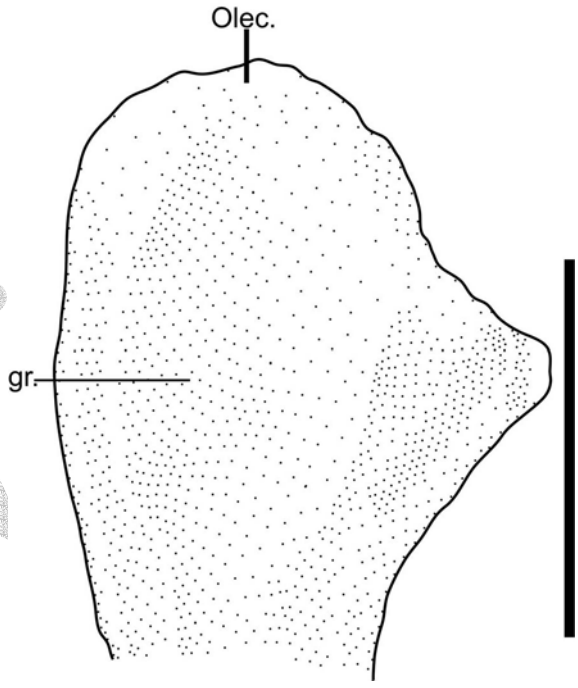

b)

Figure 10 Proximal end of the left ulna of Morphotype B (SAM –PK-1073) in a) lateral view and b) medial view.

Scale bar = 10 cm

a) SAM-PK-1073

b) SAM-PK-1073

Plate 16 Proximal end of the left ulna of Morphotype B (SAM-PK-1073) in a) lateral view and b) medial view showing the low, wide olecranon.

Scale bar = 10 cm

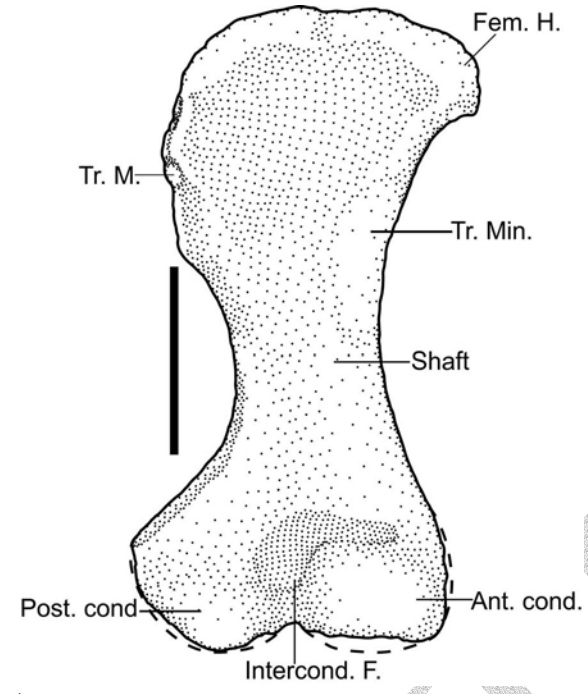

a)

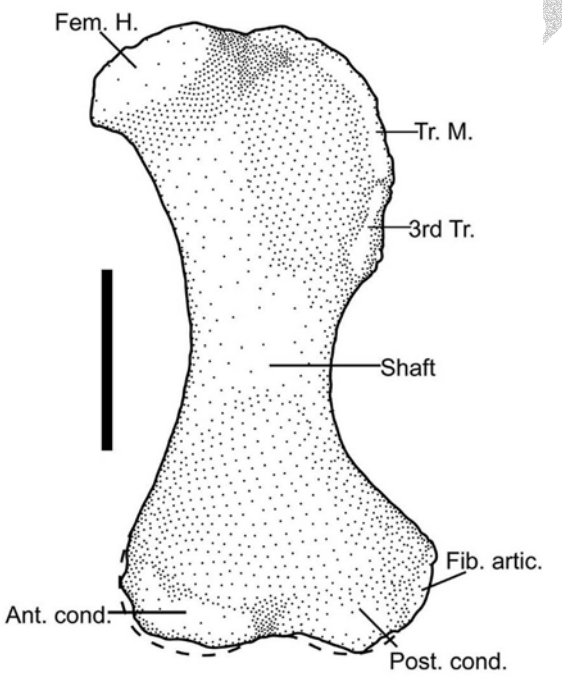

b)

Figure 11 Right femur of Morphotype B (BP/1/3518) showing a wide proximal expansion and narrow greater trochanter in a) dorsal view and the third trochanter in b) ventral view.
Scale bar = 10 cm

a) BP/1/3518

b) BP/1/3518

Plate 17 Right femur of Morphotype B (BP/1/3518) the narrow greater trochanter in a) dorsal view and the short third trochanter and antero-dorsally directed head in b) ventral view.

Scale bar = 10 cm

Plate 18 Scapulae (left and right) of British Museum specimen previously identified as *K. simocephalus* (by Pearson 1924b) (Morphotype A) show features that show them to more closely resemble Morphotype B. Scale – coin = 17 mm

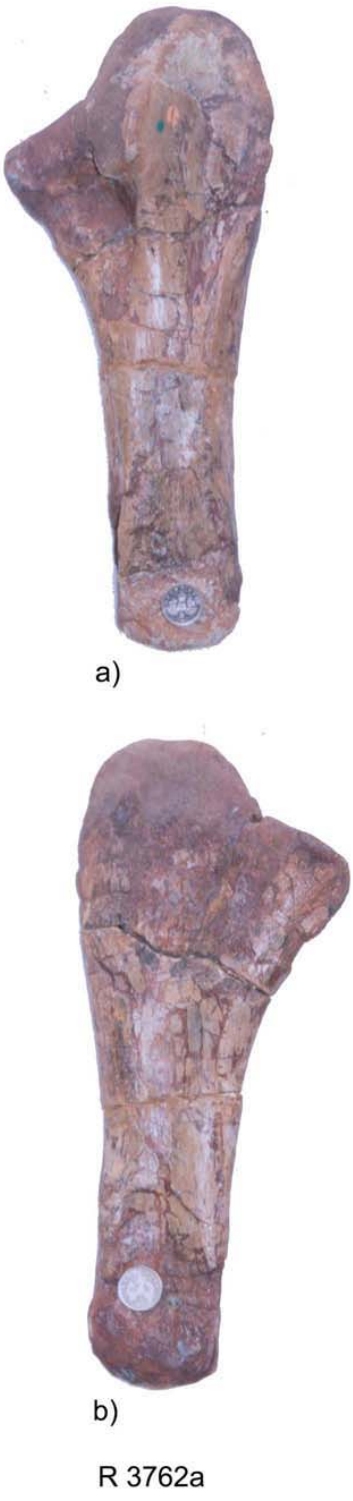

Plate 19 Ulna (left) of British Museum specimens that was previously identified as *K. simocephalus* (by Pearson 1924b) (Morphotype A) but closer examination of photographs of the material shows that it more closely resembles Morphotype B.

Scale – coin = 17mm

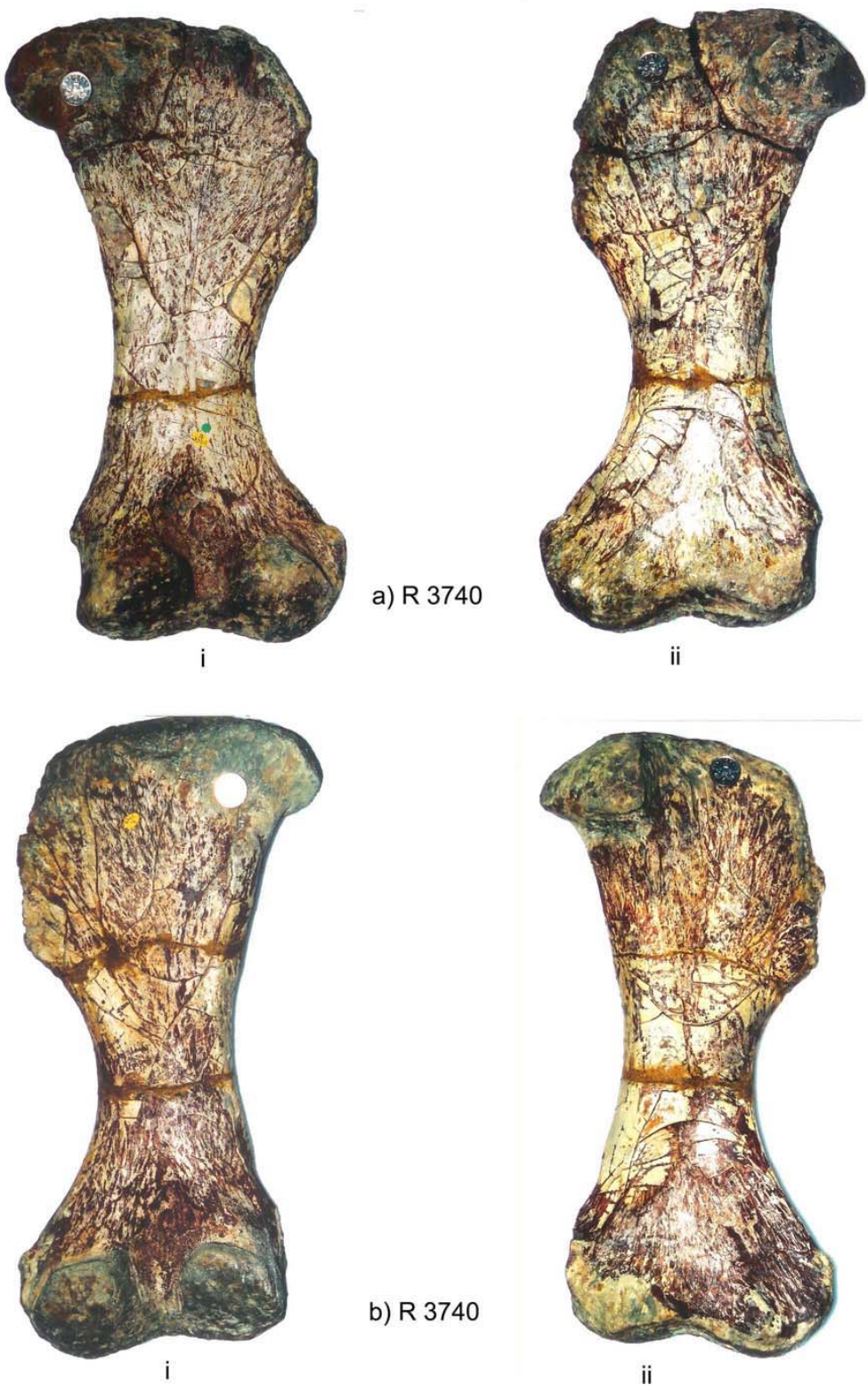

Plate 20 Left and right femora of a British Museum specimen (R 3740) previously identified as *K. simocephalus* (by Pearson 1924b) (Morphotype A), which resembles Morphotype B more closely.
Scale – coin = 17 mm

Appendix C

Comparison of Morphotype B with *K. simocephalus*

Wits ETD

a) i BP/1/5624

a) ii BP/1/994D

b) i BP/1/5624

b) ii BP/1/994D

Plate 21 Comparison of the scapula of Morphotype B [b)i & ii] with that of *K. simocephalus* showing the tubercle [b)i] and the fossa [b) ii] at the proximo-posterior corner of the acromion.

Scale bar = 10 cm

Plate 22 Comparison of the proximal end of the humerus of Morphotype B (BP/1/994A) with the humerus of *K. simocephalus* (BP/1/6160) showing the difference in the shape of the delto-pectoral crest (a) i-ii and the biccipital fossa in b) i-ii.

Scale bar = 10 cm

Plate 23 Comparison of the proximal end of the ulna of Morphotype B (SAM-PK-1073) with that of *K. simocephalus* (BP/1/6160), showing the difference in the olecranon of the two morphotypes.

Scale bar = 10 cm

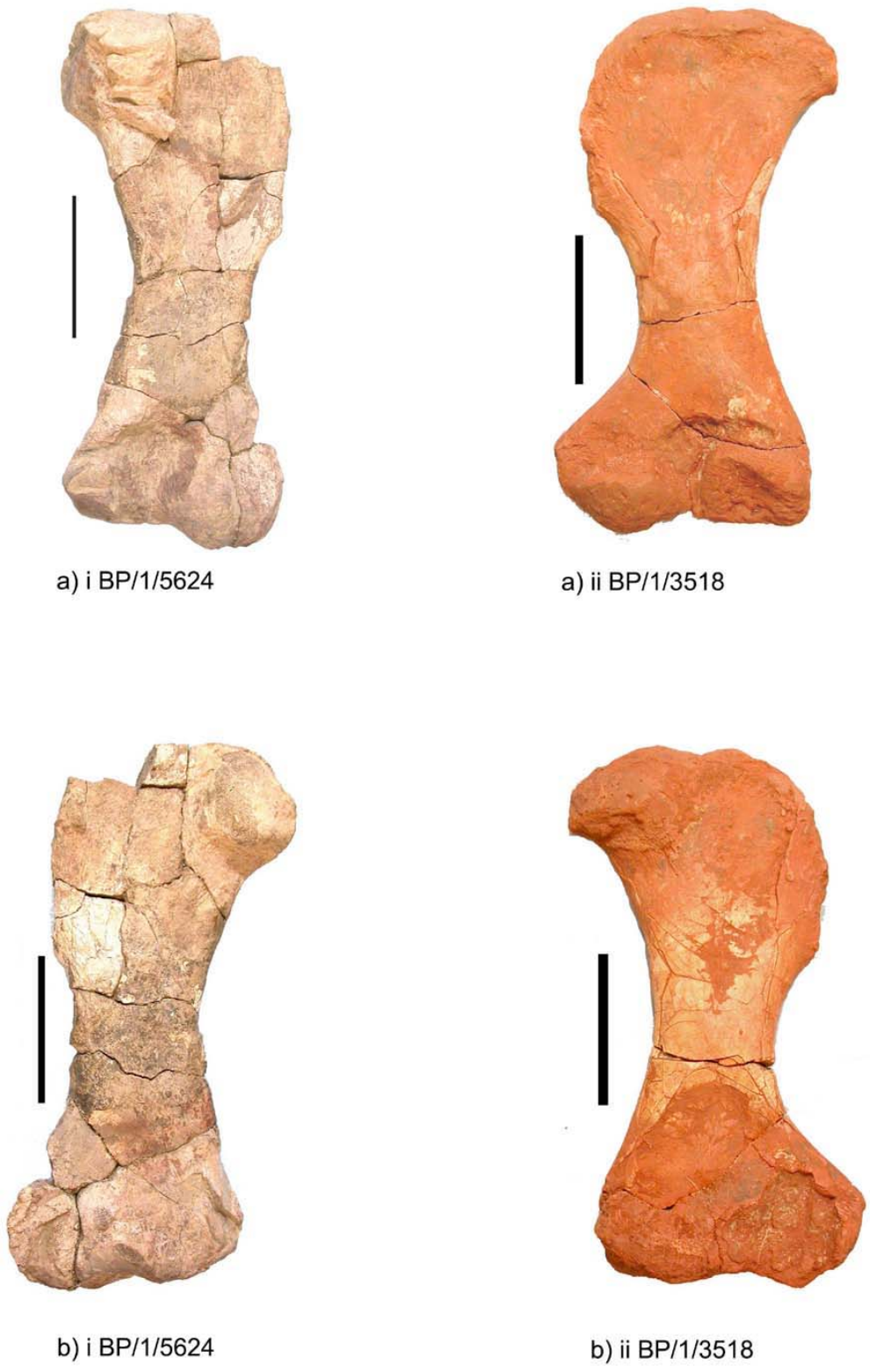

Plate 24 Comparison of the right femur of Morphotype B (BP/1/3518) and the left femur of *K. simocephalus* (BP/1/5624) clearly showing the medially inflected head in *K. simocephalus* [b)i] and the antero-dorsally directed head in Morphotype B [b)ii]. Scale bar = 10 cm

APPENDIX D

COMPARISON OF MORPHOTYPE B WITH *ZAMBIASAURUS* & *ANGONISAURUS*

Wits ETD

Plate 25 Comparison of the scapula of Morphotype B with that of *Zambiasaurus* showing the narrow scapula blades (a) and the antero-ventrally directed coracoid articulation (b). Scale bar = 10 cm; scale – coin = 17 mm

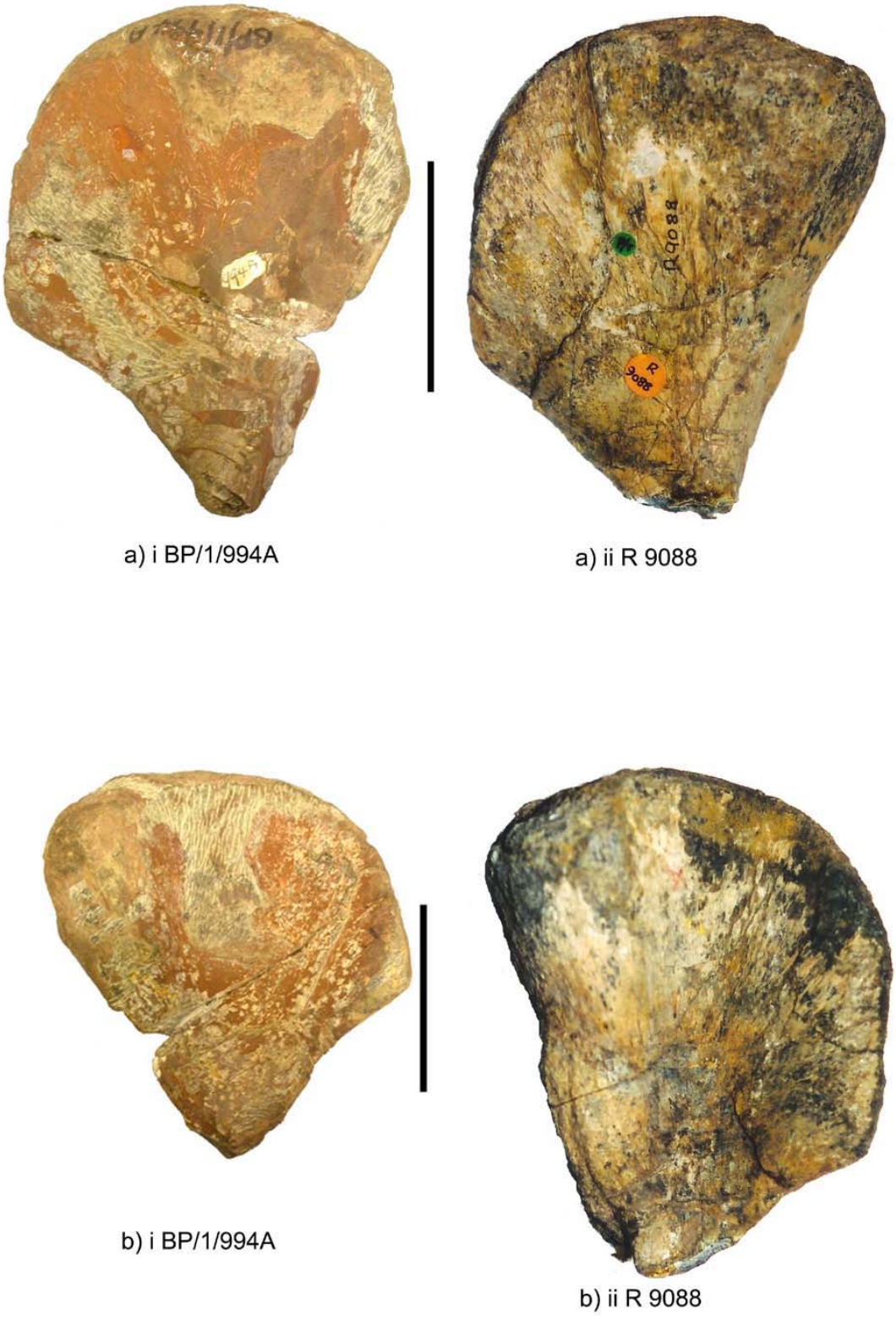

Plate 26 Comparison of the humerus of Morphotype B with that of *Zambiasaurus* showing the more posteriorly positioned head and arc shaped delto-pectoral crest [a) i-ii] and medially directed delto-pectoral crest and slightly deep biccipital fossa [b) i-ii]. Scale bar = 10 cm

Plate 27 Comparison of the lateral view of the ulna of Morphotype B with *Zambiasaurus* showing that Morphotype B has a wider olecranon in a) i-ii lateral view and a deeper groove in b) i-ii medial view.

Scale bar = 10 cm; Scale – coin = 17 mm

Plate 28 Comparison of the femur of Morphotype B with that of *Zambiasaurus* showing that the proximal end of the femur Morphotype B is wider than that of *Zambiasaurus* [a)i-ii] and that the head of the femur of *Zambiasaurus* is less well developed in this specimen [b) i-ii]. Scale bar = 10 cm

a) i BP/1/1669

a) ii R 732

b) i BP/1/1669

b) ii R 732

Plate 29 Comparison of the scapula of Morphotype B with *Angonisaurus* showing that *Angonisaurus* has a larger more robust scapula and the acromion is directed more laterally in *Angonisaurus* [a)i-ii] and there is no fossa present on the medial surface of the scapula *Angonisaurus* [b) i-ii]. Scale bar = 10 cm; scale – coin = 17 mm

Plate 30 Comparison of the humerus of Morphotype B with *Angonisaurus*, showing the triangular delto-pectoral crest in *Angonisaurus* [a)i-ii] and in b)i-ii showing an almost trapezoidal biccipital fossa in *Angonisaurus*. Scale bar = 10 cm

Plate 31 Comparison of the ulna of Morphotype B with *Angonisaurus* that shows the wedge-shaped olecranon in *Angonisaurus* [a)ii] compared with the wider one in Morphotype B [a)i] and shows a more elongated proximal end in *Angonisaurus* [b)ii] than in Morphotype B [b)i] as seen in medial view (b). Scale bar = 10 cm

APPENDIX E

POSTCRANIAL MATERIAL OF UNCERTAIN AFFINITY

Wits ETD

a) ELM 1

b) ELM 1

c) ELM 1

Plate 32 Shows some elements from the skeleton of ELM 1 that does not conform with the features of what is currently recognised as *K. simocephalus* (Morphotype A): a) radius and ulna; b) ilium and c) pubo-ischiadic plate.

Scale bar = 10 cm

Appendix F

Comparative Muscle Architecture of *K. simocephalus* & Morphotype B

Wits ETD

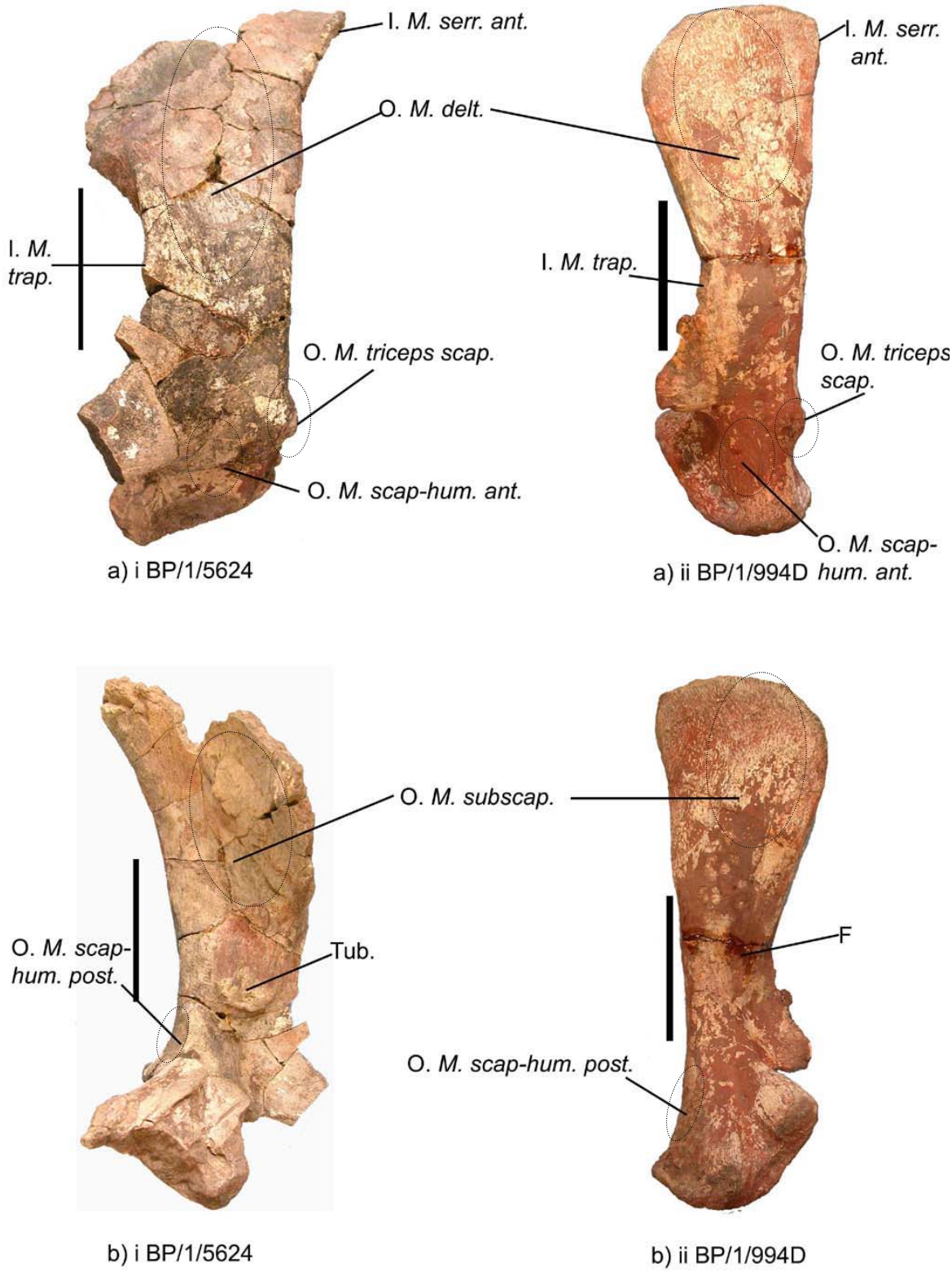

Figure 12 Muscle attachment sites on the lateral [a) i-ii] and medial [b) i-ii] surfaces of the scapulae of *K. simocephalus* [a & b) i] and Morphotype B [b) ii] showing that in most instances there is a difference in the size of the muscles between the two animals.

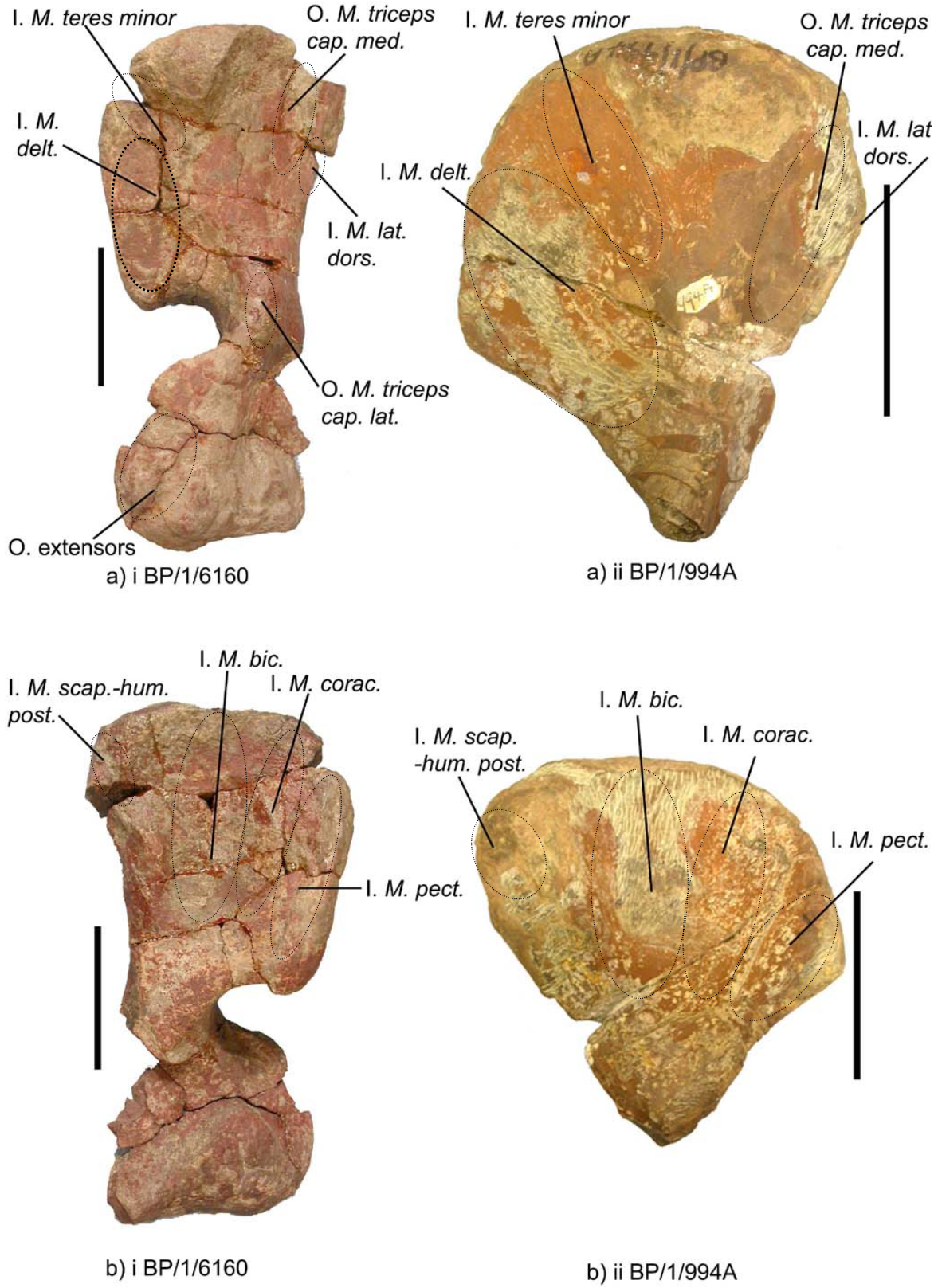

Figure 13 Muscle attachment sites on the dorsal [a) i-ii] and ventral [b) i-ii] surfaces of the humerus of *K. simocephalus* [a & b) i] and Morphotype B [a & b) ii].

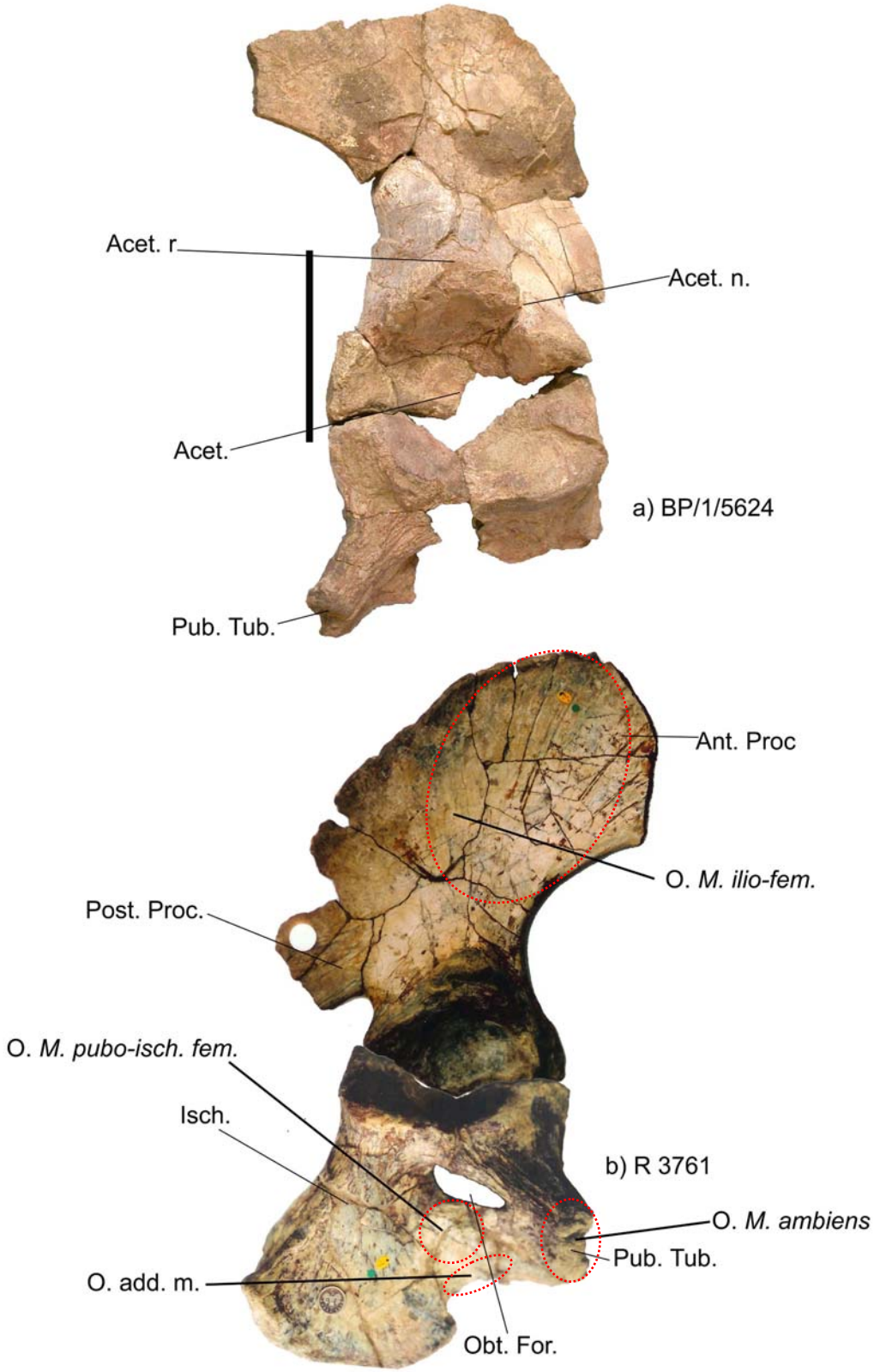

Figure 14 Muscle attachment sites on the lateral surface of the pelvic girdle of *K. simocephalus*.

Figure 15 Muscle attachment sites on the dorsal [a) i-ii] and ventral [b) i-ii] surfaces of the femora of *K. simocephalus* [a & b) i] and Morphotype B [a & b) ii].

Appendix G

Phylogenetics

Wits ETD

Character List

Character 27 of Vega – Dias *et al* (2004) was modified in this study.

Development of the acromion process: (0) well defined acromion; (1) acromion reduced to a small knob; (2) acromion reduced to a tubercle or no acromion.

The following characters were added to the character list of Vega – Dias *et al* (2004). Vega-Dias *et al* (2004) provides the description of character 1 to 44.

45. Scapula spine absent (0); present (1). In some taxa a scapula spine projects anteriorly over the anterior border of the scapula and forms a groove between the two.
    Lystrosaurus, Shansiodon, Angonisaurus, Jachaleria and *Dinodontosaurus* have no scapula spine, while *Tetragonias, K. simocephalus, Wadiasaurus, Sinokannemeyeria, Ischigualastia, Placerias* and Morphotype B all have scapula spine.
46. Projection in front of the glenoid facet of the scapula – absent (0); present (1). The bone in front of the glenoid facet of the scapula forms a thick, round projections that is directed ventrally.
    Lystrosaurus, Shansiodon, Angonisaurus, Ischigualastia, Jachaleria, Dinodontosaurus and Morphotype B have no projection in front of the glenoid facet of the scapula. *Wadiasaurus, K. simocephalus, Sinokannemeyeria,* and *Parakannemeyeria* have this projection present.
47. The coracoid articulation on the scapula faces antero-ventrally (0); faces ventrally (1).
    Lystrosaurus, Wadiasaurus, Sinokannemeyeria, Parakannemeyeria, Ischigualastia, Dinodontosaurus, Jachaleria, Placerias, K. simocephalus and Morphotype B all have antero-ventrally facing coracoid articulation on the scapula. *Shansiodon, Tetragonias, Angonisaurus* have ventrally directed coracoid articulation.
48. Glenoid facet of the scapula faces laterally (0); faces postero-ventrally (1); faces ventrally (2).
    Wadiasaurus, Parakannemeyeria, Sinokannemeyeria, Angonisaurus, Ischigualastia, Jachaleria, Dinodontosaurus, Placerias, K. simocephalus all have postero-ventrally facing glenoid facets. *Shansiodon, Tetragonias* and Morphotype B have ventrally facing glenoid facets.
49. Delto-pectoral crest of the humerus is long and rectangular (0); short and "arc" shape (1).

WitsETD

Wadiasaurus, Parakannemeyeria, Ischigualastia, Dinodontosaurus, Placerias and *K. simocephalus* have long, rectangular delto-pectoral crest. *Shansiodon, Tetragonias, Sinokannemeyeria, Placerias* and Morphotype B all have delto-pectoral crests that are short and "arc" shaped.

50. Olecranon part of the shaft (0) or separately ossified (1) (Maisch 2001).

Shansiodon, Parakannemeyeria, Sinokannemeyeria, Angonisaurus, Placerias, K. simocephalus and Morphotype B all have olecranon that are fused to the shaft while *Wadiasaurus, Ischigualastia* and *Dinodontosaurus* have separately ossified olecranon.

51. Shape of the olecranon narrow and triangular or wedge shaped (0); broad and low (1).

Shansiodon, Wadiasaurus, Sinokannemeyeria, Angonisaurus, Ischigualastia, and *K. simocephalus* all have a narrow, triangular or wedge shaped olecranon. *Tetragonias, Parakannemeyeria, Dinodontosaurus Placerias* and Morphotype B have a broad, low olecranon.

52. Delto-pectoral crest is 90° to the long axis of the humerus (0) or less than 90° (1). The delto-pectoral crest in some taxa is almost parallel with the long axis of the humerus whereas in other taxa the delto-pectoral crest is at an angle to the long axis of the bone.

Wadiasaurus, Parakannemeyeria, Ischigualastia, Dinodontosaurus, and *K. simocephalus* have the delto-pectoral crest 90° to the long axis of the humerus. *Shansiodon, Tetragonias, Sinokannemeyeria, Placerias* and Morphotype B have the delto-pectoral crest less than 90° to the long axis of the humerus.

53. The scapula blade is moderately elongated (0) or extremely long and slender (1) (Maisch 2001).

Tetragonias, Wadiasaurus, Angonisaurus, Ischigualastia, Dinodontosaurus, Placerias and *K. simocephalus* have moderately elongated blades while *Parakannemeyeria, Sinokannemeyeria* and Morphotype B have long, slender blades.

54. Ilium with moderately anterior and posterior expansions (0), preacetabular markedly enlarged (1), strongly enlarged into low elongated plate, postacetabular expansion is much reduced (2) (Maisch 2001).

Shansiodon, Parakannemeyeria, Dinodontosaurus, Placerias have moderately expanded anterior and posterior processes. *Tetragonias, Wadiasaurus, Sinokannemeyeria, Jachaleria* and *K. simocephalus* have markedly larger preacetabular region while *Angonisaurus, Ischigualastia* have a low plate anteriorly and a reduced postacetabular region.

Wits ETD

55. Femoral head continuous with the greater trochanter (0) or separated from the greater trochanter.

    Tetragonias, Wadiasaurus, Dinodontosaurus, K. simocephalus and Morphotype B have the head continuous with the greater trochanter, however, in Morphotype B there is a beginning of a separation between the head and the greater trochanter. *Shansiodon, Parakannemeyeria, Sinokannemeyeria, Ischigualastia* and *Placerias* have the head clearly separated from the greater trochanter.

56. Third trochanter absent (0) or present (1).

    In *Wadiasaurus, Ischigualastia, Dinodontosaurus* and *K. simocephalus* there is no third trochanter while in *Tetragonias* and Morphotype B there is a definite third trochanter present.

Wits ETD

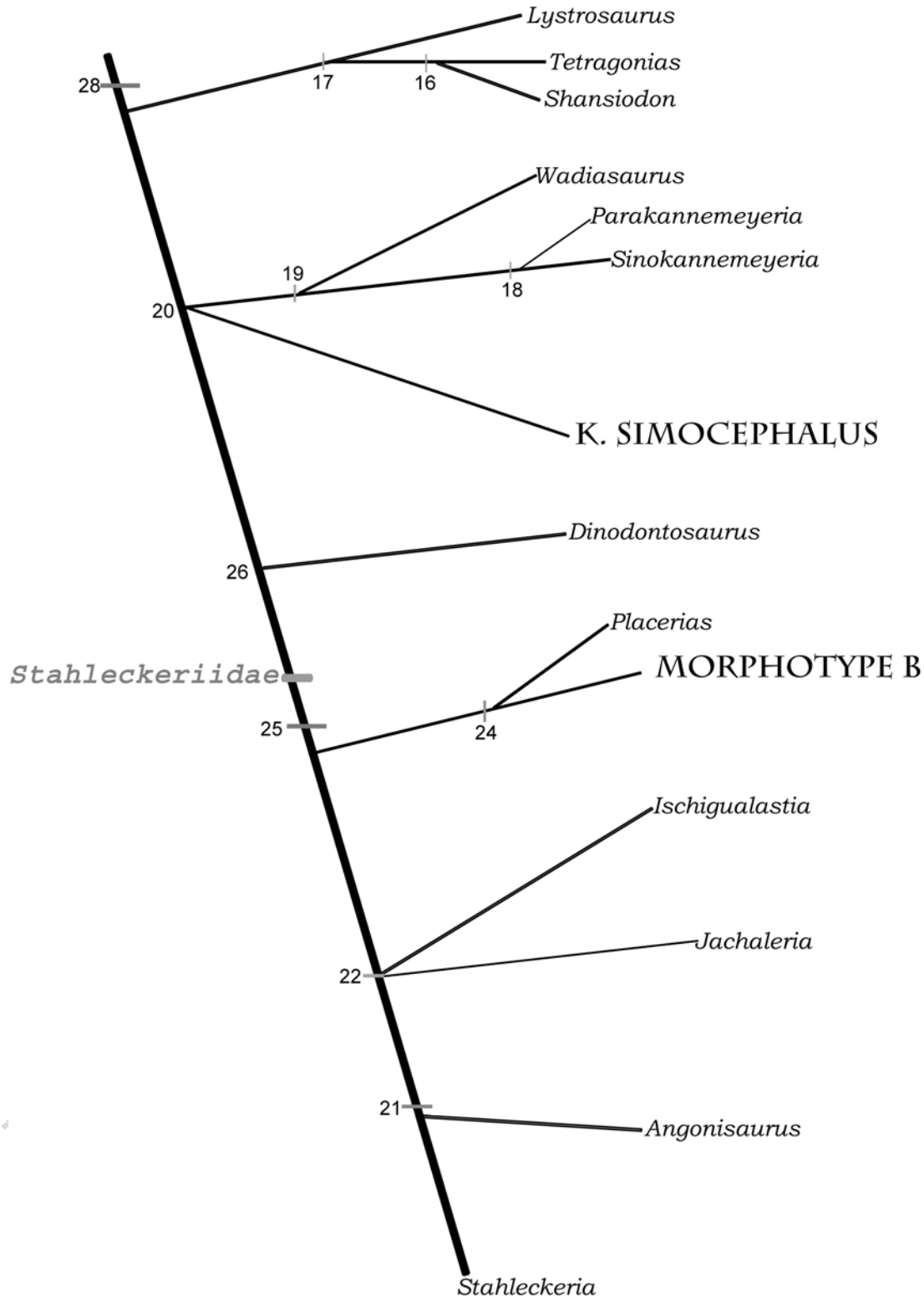

Figure 16 Phylogenetic tree showing the relationships of *K. simocephalus* and Morphotype B with certain Triassic dicynodonts using cranial and postcranial characters. Tree length: 151 steps; CI: 0.45; RI: 0.523; HI: 0.551.

Table 1 List of characters that diagnose each clade.

Character state optimised using Deltran. Unambiguous states marked with asterix. Reversal denoted (rev.), state changes to state 2 denoted with (2).

Branch	Characters
Node 28 – 17	3*, 44*, 48, 49, 52*
Node 17 – 16	13*, 22*, 26*, 33*, 47*
Node 28 – 27	15* (2), 16*, 28*, 45*, 46*, 48, 54*
Node 20 – 19	17*, 33*, 36 (2)
Node 19 – 18	1*, 8*, 10*, 14*, 15*, 16*, 19*, 20*, 26*, 37*, 53*, 55*
Node 27 – 26	11. 13*, 25*, 35*, 37*, 41
Node 26 – 25	7*, 15 (2), 23*, 33*, 34 (2), 36*, 43
Node 25 – 23	2*, 4*, 16, 19, 24, 27* (2), 28*, 29*, 30, 32*, 40, 42
Node 23 – 21	12, 13 (rev), 14*, 18*, 21*, 39
Node 25 – 24	45*, 49*, 51, 52*

WitsETD

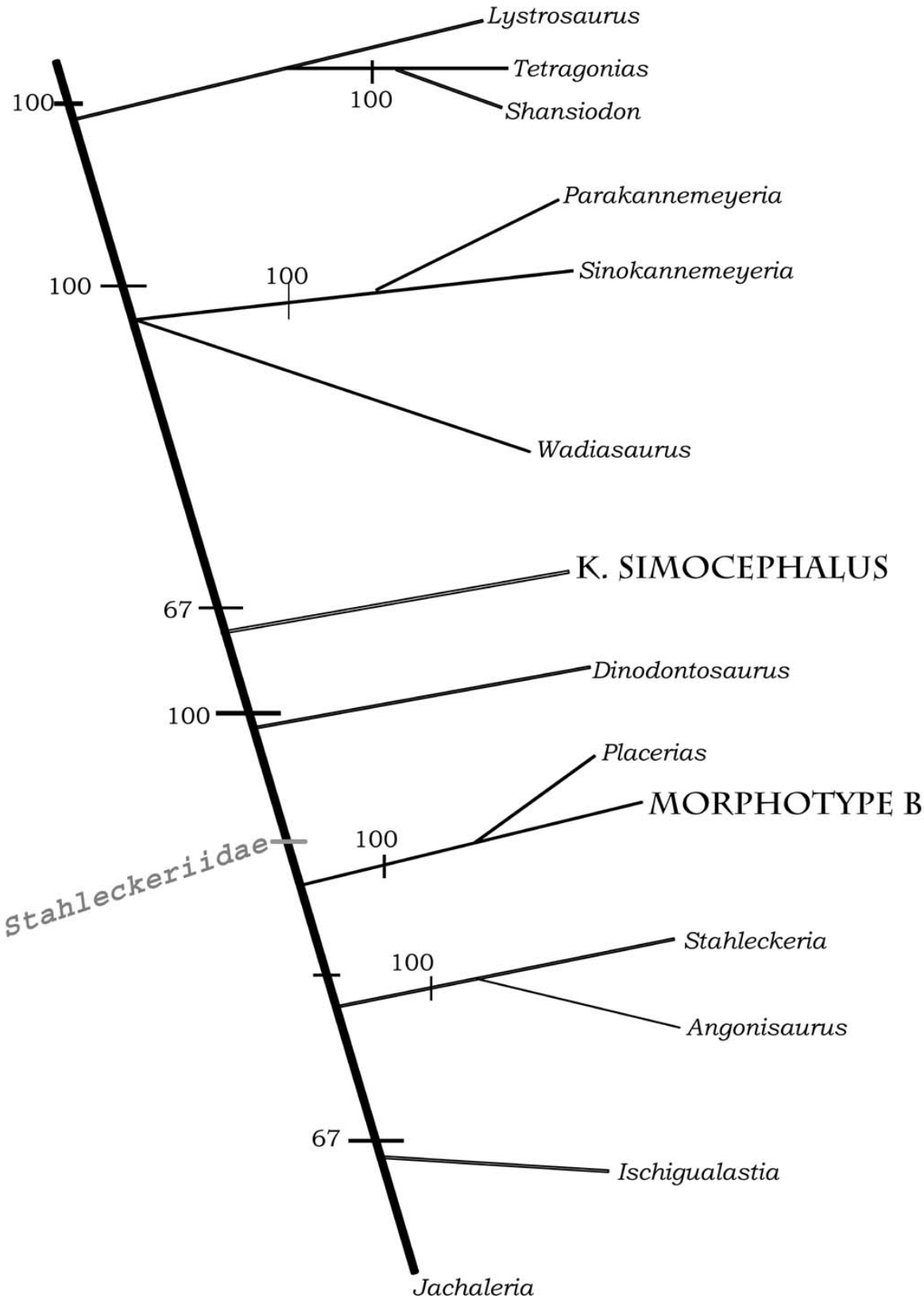

Figure 17 Majority rule consensus tree of the relationships of *K. simocephalus* and Morphotype B among certain Triassic dicynodonts using cranial and postcranial characters.

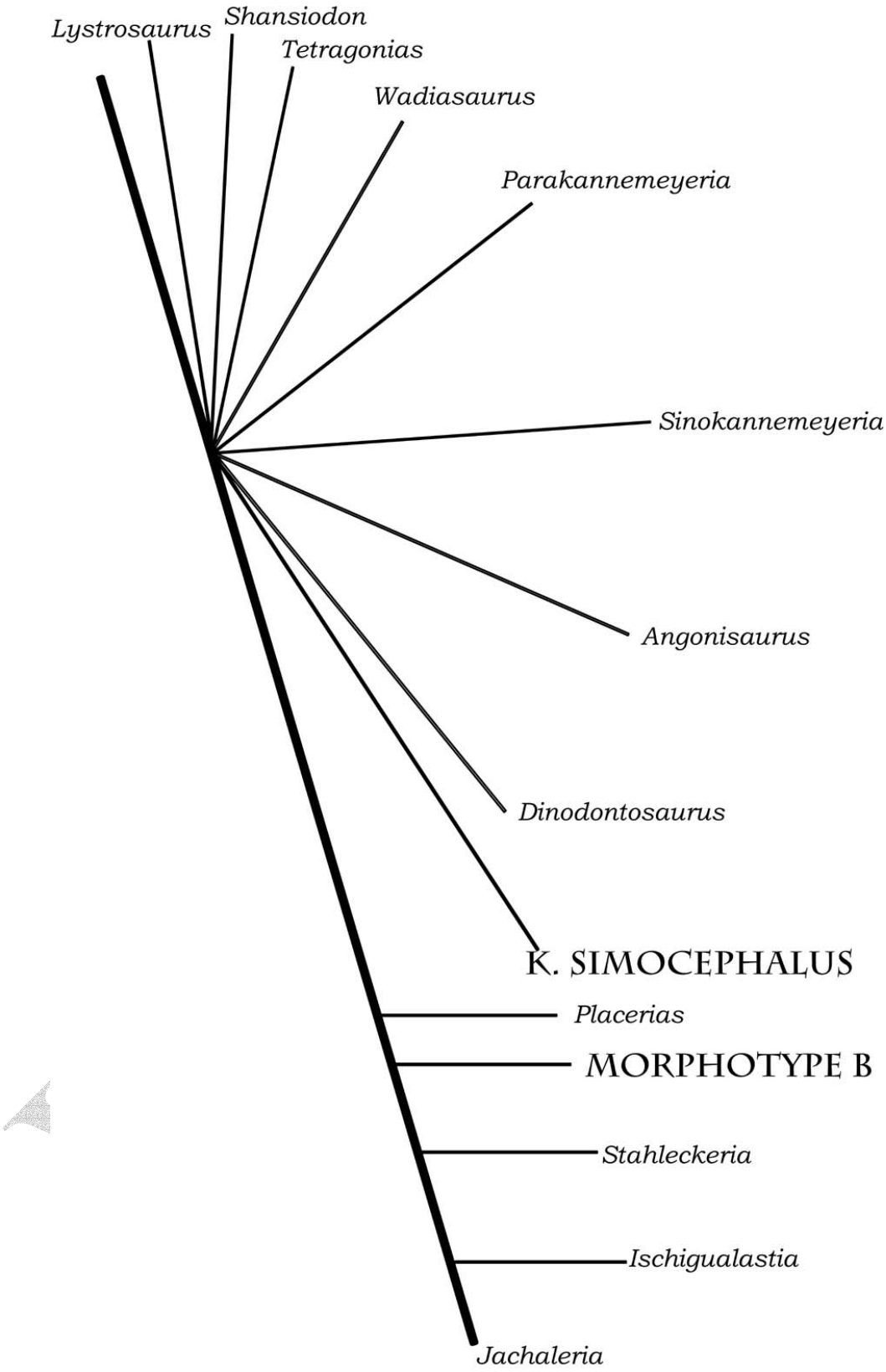

Figure 18 Consensus tree of the relationships of *K. simocephalus* and Morphotype B with some genera of Triassic dicynodonts using only postcranial characters. Tree length: 86 steps; CI: 0.43; RI: 0.5 and HI: 0.57.

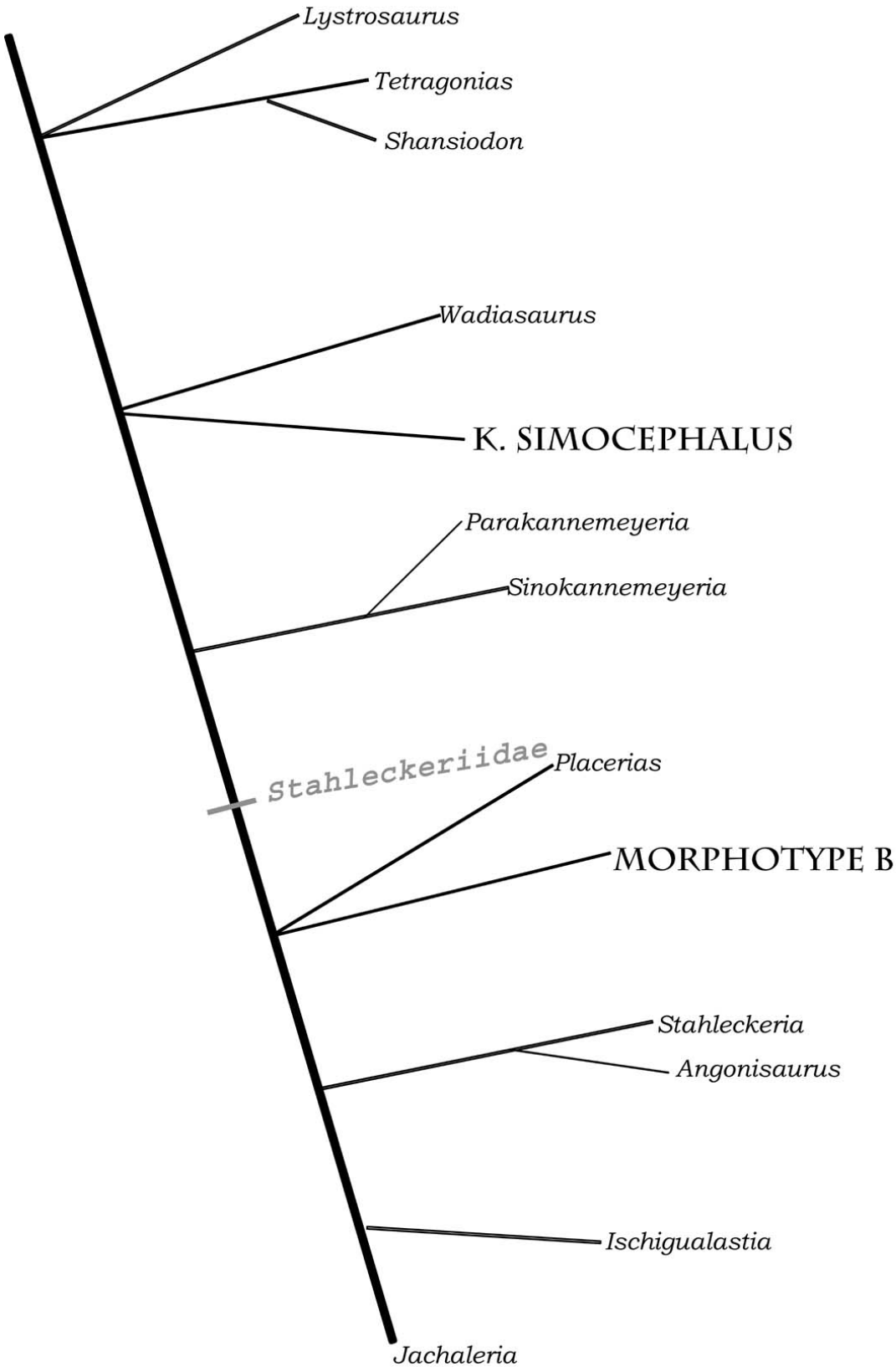

Figure 19 Relationships of *K. simocephalus* and Morphotype B among certain Triassic dicynodonts using cranial and postcranial characters and excludes *Dinodontosaurus*. Tree Length: 138 steps; CI: 0.486; RI: 0.545; HI: 0.514.

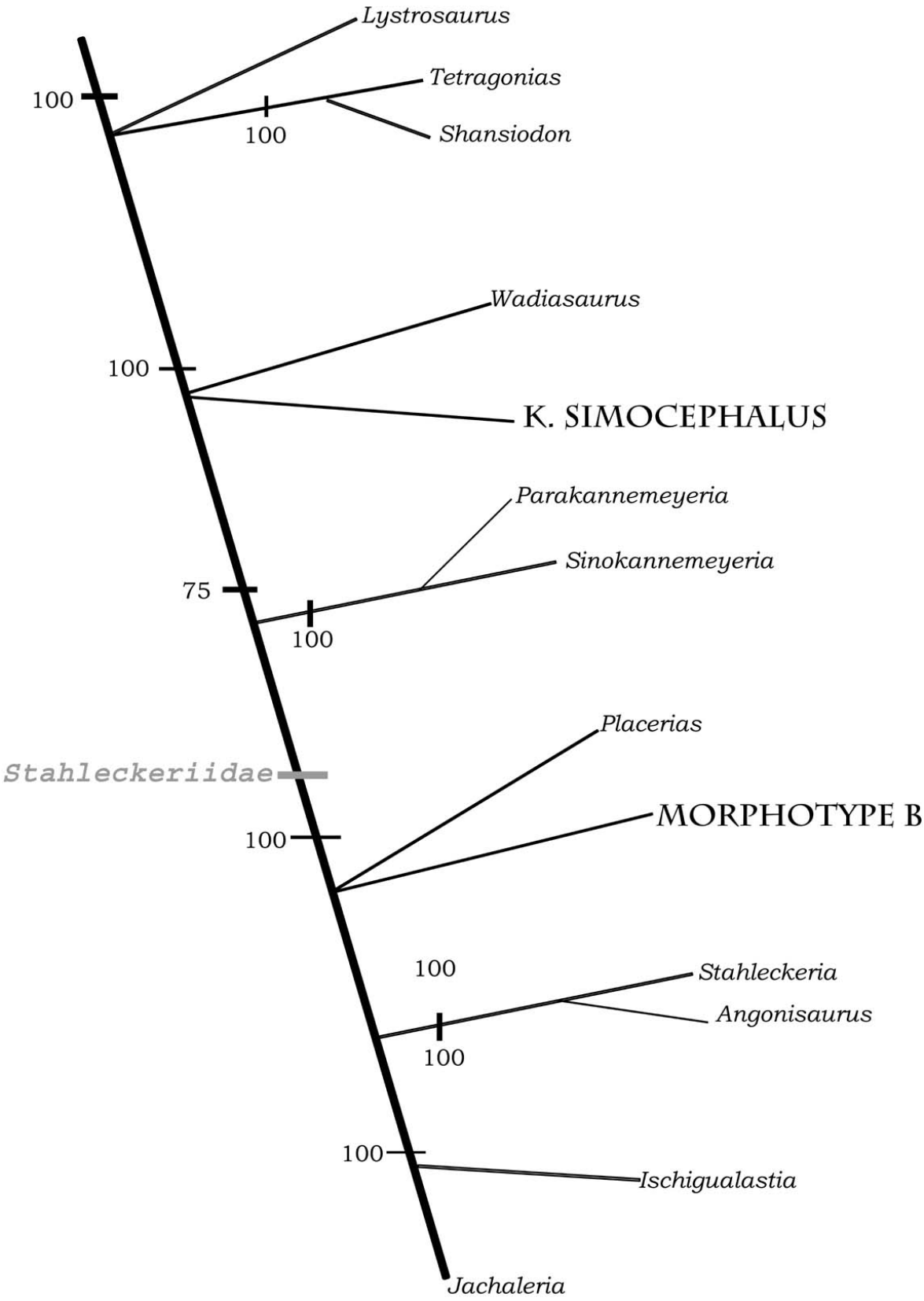

Figure 20 Majority rule consensus tree of the relationships of *K. simocephalus* and Morphotype B among certain Triassic dicynodonts genera using cranial and postcranial characters which excludes *Dinodontosaurus*.

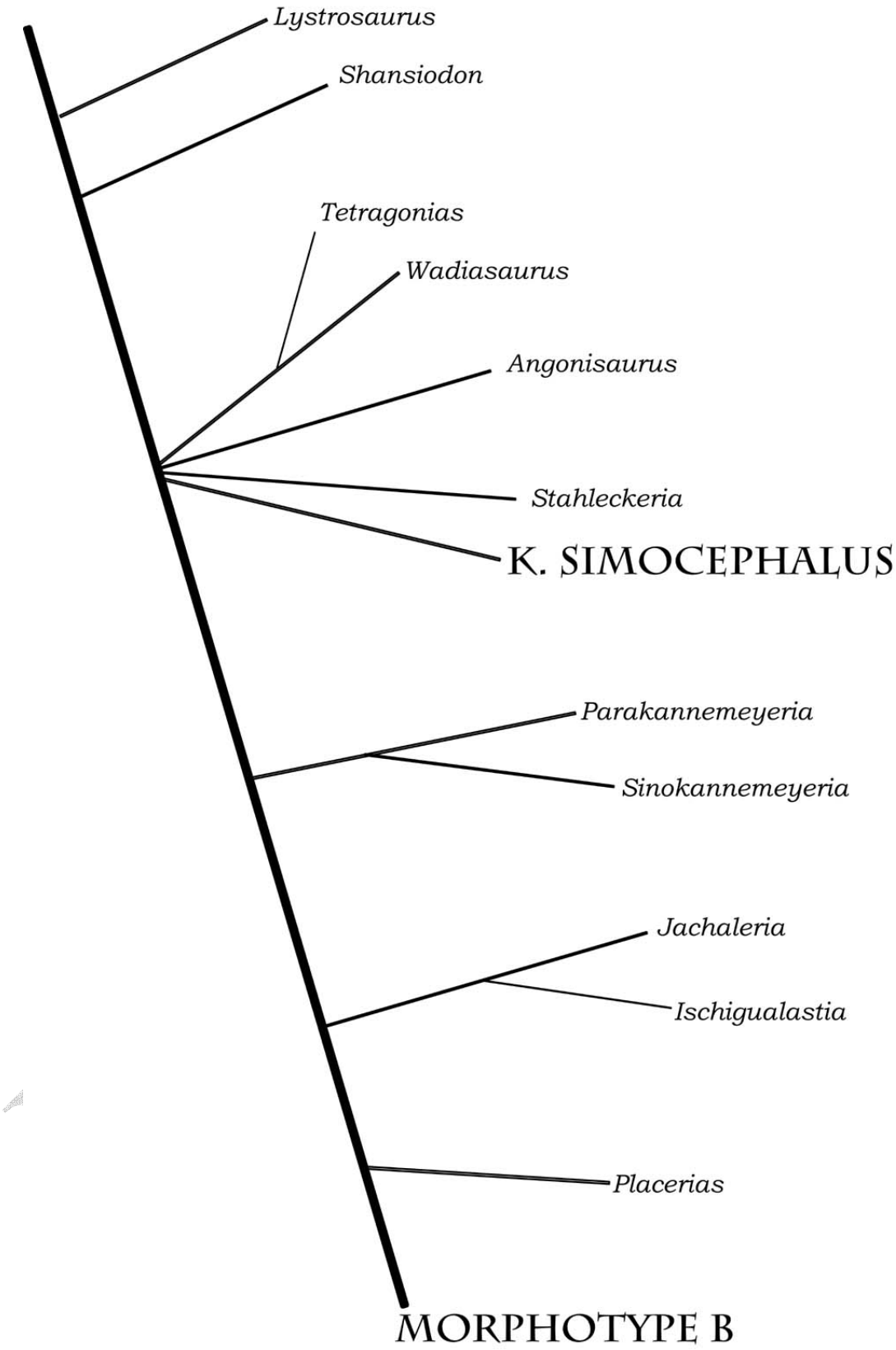

Figure 21 Relationships of *K. simocephalus* and Morphotype B with certain Triassic dicynodonts using only postcranial characters and excludes *Dinodontosaurus*. Tree length: 79; CI: 0.456; RI: 0.511 and HI: 0.544.

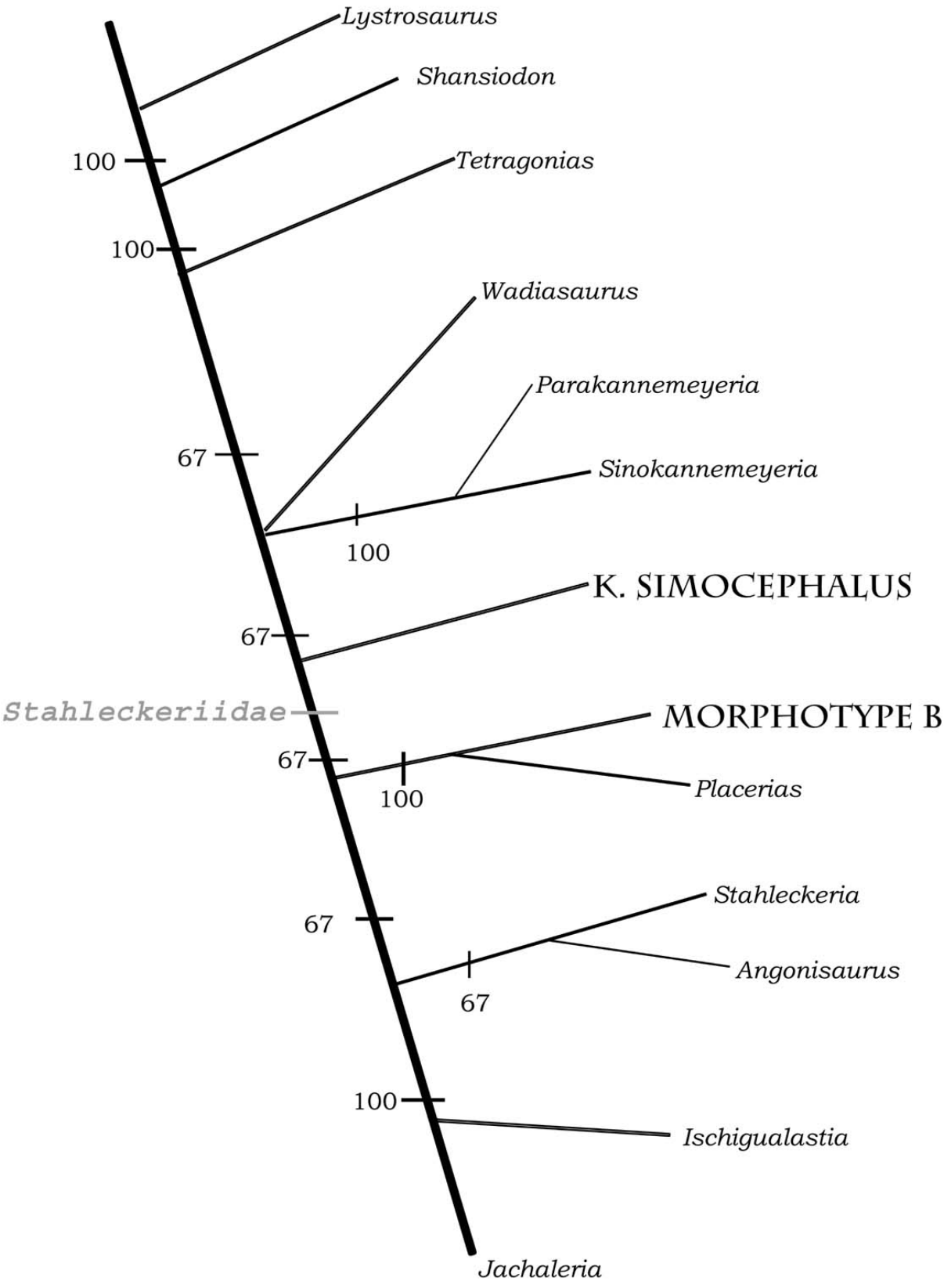

Figure 22 Majority rule consensus tree for the postcranial analysis of the relationships of *K. simocephalus* and Morphotype B among certain Triassic dicynodonts and excludes *Dinodontosaurus*.

Table 2 Data Matrix of taxa and characters used in the phylogenetic analysis.

	1	**2**	**3**	**4**	**5**	**6**	**7**	**8**	**9**	**10**	**11**	**12**	**13**	**14**
Dicynodon	0	0	0	0	0	0	0	0	0	0	0	0	0	0
Lystrosaurus	0	0	1	0	1	0	0	0	1	1	0	1	0	0
Shansiodon	0	0	1	?	?	1	?	0	0	?	?	0	1	?
Tetragonias	0	0	1	0	0	0	0	0	1	2	?	0	1	0
Wadiasaurus	0	0	0	?	2	0	?	0	0	?	?	0	?	0
Parakannemeyeria	1	0	0	0	0	0	1	1	0	2	0	0	0	1
Sinokannemeyeria	1	0	0	0	0	0	?	1	0	2	0	0	0	1
Angonisaurus	0	1	1	?	?	0	?	0	?	?	?	1	0	1
Stahleckeria	0	1	0	1	0	0	1	0	0	1	1	1	0	1
Ischigualastia	0	1	0	1	1	1	1	0	0	0	1	0	1	0
Jachaleria	0	1	1	1	0	2	1	0	1	1	1	1	1	0
Dinodontosaurus	0	0	0	0	1	0	0	0	0	0	1	0	1	0
Placerias	2	0	0	0	?	0	1	0	1	0	1	0	1	0
K. simocephalus	0	0	0	?	1	1	0	0	0	0	1	0	0	0
Morphotype B	?	?	?	?	?	?	?	?	?	?	?	?	?	?

WITHDRAWN

Table 2 continued

	15	16	17	18	19	20	21	22	23	24	25	26	27	28
													*	
Dicynodon	0	0	0	0	0	0	0	0	0	0	0	0	0	0
Lystrosaurus	0	0	0	0	0	1	0	0	0	0	0	0	0	0
Shansiodon	0	0	0	?	0	0	0	1	0	0	0	1	0	0
Tetragonias	0	0	0	0	0	0	0	1	0	0	0	1	0	1
Wadiasaurus	1	2	1	0	0	0	0	0	0	0	0	0	0	1
Parakannemeyeria	0	1	1	0	1	1	0	0	0	0	0	1	0	1
Sinokannemeyeria	0	1	1	0	1	1	0	0	0	1	0	1	0	1
Angonisaurus	?	0	0	1	1	0	1	0	1	1	?	0	0	1
Stahleckeria	2	0	0	1	0	1	1	0	1	0	1	0	0	1
Ischigualastia	2	1	0	0	1	0	0	0	1	1	1	1	2	0
Jachaleria	2	1	0	0	1	0	0	0	1	1	?	0	2	0
Dinodontosaurus	1	0	1	1	0	1	0	0	0	0	1	1	0	1
Placerias	2	1	0	0	0	0	0	0	1	?	1	0	0	1
K. simocephalus	1	2	0	0	0	0	0	0	0	0	0	0	0	1
Morphotype B	?	?	?	?	?	?	?	?	?	?	?	0	1	1

WITHDRAWN

Table 2 continued

	29	30	31	32	33	34	35	36	37	38	39	40	41	42
Dicynodon	0	0	?	?	0	0	0	0	0	0	0	0	0	0
Lystrosaurus	1	1	0	0	0	2	0	0	0	0	0	0	0	0
Shansiodon	0	0	?	?	1	0	0	0	0	0	?	?	?	0
Tetragonias	0	0	0	0	1	0	1	0	0	0	0	0	1	0
Wadiasaurus	1	?	?	1	1	0	?	2	0	1	?	0	0	0
Parakannemeyeria	0	0	?	?	1	0	0	2	1	0	?	0	0	0
Sinokannemeyeria	0	0	0	0	1	0	?	2	1	0	?	?	?	1
Angonisaurus	0	?	?	?	?	?	?	?	?	?	1	1	0	?
Stahleckeria	0	0	0	1	1	2	1	1	1	1	1	1	1	1
Ischigualastia	1	1	?	?	?	1	?	1	1	?	?	?	?	1
Jachaleria	1	1	1	1	?	?	?	?	1	0	0	1	1	?
Dinodontosaurus	0	0	0	0	0	0	1	0	1	0	1	1	1	?
Placerias	0	?	0	0	1	2	?	1	1	?	?	0	1	0
K. simocephalus	0	1	?	?	0	0	0	0	0	0	0	0	1	1
Morphotype B	0	1	?	?	?	?	?	?	?	?	?	?	?	1

Wits ETD

Table 2 continued

	43	44	45	46	47	48	49	50	51	52	53	54	55	56
Dicynodon	0	1	0	0	0	0	?	0	0	0	0	0	0	0
Lystrosaurus	0	0	0	0	0	2	1	0	?	1	?	0	0	0
Shansiodon	0	0	0	0	1	2	1	0	0	1	?	0	1	?
Tetragonias	0	0	1	1	1	2	1	0	1	1	0	1	0	1
Wadiasaurus	1	1	1	1	0	1	0	1	0	0	0	1	0	0
Parakannemeyeria	0	1	?	1	0	1	0	0	1	0	1	0	1	?
Sinokannemeyeria	0	1	1	1	0	1	1	0	0	1	1	1	1	?
Angonisaurus	?	?	0	0	1	1	?	0	0	?	0	2	?	?
Stahleckeria	1	1	?	?	?	?	?	?	?	?	?	?	?	?
Ischigualastia	1	0	1	0	0	0	0	1	0	0	0	2	1	0
Jachaleria	?	?	0	0	0	1	?	?	?	?	?	1	?	?
Dinodontosaurus	2	1	0	0	0	1	0	1	1	0	0	1	0	0
Placerias	1	1	1	?	0	1	1	?	1	1	0	?	1	?
K. simocephalus	0	1	1	1	0	1	0	0	0	0	0	1	0	0
Morphotype B	1	1	1	0	0	1	1	0	1	1	1	?	0	1

WITHDRAWN

APPENDIX H

PLATES OF THE ARTICULATING SURFACES OF THE LONG BONES OF *K. SIMOCEPHALUS* AND MORPHOTYPE B

Wits ETD

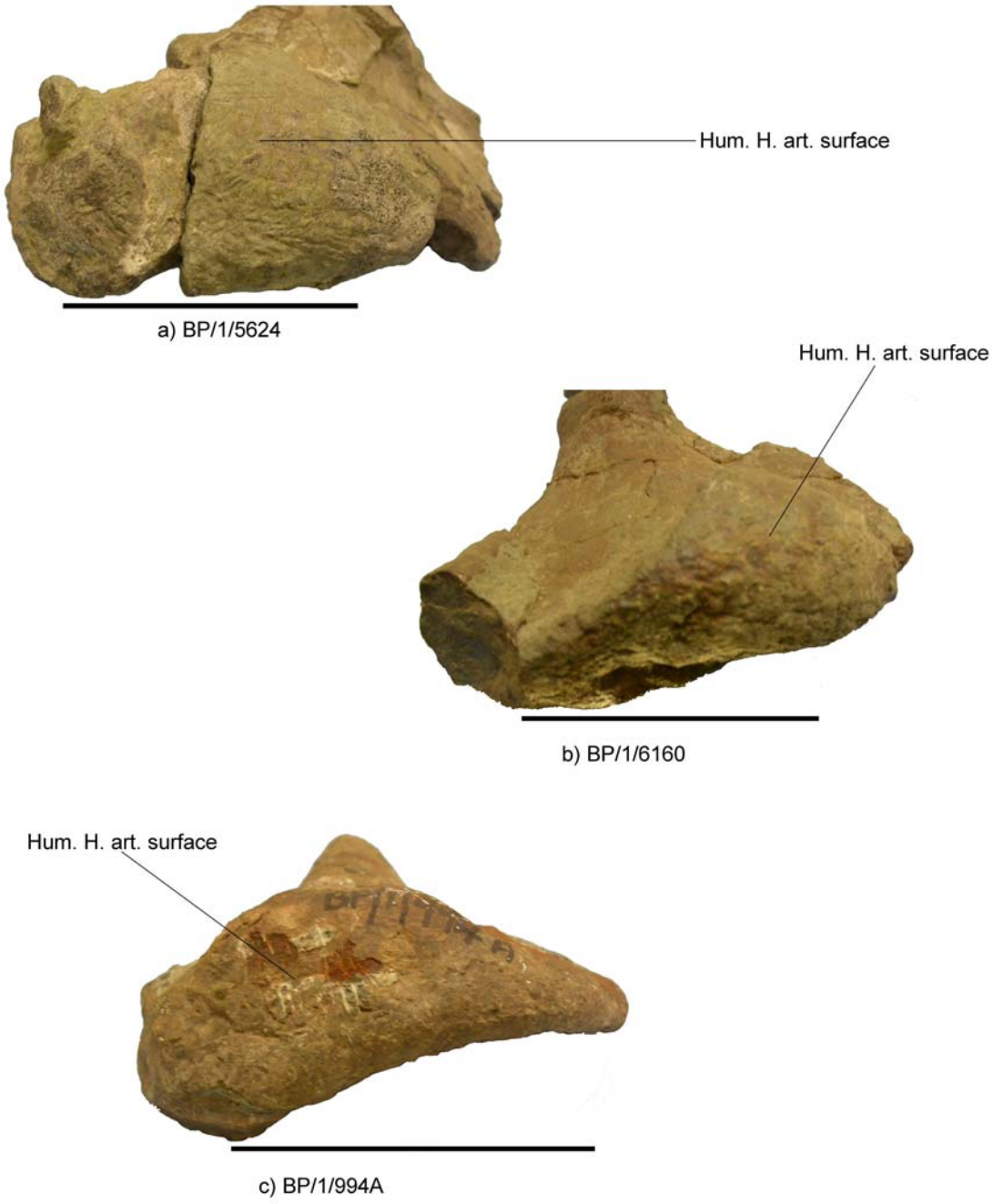

Plate 33 Proximal articulating surface of the humerus of *K. simocephalus* (a & b) and Morphotype B (c).

Scale = 10 cm

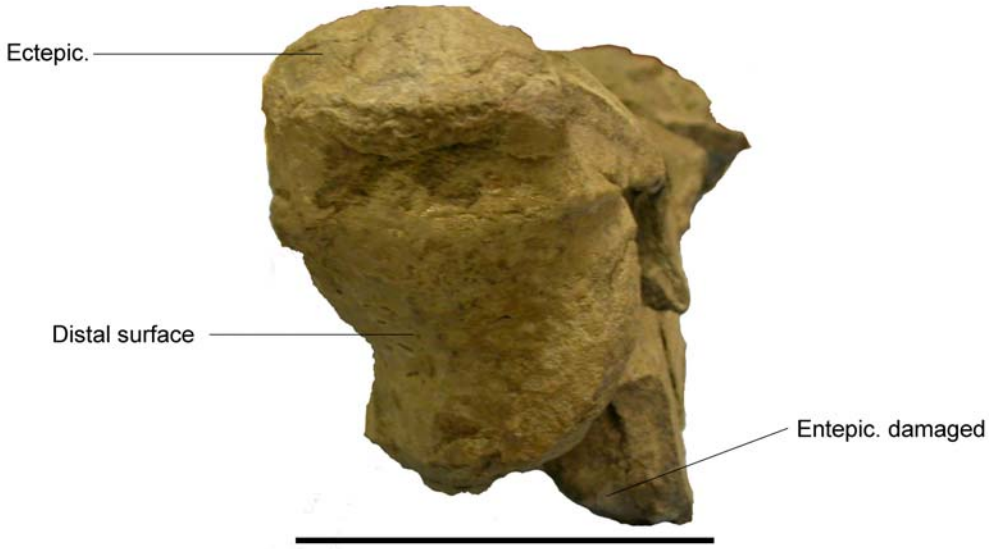

a) BP/1/5624

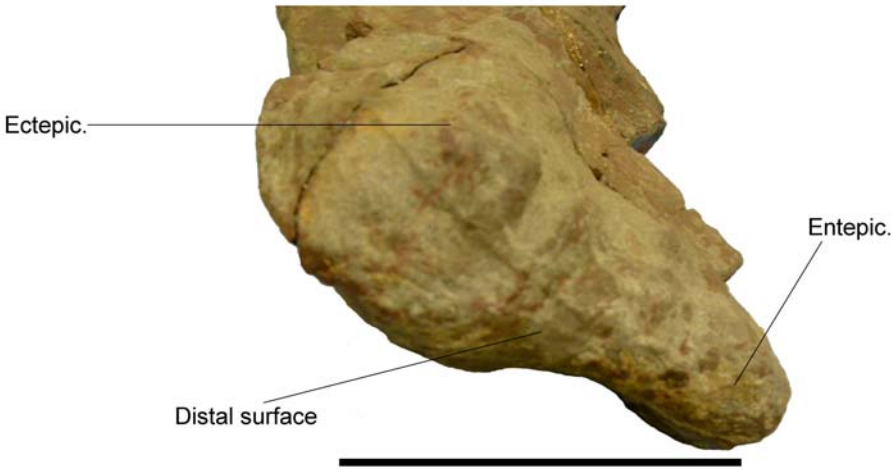

b) BP/1/6160

Plate 34 Distal articulating surface of the humerus of *K. simocephalus*.

Scale = 10 cm

a) BP/1/6160

b) BP/1/6160

c) BP/1/6160

Plate 35 a) Proximal articulating surface of the ulna and radius of *K. simocephalus*; b) Distal articulating surface of the radius of *K. simocephalus*; c) Distal articulating surface of the ulna of *K. simocephalus*.

Scale = 10 cm

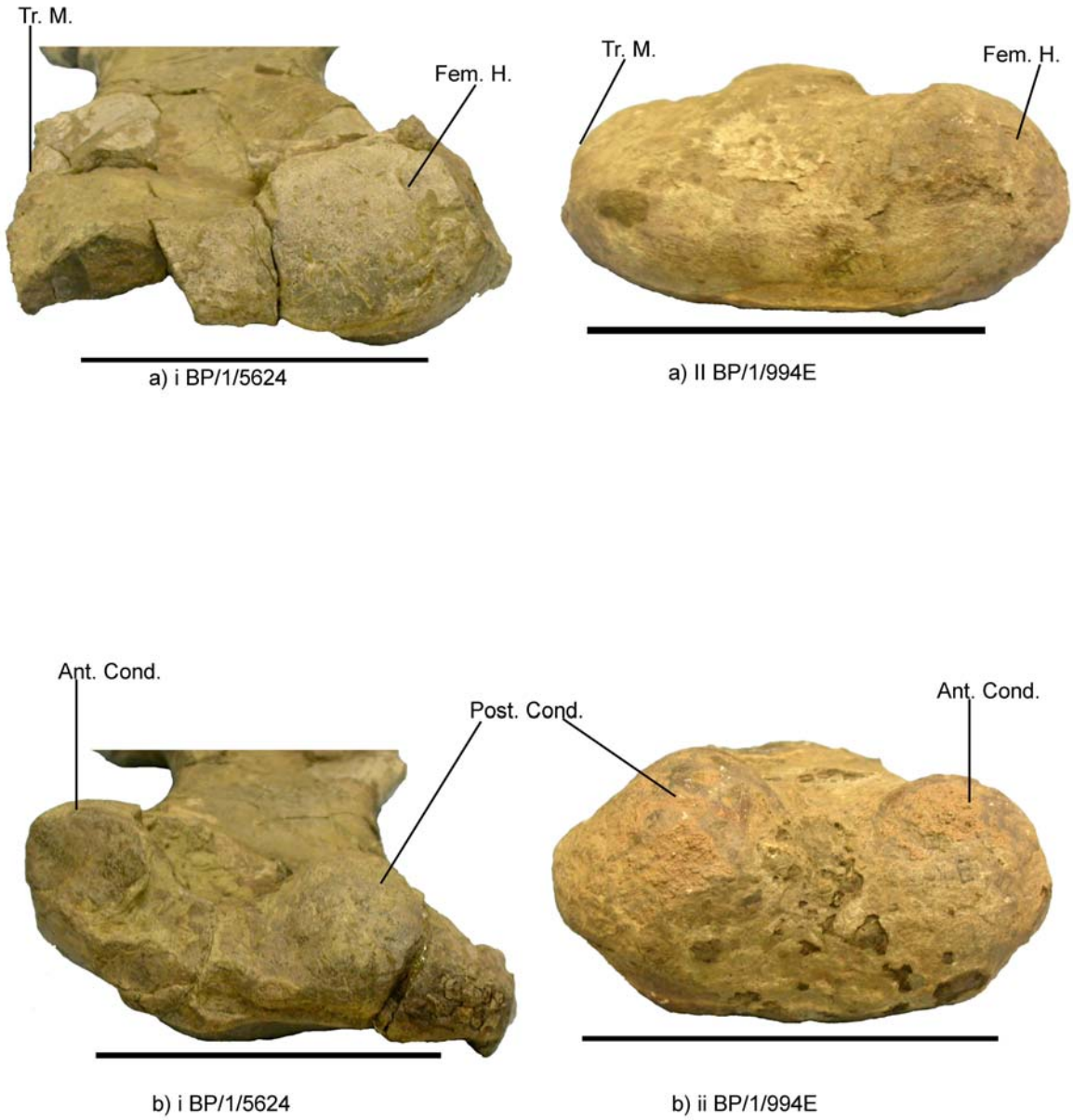

Plate 36 Proximal articulating surface of the femur of a)i. *K. Simocephalus* (dorsal view); a) ii Morphotype B (ventral view). Distal articulating surface of the femur of b) i. *K. simocephalus* (dorsal view); b) ii Morphotype B (dorsal view).

Scale = 10 cm

a) BP/1/5624

b) BP/1/5624

Plate 37 a) Proximal articulating surface of the tibia of *K. simocephalus*; b) Distal articulating surface of the tibia of *K. simocephalus*.

Scale = 10 cm